UNIVERSITY OF CAPE TOWN

Faculty of Engineering and the Built Environment

Department of Civil Engineering

A comparative study on the structural behaviour of concrete arch dams subjected to swelling due to aggregate silica reactions

By

Hermann Theodor Stehle

Submitted in partial fulfilment of the requirements for the degree

M.Eng

Civil Infrastructure Management and Maintenance

Supervisor: **Professor Pilate Moyo**

Acknowledgements

I would like to thank Professor Pilate Moyo for his supervision and guidance throughout this dissertation.

I would like to express my gratitude towards the late Doctor Chris Oosthuizen for urging me to further my studies and for his continual sharing of knowledge.

I would like to acknowledge the National Department of Water and Sanitation for allowing me to the opportunity to further my studies.

Plagiarism declaration

I know the meaning of plagiarism and declare that all the work in the document, save for that which is properly acknowledged, is my own. This thesis/dissertation has been submitted to the Turnitin module (or equivalent similarity and originality checking software) and I confirm that my supervisor has seen my report and any concerns revealed by such have been resolved with my supervisor

Signature:..Signed by candidate... Date: .....21/10/2018.....

Abstract

South Africa is considered a water-scarce country and this fact alone stresses the absolute need to preserve its water resources. As time goes by, the ageing of dams in South Africa is becoming an increasingly important factor to consider from a dam safety perspective. When considering concrete dams, Alkali Aggregate Reactions (AAR) which is the collective term referring to the potential chemical reactions between the cement and the coarse aggregate in the concrete, are a major cause of ageing. AAR causes internal swelling of concrete leading to stresses that eventually manifest on a macroscopic level as *inter alia* cracks, deformation and opening of horizontal construction joints. Although the effect of AAR expansion on arch dams is complex, certain behavioural phenomena have been identified as typical indicators of swelling concrete. These are well covered by literature.

This thesis aims to compare the structural behaviour of concrete arch dams in South Africa that are subjected to swelling due to AAR. Three arch dams, namely Hartebeeskuil Dam, Poortjieskloof Dam and Thabina Dam (all located in different climatic regions), were identified and their behavioural patterns were investigated by using visual techniques along with the interpretation of instrumentation results. The typical instrumentation results that were used for interpretation purposes included geodetic surveying results, crack width gauge results, in situ stress measurement results and trivec measurement results.

Poortjieskloof Dam, the oldest of the three dams, showed permanent upstream displacement trends of both flanks, but the centre of the arch showed a downstream displacement trend. Both flanks show swelling towards the abutments and rising crest levels are evident throughout the length of the dam wall. The dam wall was cracked quite severely on the downstream face and the horizontal joints showed clear separation. The most recent displacement trends suggest that the rate of AAR is decreasing.

Hartebeeskuil Dam, the second oldest of the three dams, showed permanent upstream displacement trends throughout the length of the dam wall. Both flanks show swelling towards the abutments and crest levels at both flanks show some settlement. The central section of the arch show rising crest levels. The results of in situ stress measurements carried out in 1999 showed that the downstream section of the arch is experiencing tensile stresses while the upstream section of the arch is mostly experiencing compressive stresses. The cracking patterns on both the upstream and downstream faces seem to agree with these findings. The results generally seem to suggest that the AAR mainly occurs on the upstream side of the arch and that the effective arch has become thinner due to the tension zone on the downstream side. The most recent displacement trends suggest that the rate of AAR is not showing any signs of decreasing.

Thabina Dam, the youngest of the three dams, showed permanent upstream trends of the right flank while the central region and left flank of the arch showed downstream trends. The flanks have moved permanently towards each other and the crest levels have increased throughout the length of the arch section. The most recent trends show increasing rates of strain especially in the vertical (z) and tangential (y) directions. More recently the entire arch has started showing upstream displacement trends. These may indicate the onset of a swelling mechanism in the concrete, most likely AAR, but extensive testing is required to prove this.

Table of Contents

Acknowledgements i
Plagiarism declaration ii
Abstract iii
List of Figures viii
List of Tables xiv
List of Abbreviations xv
Nomenclature xvi
1. Introduction 1
1.1. Background 1
1.2. Problem Statement 2
1.3. The Significance of the Research 2
1.4. Research Objectives 2
1.5. Research Limitations 2
1.6. Thesis Structure 3
2. Literature Review 5
2.1. Introduction 5
2.2. Types of Expansive Chemical Reactions in Concrete Dams 5
2.2.1. Alkali Aggregate Reactions 5
2.2.2. External Sulphate Attack 7
2.2.3. Internal Sulphate Reactions 7
2.2.4. Delayed Ettringite Formation 7
2.3. Factors that Influence AAR 8
2.3.1. Materials 8
2.3.2. Environmental Conditions 9
2.3.3. Time 10
2.4. Concrete Arch Dams 12
2.4.1. Construction 12
2.4.2. General Arch Function 13
2.4.3. Different Types of Arch Dams 15
2.5. Concrete Arch Dams Experiencing Expansion due to Chemical Reaction 15
2.5.1. Surveillance of Arch Dams 15
2.5.2. Expansion Phenomena in Arch Dams 16
2.5.3. The Role of Creep 17

2.6. Case Studies 18
2.6.1. Cahora Bassa Dam (Mozambique) 18
2.6.2. Kouga Dam (South Africa) 18
3. Methodology 20
3.1. Introduction 20
3.2. Systematic Approach 20
3.2.1. Visual Inspections 20
3.2.2. Geodetic Surveys 20
3.2.3. Three-Dimensional Crack Width Gauges 21
3.2.4. Trivec Installations 21
3.2.5. In Situ Stress Measurements 23
4. Hartebeeskuil Dam 24
4.1. Introduction 24
4.2. Visual Inspection 25
4.2.1. Right Flank 25
4.2.2. Spillway Section 27
4.2.3. Left Flank 28
4.3. Geodetic Survey Results 29
4.3.1. Tangential Movements 30
4.3.2. Radial Movements 32
4.3.3. Vertical Movements 34
4.4. Crack Width Gauges 36
4.4.1. Tangential Crack on Crest 36
4.4.2. Vertical Joints on Right Flank Crest 37
4.4.3. Vertical Joints on Right Flank Base 39
4.4.4. Horizontal Lift Joints on Right Flank 41
4.5. In Situ Stress Measurements 42
4.6. Chapter Summary 43
5. Poortjieskloof Dam 44
5.1. Introduction 44
5.2. Visual Inspection 45
5.2.1. Left Flank 45
5.2.2. Spillway Section 48
5.2.3. Right Flank 49
5.3. Geodetic Survey Results 49

5.3.1. Tangential Movements 50
5.3.2. Radial Movements 54
5.3.3. Vertical Movements 59
5.4. Crack Width Gauges 63
5.4.1. Vertical Joints on Left Flank Crest 63
5.4.2. Vertical Joints on Right Flank Crest 64
5.4.3. Vertical Joints Measured on Left Flank Downstream Face 66
5.4.4. Vertical Joints Measured on Right Flank Downstream Face 67
5.4.5. Horizontal Joints and Cracks Measured on the Downstream Face 68
5.5. Trivec Results 71
5.5.1. Trivec Installation 1 71
5.5.2. Trivec Installation 2 73
5.5.3. Trivec Installation 3 75
5.5.4. Trivec installation 4 77
5.6. Chapter Summary 79
6. Thabina Dam 81
6.1. Introduction 81
6.2. Visual Inspection 82
6.2.1. Left Flank (Gravity Section) 82
6.2.2. Right Flank (Arch Section) 83
6.3. Crack Width Gauges 84
6.3.1. Vertical Joints on the Crest of the Gravity Section 85
6.3.2. Vertical Joints on the Central Crest of the Arch Section 87
6.3.3. Vertical Joints on the Right Flank Arch Section 88
6.4. Trivec Results 89
6.4.1. Trivec Installation 1 90
6.4.2. Trivec Installation 2 92
6.4.3. Trivec Installation 3 94
6.5. Chapter Summary 96
7. Discussion of Results 98
7.1. Introduction 98
7.2. Comparative Results 98
7.3. Comparative Discussion 99
8. Conclusions and Recommendations 103
8.1. Summary 103

8.2. Conclusions 103
8.3. Recommendations 104
9. References 105

List of Figures

Figure 2-1: Typical ASR crack pattern and staining 5
Figure 2-2: Cracks associated with ASR generally display wide crack widths and staining around them caused by the silicate gel 5
Figure 2-3: Micro-cracking in the concrete due to ASR (Menendez, 2016) 6
Figure 2-4: White reaction product on the rims of the coarse aggregate (Oberholster, 2009: 208) 6
Figure 2-5: Differences in AAR expansion due to temperature (Saouma & Perotti, 2006: 195) .. 10
Figure 2-6: Normalized expansion curve with time (Saouma & Perotti, 2006) 11
Figure 2-7: Typical accumulated expansion strain trend versus time for concrete dam walls adapted from Charlwood (2016: 33) 12
Figure 2-8: The construction of Flaming Gorge Dam in the United States of America (USA) (USBR, 2017) 13
Figure 2-9: The construction of Glen Canyon Dam in the USA (USBR, 2017) 13
Figure 2-10: The typical principal compression stress vectors on a developed arch elevation (Shaw, 2015: 324) 14
Figure 2-11: The typical principal compression stress vectors on a horizontal arch section (Shaw, 2015: 324) 14
Figure 2-12: Typical deflected arch unit (Ghanaat, 1993: 2-4) 14
Figure 2-13: Typical deflected cantilever unit (Ghanaat, 1993: 2-4) 14
Figure 2-14: Typical separation of a horizontal construction lift joint at Poortjieskloof Dam in South Africa 17
Figure 2-15: Typical peripheral cracks at Poortjieskloof Dam in South Africa 17
Figure 2-16: Time-dependent increase in strain under constant stress (Alexander & Beushausen, 2009: 119) 17
Figure 2-17: Time-dependent decrease in stress under constant strain (Alexander & Beushausen, 2009: 119) 17
Figure 2-18: Cahora Bassa Dam (Carvalho *et al.*, 2016: 6-87) 18
Figure 2-19: Close-up view of Cahora Bassa Dam from the downstream side (Botha *et al.*, 2016: 2a-210) 18
Figure 2-20: Kouga Dam as viewed from the downstream side (Mahlabela & Oosthuizen, 2012: 233) 19
Figure 2-21: Kouga Dam as viewed from the right flank (Hattingh, 2011) 19
Figure 3-1: A typical DWAF2001 3-D crack-width-tilt gauge with assembly unit (Dorfling, 2008: 45) 21
Figure 3-2: The typical components of the Trivec system used in South Africa (Naude, 2002: 4) 22
Figure 3-3: The over-coring method for in situ stress measurement (Geotechnisches Ingenieurbüro, 2004) 23
Figure 4-1: Hartebeeskuil Dam as viewed from the downstream side 24
Figure 4-2: Hartebeeskuil Dam: The upstream concrete face of the right flank displaying horizontal cracks 25
Figure 4-3: Hartebeeskuil Dam: The upstream concrete face viewed towards the inlet tower ... 25
Figure 4-4: Hartebeeskuil Dam: A major tangential crack on the right flank crest 26

Figure 4-5: Hartebeeskuil Dam: An indication of the crack width and previous core drill hole that determined the depth of the crack 26
Figure 4-6: Hartebeeskuil Dam: AAR cracking pattern on the far-right abutment steps 26
Figure 4-7: Hartebeeskuil Dam: Crack width and typical ASR crack staining 26
Figure 4-8: Hartebeeskuil Dam: Typical parallel peripheral cracks in the vicinity of the right flank "pulvino" 27
Figure 4-9: Hartebeeskuil Dam: Parallel cracks evident on the right flank downstream face 27
Figure 4-10: Hartebeeskuil Dam: Close-up view of one of the peripheral cracks on the right flank downstream face 27
Figure 4-11: Hartebeeskuil Dam: Parallel cracks in the vicinity of the "pulvino" 27
Figure 4-12: Hartebeeskuil Dam: Tangential crack between two radial cracks on the spillway crest 28
Figure 4-13: Hartebeeskuil Dam: General view of the spillway crest 28
Figure 4-14: Hartebeeskuil Dam: Calcite staining visible on the downstream face of the spillway section 28
Figure 4-15: Hartebeeskuil Dam: Spillway and left flank downstream face 29
Figure 4-16: Hartebeeskuil Dam: Close-up view of left flank downstream face 29
Figure 4-17: Hartebeeskuil Dam: Typical peripheral cracks on the left flank 29
Figure 4-18: Plan layout of the crest geodetic survey targets at Hartebeeskuil Dam 29
Figure 4-19: Tangential movements of T77 and T87 at Hartebeeskuil Dam 30
Figure 4-20: Tangential movements of T85 and T84 at Hartebeeskuil Dam 30
Figure 4-21: Tangential movements of T83 at Hartebeeskuil Dam 30
Figure 4-22: Tangential movements of T78 and T79 at Hartebeeskuil Dam 31
Figure 4-23: Tangential movements of T80 and T81 at Hartebeeskuil Dam 31
Figure 4-24: Tangential movements of T82 at Hartebeeskuil Dam 31
Figure 4-25: Radial movements of T77 and T87 at Hartebeeskuil Dam 32
Figure 4-26: Radial movements of T85 and T84 at Hartebeeskuil Dam 32
Figure 4-27: Radial movements of T83 at Hartebeeskuil Dam 32
Figure 4-28: Radial movements of T78 and T79 at Hartebeeskuil Dam 33
Figure 4-29: Radial movements of T80 and T81 at Hartebeeskuil Dam 33
Figure 4-30: Radial movements of T82 at Hartebeeskuil Dam 33
Figure 4-31: Vertical movements of T77 and T87 at Hartebeeskuil Dam 34
Figure 4-32: Vertical movements of T85 and T84 at Hartebeeskuil Dam 34
Figure 4-33: Vertical movements of T83 at Hartebeeskuil Dam 34
Figure 4-34: Vertical movements of T78 and T 79 at Hartebeeskuil Dam 35
Figure 4-35: Vertical movements of T80 and T81 at Hartebeeskuil Dam 35
Figure 4-36: Radial movements of T82 at Hartebeeskuil Dam 35
Figure 4-37: Radial movements of the tangential crest crack at Hartebeeskuil Dam 36
Figure 4-38: Tangential movements of the tangential crest crack at Hartebeeskuil Dam 37
Figure 4-39: Vertical movements of the tangential crest crack at Hartebeeskuil Dam 37
Figure 4-40: Hartebeeskuil Dam: The positions of the vertical joints and block numbers 38
Figure 4-41: Radial movements of crest vertical joints at Hartebeeskuil Dam 38
Figure 4-42: The opening/closing of crest vertical joints at Hartebeeskuil Dam 38
Figure 4-43: The vertical movements of crest vertical joints at Hartebeeskuil Dam 39
Figure 4-44: Radial movements of base vertical joints at Hartebeeskuil Dam 40
Figure 4-45: The opening/closing of base vertical joints at Hartebeeskuil Dam 40
Figure 4-46: The vertical movements of base vertical joints at Hartebeeskuil Dam 40

Figure 4-47: Radial movements of horizontal lift joints at Hartebeeskuil Dam 41
Figure 4-48: Tangential movements of horizontal lift joints at Hartebeeskuil Dam 41
Figure 4-49: Vertical movements of horizontal lift joints at Hartebeeskuil Dam 42
Figure 5-1: Poortjieskloof Dam 44
Figure 5-2: Poortjieskloof Dam: General view of left flank upstream face 45
Figure 5-3: Poortjieskloof Dam: Close-up view of left flank upstream face 45
Figure 5-4: Poortjieskloof Dam: Map cracking on concrete step structure left of the NOC 46
Figure 5-5: Poortjieskloof Dam: The left flank NOC 46
Figure 5-6: Poortjieskloof Dam: Some more map cracking on the concrete step structure 46
Figure 5-7: Poortjieskloof Dam: Clear parallel peripheral cracking patterns visible on the left flank downstream face 47
Figure 5-8: Poortjieskloof Dam: Close-up view of the cracking patterns on left flank downstream face 47
Figure 5-9: Poortjieskloof Dam: Some seepage through horizontal lift joints bordering the left abutment 47
Figure 5-10: Poortjieskloof Dam: Excessive map cracking patterns surrounding the outlet structure; also, note the staining 47
Figure 5-11: Poortjieskloof Dam: View of spillway crest 48
Figure 5-12: Poortjieskloof Dam: General view of spillway downstream face 48
Figure 5-13: Poortjieskloof Dam: Increased cracking in the area surrounding the outlet structure 48
Figure 5-14: Poortjieskloof Dam: Clear separation of first horizontal construction lift joint above apron 48
Figure 5-15: Poortjieskloof Dam: Unfavourable cracking patterns on the right flank 49
Figure 5-16: Poortjieskloof Dam: General view of the right flank downstream face 49
Figure 5-17: Poortjieskloof Dam: A prominent crack parallel to the abutment 49
Figure 5-18: Poortjieskloof Dam: Close-up view of the far-right flank downstream face 49
Figure 5-19: Upstream elevation of the geodetic survey targets at Poortjieskloof Dam 50
Figure 5-20: Plan view of the geodetic survey network at Poortjieskloof Dam 50
Figure 5-21: Tangential movements of T27, T29 and T80 at Poortjieskloof Dam 51
Figure 5-22: Tangential movements of T28, T30 and T31 at Poortjieskloof Dam 51
Figure 5-23: Tangential movements of T01, T02 and T32 at Poortjieskloof Dam 51
Figure 5-24: Tangential movements of T70 and T71 at Poortjieskloof Dam 52
Figure 5-25: Tangential movements of T33 at Poortjieskloof Dam 52
Figure 5-26: Tangential movements of T34 at Poortjieskloof Dam 52
Figure 5-27: Tangential movements of T72 at Poortjieskloof Dam 53
Figure 5-28: Tangential movements of T39, T37 and T81 at Poortjieskloof Dam 53
Figure 5-29: Tangential movements of T40, T38 and T35 at Poortjieskloof Dam 53
Figure 5-30: Tangential movements of T04, T03 and T36 at Poortjieskloof Dam 54
Figure 5-31: Tangential movements of T74 and T73 at Poortjieskloof Dam 54
Figure 5-32: Radial movements of T27, T29 and T80 at Poortjieskloof Dam 55
Figure 5-33: Radial movements of T28, T30 and T31 at Poortjieskloof Dam 55
Figure 5-34: Radial movements of T01, T02 and T32 at Poortjieskloof Dam 55
Figure 5-35: Radial movements of T70 and T71 at Poortjieskloof Dam 56
Figure 5-36: Radial movements of T33 at Poortjieskloof Dam 56
Figure 5-37: Radial movements of T34 at Poortjieskloof Dam 56
Figure 5-38: Radial movements of T72 at Poortjieskloof Dam 57

Figure 5-39: Radial movements of T39, T37 and T81 at Poortjieskloof Dam 57
Figure 5-40: Radial movements of T40, T38 and T35 at Poortjieskloof Dam 57
Figure 5-41: Radial movements of T04, T03 and T36 at Poortjieskloof Dam 58
Figure 5-42: Radial movements of T74 and T73 at Poortjieskloof Dam 58
Figure 5-43: Vertical movements of T27, T29 and T80 at Poortjieskloof Dam 59
Figure 5-44: Vertical movements of T28, T30 and T31 at Poortjieskloof Dam 59
Figure 5-45: Vertical movements of T01, T02 and T32 at Poortjieskloof Dam 60
Figure 5-46: Vertical movements of T70 and T71 at Poortjieskloof Dam 60
Figure 5-47: Vertical movements of T33 at Poortjieskloof Dam 60
Figure 5-48: Vertical movements of T34 at Poortjieskloof Dam 61
Figure 5-49: Vertical movements of T72 at Poortjieskloof Dam 61
Figure 5-50: Vertical movements of T39, T37 and T81 at Poortjieskloof Dam 61
Figure 5-51: Vertical movements of T40, T38 and T35 at Poortjieskloof Dam 62
Figure 5-52: Vertical movements of T04, T03 and T36 at Poortjieskloof Dam 62
Figure 5-53: Vertical movements of T74 and T73 at Poortjieskloof Dam 62
Figure 5-54: Radial movements of the vertical joints on the left flank NOC 63
Figure 5-55: Tangential movements of the vertical joints on the left flank NOC 64
Figure 5-56: Vertical movements of the vertical joints on the left flank NOC 64
Figure 5-57: Radial movements of the vertical joints on the right flank NOC 65
Figure 5-58: Tangential movements of the vertical joints on the right flank NOC 65
Figure 5-59: Vertical movements of the vertical joints on the right flank NOC 65
Figure 5-60: Radial movements of the vertical joints on the left flank downstream face 66
Figure 5-61: Tangential movements of the vertical joints on the left flank downstream face 66
Figure 5-62: Vertical movements of the vertical joints on the left flank downstream face 67
Figure 5-63: Radial movements of the vertical joints on the right flank downstream face 67
Figure 5-64: Tangential movements of the vertical joints on the right flank downstream face 68
Figure 5-65: Vertical movements of the vertical joints on the right flank downstream face 68
Figure 5-66: Radial movements of the horizontal joints on the downstream face of Block 3 69
Figure 5-67: Tangential movements of the horizontal joints on the downstream face of Block 3 69
Figure 5-68: Vertical movements of the horizontal joints on the downstream face of Block 3 69
Figure 5-69: Radial movements of the horizontal cracks on the downstream face of Block 7 and 8 70
Figure 5-70: Tangential movements of the horizontal cracks on the downstream face of Block 7 and 8 70
Figure 5-71: Vertical movements of the horizontal cracks on the downstream face of Block 7 and 8 70
Figure 5-72: The positions of the Trivec boreholes at Poortjieskloof Dam 71
Figure 5-73: Summer radial displacements of Trivec borehole Pokr1 72
Figure 5-74: Winter radial displacements of Trivec borehole Pokr1 72
Figure 5-75: Summer tangential displacements of Trivec borehole Pokr1 72
Figure 5-76: Winter tangential displacements of Trivec borehole Pokr1 72
Figure 5-77: Summer vertical displacements of Trivec borehole Pokr1 73
Figure 5-78: Winter vertical displacements of Trivec borehole Pokr1 73
Figure 5-79: Summer radial displacements of Trivec borehole Pokr2 74
Figure 5-80: Winter radial displacements of Trivec borehole Pokr2 74
Figure 5-81: Summer tangential displacements of Trivec borehole Pokr2 74

Figure 5-82: Winter tangential displacements of Trivec borehole Pokr2 74
Figure 5-83: Summer vertical displacements of Trivec borehole Pokr2 75
Figure 5-84: Winter vertical displacements of Trivec borehole Pokr2 75
Figure 5-85: Summer radial displacements of Trivec borehole Pokr3 76
Figure 5-86: Winter radial displacements of Trivec borehole Pokr3 76
Figure 5-87: Summer tangential displacements of Trivec borehole Pokr3 76
Figure 5-88: Winter tangential displacements of Trivec borehole Pokr3 76
Figure 5-89: Summer vertical displacements of Trivec borehole Pokr3 77
Figure 5-90: Winter vertical displacements of Trivec borehole Pokr3 77
Figure 5-91: Summer radial displacements of Trivec borehole Pokr4 78
Figure 5-92: Winter radial displacements of Trivec borehole Pokr4 78
Figure 5-93: Summer tangential displacements of Trivec borehole Pokr4 78
Figure 5-94: Winter tangential displacements of Trivec borehole Pokr4 78
Figure 5-95: Summer vertical displacements of Trivec borehole Pokr4 79
Figure 5-96: Winter vertical displacements of Trivec borehole Pokr4 79
Figure 6-1: Thabina Dam 81
Figure 6-2: The right flank downstream face as viewed from the right flank NOC 83
Figure 6-3: The stepped downstream profile of the spillway as viewed from the left flank NOC 83
Figure 6-4: The prominent crack near the base of the right flank abutment area 83
Figure 6-5: View of the horizontal lift joint that displays active seepage 84
Figure 6-6: General view of the downstream face of the arch 84
Figure 6-7: The positions of the blocks comprising the arch section at Thabina Dam 84
Figure 6-8: Radial movements of the vertical joints on the left flank NOC 85
Figure 6-9: Tangential movements of the vertical joints on the left flank NOC 85
Figure 6-10: Vertical movements of the vertical joints on the left flank NOC 86
Figure 6-11: Radial movements of the vertical joints on the NOC of the central arch section 87
Figure 6-12: Tangential movements of the vertical joints on the NOC of the central arch section 87
Figure 6-13: Vertical movements of the vertical joints on the NOC of the central arch section 88
Figure 6-14: Radial movements of the vertical joints on the NOC of the right flank arch section 88
Figure 6-15: Tangential movements of the vertical joints on the NOC of the right flank arch section 89
Figure 6-16: Vertical movements of the vertical joints on the NOC of the central arch section 89
Figure 6-17: The positions of the Trivec boreholes at Thabina Dam 90
Figure 6-18: Summer radial displacements of Trivec borehole Thar1 91
Figure 6-19: Winter radial displacements of Trivec borehole Thar1 91
Figure 6-20: Summer tangential displacements of Trivec borehole Thar1 91
Figure 6-21: Winter tangential displacements of Trivec borehole Thar1 91
Figure 6-22: Summer vertical displacements of Trivec borehole Thar1 92
Figure 6-23: Winter vertical displacements of Trivec borehole Thar1 92
Figure 6-24: Summer radial displacements of Trivec borehole Thar2 93
Figure 6-25: Winter radial displacements of Trivec borehole Thar2 93
Figure 6-26: Summer tangential displacements of Trivec borehole Thar2 93
Figure 6-27: Winter tangential displacements of Trivec borehole Thar2 93
Figure 6-28: Summer vertical displacements of Trivec borehole Thar2 94
Figure 6-29: Winter vertical displacements of Trivec borehole Thar2 94
Figure 6-30: Summer radial displacements of Trivec borehole Thar3 95

Figure 6-31: Winter radial displacements of Trivec borehole Thar3 95
Figure 6-32: Summer tangential displacements of Trivec borehole Thar3 95
Figure 6-33: Winter tangential displacements of Trivec borehole Thar3 95
Figure 6-34: Summer vertical displacements of Trivec borehole Thar3 96
Figure 6-35: Winter vertical displacements of Trivec borehole Thar3 96
Figure 7-1: Schematic of permanent x-y displacement of Hartebeeskuil Dam 99
Figure 7-2: Schematic of permanent x-y displacement of Poortjieskloof Dam 100
Figure 7-3: Schematic of permanent x-y displacement of Thabina Dam 102

List of Tables

Table 2-1: Potentially reactive aggregate sources in South Africa as adapted from Oberholster (2009: 192) 9
Table 2-2: Different static and dynamic loads that act on arch dams as adapted from Vezi (2014: 6-10), Kroon (1984: 5-1 to 5-8) and Prins (2014: 154) 14
Table 2-3: The different types of arch dams according to its thickness as adapted from Shaw (2015: 323) 15
Table 2-4: Typical instrumentation used for measuring an arch dam's load response as adapted from Oosthuizen (2015) 16
Table 3-1: Relative accuracies of different crack gauges used in South Africa as adapted from Oosthuizen *et al.* (2003: 604) 21
Table 4-1: Results gained from the in-situ stress measurements conducted in 1999 42
Table 7-1: Summary of comparative displacement and strain rates 98
Table 7-2: Average strain and displacement rates at Hartebeeskuil Dam since 2010 100
Table 7-3: Average strain and displacement rates at Poortjieskloof Dam since 2010 101
Table 7-4: Average strain and displacement rates at Thabina Dam since 2010 102

List of Abbreviations

AAR	Alkali Aggregate Reactions
ACR	Alkali Carbonate Reaction
ASR	Alkali Silica Reaction
CSIRO	Commonwealth Scientific and Industrial Research Organisation
DEF	Delayed Ettringite Formation
DWAF	Department of Water Affairs and Forestry
DWS	Department of Water and Sanitation
ESA	External Sulphate Attack
HI	Hollow Inclusion
ICOLD	International Commission on Large Dams
ISR	Internal Sulphate Reactions
NOC	Non-overspill crest
NWA	National Water Act
RL	Reduced Level
SCM	Supplementary Cementitious Material
uPVC	Un-plasticized polyvinyl chloride
USA	United States of America
USACE	United States Army Corps of Engineers
USBR	United States Bureau of Reclamation

Nomenclature

Latin Upper Case

°C	Degrees Celsius
K	Kelvin (Temperature) or Canyon Shape Factor
MPa	Megapascal

Latin Lower Case

km	Kilometres
m	Metres
mm	Millimetres
t	Time

Greek Lower Case

τ_L	Latency time
τ_c	Characteristic time
ξ	Normalised volumetric expansion
σ	Stress
ε	Strain
με	Micro-strain

1. Introduction

1.1. Background

Dams in general are some of the most magnificent civil engineering structures in the world. They perform the vital function of providing gross storage water for domestic usage, irrigation, industrial usage, hydro-electricity generation, and even recreational purposes. All these functions together play a large role in society as a whole, which is the very reason why it is of utmost importance to ensure that these structures are looked after well. Dam engineering is thus concerned with ensuring that dams are structurally safe and meet performance specifications while minimising threats to the environment (ICOLD, 1994: 13).

From a dam safety engineering point of view, understanding the long-term behaviour of the materials used for the design and construction of dams is very important (Hattingh & Oosthuizen, 2012: 1). Dams are usually constructed by using either mass concrete, earth-fill, rock-fill or rubble-masonry materials depending on the founding conditions and geometry of the dam site. Concrete dams are generally divided into concrete gravity, concrete buttress, concrete gravity-arch and concrete arch dams, each with a unique structural function.

According to the ICOLD Bulletin 93 (1994: 17), the ageing of concrete is considered a major class of deterioration in dams and appurtenant works. Major ageing scenarios in concrete dams include chemical reactions resulting in swelling, shrinkage, creep, loss of strength under permanent and repeated actions, poor resistance to freezing and thawing, ageing of structural joints and ageing of pre-stressed structures (ICOLD, 1994: 21).

Swelling in concrete due to chemical reaction between the cement and the coarse aggregate contributes significantly to ageing of concrete dams. These reactions are collectively referred to as Alkali-Aggregate Reactions (AAR). There are also other reactions that can lead to swelling of concrete, namely sulphate related reactions either internally, known as Internal Sulphate Attack (ISA), or externally, known as External Sulphate Attack (ESA) where sulphates enter the concrete from the surrounding environment. A third reaction (also involving sulphates) that may cause swelling of concrete is known as Delayed Ettringite Formation (DEF) which usually occurs due to elevated temperatures during the initial hydration of the concrete (Charlwood *et al.*, 2013).

The macroscopic structural effects of swelling concrete in dams have been observed comprehensively world-wide. These macroscopic structural effects include surface cracking and dimensional changes of the structure such as rising crest levels and permanent upstream or downstream displacements (Amberg, 2011).

Swelling due to chemical reaction has been proven to degrade some mechanical properties of concrete such as the tensile strength, the bending capacity, the static modulus of elasticity and the dynamic modulus of elasticity (Liu *et al.*, 2012: 567).

It is very important to understand the effects of expanding concrete on dams so that meaningful safety evaluations can be carried out that will eventually lead to feasible remedial measures if required. Most remedial measures to alleviate the effects of swelling in dams are of a temporary nature, because the swelling effect is an ongoing process and will only stop once the reaction

has been exhausted or when one or more of the reactants have been permanently removed. Concrete naturally deals with expansion by means of a mechanism known as creep (discussed in the next chapter) and the challenge is to determine whether any remedial measures will indeed be necessary.

1.2. Problem Statement

There are three main factors that affect the probability of occurrence and rate of AAR, namely climate (more specifically, temperature and humidity), the chemical make-up of the concrete mix used during the construction, and the availability of moisture (this would relate with the water levels in a dam). This thesis is a comparative study of the observed behaviour of concrete arch dam walls subjected to the swelling effect of AAR by looking at three specific case studies in South Africa. These three dams are all located in areas with varying climatic conditions, while the water level records and mix designs of the concrete also differ. The aim of the study is to determine how the concrete arch structures differ in behaviour and to draw conclusions on what mistakes with regards to swelling concrete can be eliminated in the future during the construction of arch dams in South Africa.

1.3. The Significance of the Research

The study is being undertaken to increase the knowledge about swelling in concrete arch dam walls in South Africa due to AAR. The knowledge will prove valuable for dam safety engineers conducting dam safety evaluations on concrete arch dam walls by providing a framework to identify swelling phenomena in different climate regions and where there are differences in chemical make-up of the concrete.

1.4. Research Objectives

The objectives of this study are listed below;

- use literature to discuss AAR and its microscopic and macroscopic effects on concrete arch dams;
- obtain data from geodetic surveys, trivec installations and crack width gauges and compare the results of three arch dams in South Africa;
- draw conclusions from observed structural behavioural patterns;

1.5. Research Limitations

The results contained in this thesis are based on readings that were taken by the Department of Water and Sanitation (DWS) over the years. Although deemed fairly reliable, the DWS cannot guarantee that all the results are necessarily correct. There is still a human element involved in taking these readings and, therefore, mistakes are inevitable. Unfortunately, there are also some gaps in the records, which is information that the DWS will never be able to retrieve. This study is limited by the records of instrumentation readings that were available.

The confirmation of the presence of AAR by recognized diagnostic methods was not included in the scope of this study. This study was limited to the gathering of as much of the archived information on the dams as possible, which included previous studies/tests that were conducted to confirm the presence of AAR. Pootjieskloof Dam and Hartebeeskuil Dam were specifically selected because of their known history of performance issues which were attributed to AAR swelling over the years and is well documented by the Department of Water and Sanitation. The

decision to include Thabina Dam was based on the fact that the dam is situated in a totally different geographical area and was constructed with different materials. Although AAR has not yet been confirmed at Thabina Dam by any of the recognized diagnostic methods, increasing evidence of behavioural patterns which could be linked to AAR has been picked up through instrumentation readings.

Unfortunately, very little as-built information was available and the limited information on construction materials used during construction were gathered from dam safety inspection reports.

This study is limited to studying the behaviour of the arch dams by visual techniques and the interpretation of measured instrumentation results. Any form of theoretical structural simulations, such as finite element analyses, fall outside of the scope of this study.

This study includes only three case studies. Including any more dams would result in a very tedious and lengthy discussion of the interpretation of instrumentation results. Although a comparison is made, the study does not represent all possible scenarios relating to the swelling of concrete arch dams.

1.6. Thesis Structure

Chapter 1 - Introduction

This chapter considers swelling chemical reactions within concrete as an ageing mechanism in dams. The objectives, scope and limitations of the study are presented.

Chapter 2 – Literature Review

This chapter presents literature relating to different chemical reactions in concrete that causes swelling. The focus is primarily on Alkali Aggregate Reaction (AAR) which is the most prominent cause of swelling in concrete dam wall structures. The effect of AAR swelling specifically on concrete arch dams are investigated and two case studies in Southern Africa are briefly presented.

Chapter 3 – Methodology

This chapter presents the systematic approach that was followed during the study. The typical instruments and techniques that were used, are explained.

Chapter 4 – Hartebeeskuil Dam

This chapter presents the visual inspection and instrumentation results for the Hartebeeskuil Dam in the Western Cape. The results are interpreted in order to determine the structural behaviour of the dam wall.

Chapter 5 – Poortjieskloof Dam

This chapter presents the visual inspection and instrumentation results for the Poortjieskloof Dam in the Western Cape. The results are interpreted in order to determine the structural behaviour of the dam wall.

Chapter 6 – Thabina Dam

This chapter presents the visual inspection and instrumentation results for the Thabina Dam in the Limpopo Province. The results are interpreted in order to determine the structural behaviour of the dam wall.

Chapter 7 – Discussion of Results

This chapter presents a discussion on the instrumentation results for the three dams.

Chapter 8 – Conclusions and Recommendations

Concludes the study and makes recommendations for future work related to this topic.

Chapter 9 – References

Contains a list of literature used in this research.

2. Literature Review

2.1. Introduction

Swelling in concrete due to chemical reaction is a significant cause of ageing in dams (Amberg, 2011). There are several chemical reactions in concrete which cause swelling. They include Alkali Aggregate Reactions (AAR), internal sulphate reactions (ISR) and external sulphate attack (ESA). In South Africa AAR is the most prominent of these.

The distinctive evidence of swelling in dams are surface cracking and dimensional changes of the structure such as rising crest levels and permanent upstream or downstream displacements. Other consequences of swelling include the degradation of some mechanical properties of the concrete (Amberg, 2011 & Liu *et al.*, 2012: 567).

In most cases dams will only exhibit signs of expansion about 20 - 30 years after construction (Amberg, 2011). As most of the concrete dams in South Africa are older than this, those dams that are subjected to swelling are showing signs of deterioration through cracking patterns and permanent displacements. It is very important to understand the effects of expansion on dams so that meaningful safety evaluations can be conducted that will eventually lead to feasible remedial works if required (Hattingh & Oosthuizen, 2012: 3).

The only way to stop the swelling action due to AAR is to stop the chemical reaction. This is generally impossible as long as the reacting chemicals are present. Hence, remedial action is generally temporary.

2.2. Types of Expansive Chemical Reactions in Concrete Dams

2.2.1. Alkali Aggregate Reactions

Alkali aggregate reactions is the broader term describing the chemical reaction between certain specific mineralogical types of aggregates and alkali of cement in the presence of moisture (Charlwood, 2009: 4). There are two major types of AAR, namely alkali silica reaction (ASR) and alkali carbonate reaction (ACR).

Figure 2-1: Typical ASR crack pattern and staining

Figure 2-2: Cracks associated with ASR generally display wide crack widths and staining around them caused by the silicate gel

During ASR the alkalis in the cement reacts with certain siliceous aggregates such as opals, chalcedony, cherts, andesites, basalts and some quartz (Charlwood, 2009: 4). Alkalis may also

come from other constituents in the concrete mix, such as water or adjuvant (admixtures or additives) and they may also penetrate the concrete from the environment. The alkalis are dissolved in the mixing water during the mixing of concrete and in the pore water. The resultant alkaline solution reacts with the reactive silica-containing aggregates as described by the chemical equations (Saouma & Perotti, 2006: 194).

- The first step: silica (aggregate) + alkali (cement) → alkali-silica gel
  - $[xSiO_2] + [yNa(K)OH] \rightarrow \left[Na(K)_ySi_xO_z\ aq\right]$ (2.1)
- The second step: alkali-silica gel + moisture → expanded alkali-silica gel
  - $\left[Na(K)_ySi_xO_z\ aq\right] + [H_2O] \rightarrow [Na(K)_ySi_xO_z \cdot wH_2O]$ (2.2)

The silica minerals (especially the poorly crystallized ones) are transformed into an alkali-silica gel (see the white reaction product shown in Figure 2-4) which is hygroscopic in nature. This causes a swelling action on the microscopic level which causes the aggregate to develop cracks leading to the expansion and cracking of the surrounding cement paste as shown in Figure 2-3 (Charlwood *et al.*, 2013).

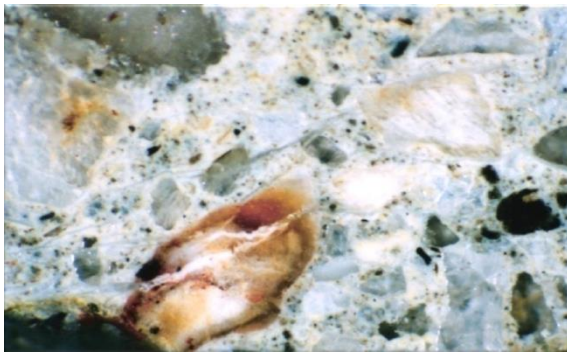

Figure 2-3: Micro-cracking in the concrete due to ASR (Menendez, 2016)

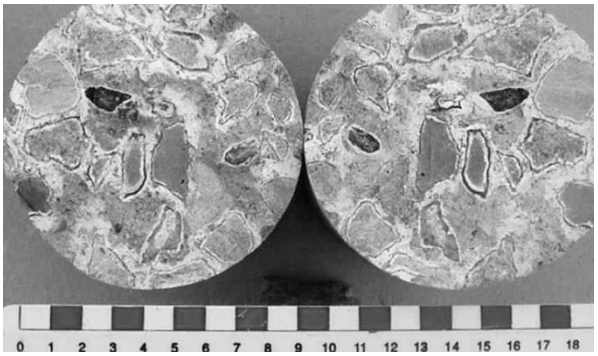

Figure 2-4: White reaction product on the rims of the coarse aggregate (Oberholster, 2009: 208)

ACR refers to the reaction between the alkaline pore solution and certain argillaceous dolomitic limestones and argillaceous calcitic dolostones. No expansive alkali-silica gel is formed, and the harmful expansion is believed to be caused by the reaction of the alkali hydroxides with the small dolomite crystals in the clay matrix. This reaction is also referred to as dedolomitisation and additional expansion may occur if the dry clay absorbs moisture and causes the expansion of the already dedolomitised limestones (Oberholster, 2009: 189-190). These are the ACR equations below (ICOLD, 1991: 16-17).

- Dedolomitisation:
  - $CaMg(CO_3)_2 + 2NaOH \rightarrow MG(OH)_2 + CaCO_3 + Na_2CO_3$ (2.3)
- The alkali hydroxide (for instance NaOH) is regenerated:
  - $Na_2CO_3 + Ca(OH)_2 \rightarrow 2NaOH + CaCO_3$ (2.4)

AAR is mainly affected by temperature, humidity, water supply, pH of the pore solution, mineralogy of the aggregates and the composition of the cement paste (Charlwood *et al.*, 2013). AAR may lead to strain and displacement, a network of cracks and a weakening of the concrete's mechanical properties such as strength and Young's modulus. According to Liu *et al.* (2012: 571) expansion due to AAR reduces the splitting tensile strength, the ultimate tensile strength, the bending strength, and the static and dynamic modulus of elasticity of concrete.

In cases where precautions were taken to limit AAR in a concrete structure, certain phenomena may explain the continuation of the reaction (Charlwood, 2011). Alkalis resulting from the recycling process of the alkali-silica gel and the re-supply from certain aggregates may become available in significant quantities later and cause AAR to start very slowly and show as expansion much later. These processes may cause AAR to continue essentially indefinitely even if precautions of using low alkali cements were taken (Charlwood, 2011).

2.2.2. External Sulphate Attack

External sulphate attack (ESA) refers to possibly expansive reactions that involves sulphates that penetrate the concrete from the environment. The expansion associated with the reactions of sulphate ions and constituents of the cement paste is typically caused by the formation of secondary ettringite. It is widely believed that the expansion is plainly caused by the fact that the ettringite occupies a greater volume than the reacting components (Charlwood *et al.*, 2013). Charlwood *et al.* (2013), however, argue that the formation of ettringite does not necessarily lead to an increase in volume, unless the water needed for the reaction comes from outside the system and even this alone is not sufficient to cause severe expansion. The expansion will occur when the formation of ettringite occurs under conditions of super-saturation and in regions where its growth is confined.

2.2.3. Internal Sulphate Reactions

Additional to the formation of ettringite (which forms when sulphates react with hydrated calcium aluminates), another sulphate-driven reaction could lead to the deterioration of concrete, namely the reaction of sulphates with lime to form gypsum (Lea, 1971). Rock in concrete containing iron sulphides can release sulphide ions through the process of oxidisation. In such instances, it is usually iron mono-sulphide (pyrrhotite) and iron disulphide (pyrite) that oxidises to form iron oxide and sulphate ions. Resulting expansion can be due to either the formation of ettringite (under conditions of super-saturation and constraint) or the formation of iron oxides within composite rocks which induces an increase in volume (Charlwood *et al.*, 2013).

2.2.4. Delayed Ettringite Formation

Another internal process involving sulphates known as delayed ettringite formation (DEF) can occur in concrete because of elevated temperatures (>70 - 80°C) during initial hydration. The solubility of ettringite increases with temperature and therefore instead of ettringite forming as a primary hydration product, at very high temperatures, mono-sulphate is formed and higher than normal levels of sulphate are absorbed on the C-S-H phase. Sulphate is released from the C-S-H as the concrete cools down and, in the presence of water, will react with the mono-sulphate to form ettringite which in certain instances may lead to expansion (Charlwood *et al.*, 2013).

2.3. Factors that Influence AAR

2.3.1. Materials

Cements and supplementary cementitious materials

The neutral sulphates Na_2SO_4, K_2SO_4 or the mixed salt $(Na,K)_2SO_4$ are highly soluble and are the main sources of alkalis present in cement. These alkalis will usually produce a pore solution with sufficient alkalinity to initiate and sustain AAR in the presence of reactive aggregates (Oberholster, 2009: 191). During early research between 1940 and 1960, control measures were centred on limiting the alkali content of cement, but more recently the emphasis shifted to rather limiting the alkali content per m^3 of concrete. In South Africa, for instance, the limits for alkali content are expressed in kilograms of Na_2O-eq per m^3 of concrete (Oberholster, 2009: 191; ICOLD, 1991: 25).

The alkalis from the cement that is available for reaction with the aggregates are referred to as active alkalis. In the case of South African CEM I cements, the active alkalis may comprise up to 80% of the total Na_2O-eq of the cement. The use of these active alkali-rich Portland cements with highly reactive aggregates can lead to problems after only a few years. It is thus necessary to explore the use of supplementary cementitious materials (SCMs) such as slag, silica fume, fly ash, and metakaolin to help prevent ASR. A proper understanding of the role of the SCMs is required to be able to predict the precise amount of substitution of Portland cement that is required to reduce the ASR expansion potential (ICOLD, 1991: 27; Oberholster, 2009: 199; Shappex & Scrivener, 2012: 605). The success of the use of SCMs to reduce the effects of AAR, can be attributed to the dilution of the contribution of the cement to the alkali content of the mix. In addition, the pozzolan reactions lower the calcium to silicon ratio in the C-S-H phases, which increases the capacity of the cement paste to fix alkalis (Charlwood *et al.*, 2013).

Shappex and Scrivener (2012: 606) argue that aluminium rich SCMs, such as fly ash, slagment or metakaolin are more efficient against ASR than pure silica additions such as silica fume - the reasons are still unknown especially considering that the aluminium containing SCMs do not lower the alkalinity of the pore solution as efficiently as silica fume. In the case of dams, the required concrete strength is usually not that high, enabling designers to make large substitutions of cement with the correct SCMs (Charlwood *et al.*, 2013).

Aggregates

Both factors connected with constituent minerals and factors connected with rocks formed by the combinations of minerals, have an influence on the reactivity of aggregates used in a given concrete mix. The International Commission On Large Dams (ICOLD) Bulletin 79 (1991: 23) have identified the following minerals that are most commonly associated with AAR;

- siliceous polyphased minerals;
- silicates such as:
    - amorphous minerals like opal and volcanic glass;
    - cryptocrystalline minerals like chalcedony;
    - crystalline minerals like quartz, feldspar and phyllosilicates.

The reactivity of the minerals is partly governed by the rock mass that they are contained in. There are two major rock-dependent categories, namely structural factors and composition

factors. Grain size plays a big role and generally larger grain sizes are more susceptible to reactivity than very fine-grained rocks - there are exceptions, such as the Malmesbury Group in South Africa, as noted in ICOLD Bulletin 79 (1991: 25). Other structural parameters such as the permeability, the porosity and the specific surface of a rock are also important to determine (ICOLD, 1991: 25).

The mineralogical composition of the rock plays an important role and it involves determining which minerals are present in the rock and their relative concentration. When considering sedimentary rocks, it will be sensible to become acquainted with the type and contents of the cementitious binding materials within the rock matrix. A crystalline or lithographic limestone can become reactive if it contains a siliceous or clay fraction disseminated within the mass (ICOLD, 1991: 25).

In South Africa, several aggregate sources have been identified as potentially alkali reactive and these are summarized in Table 2-1.

Table 2-1: Potentially reactive aggregate sources in South Africa as adapted from Oberholster (2009: 192)

Province	Aggregate source
Western Cape	• Malmesbury Group - hornfels, spotted hornfels, quartz-albite-epidote hornfels, meta-greywacke, quartzite, mylonite, phyllite, sandstone, lava • Cape Granite Suite - very rarely • Cape Super Group - occasionally orthoquartzite of the Table Mountain Group; arkose of the Bokkeveld Group • Quaternary Period - occasionally river gravels
Eastern Cape	• Cape Super Group - occasionally orthoquartzite of the Table Mountain Group • Enon Formation - quartzite pebbles • Quaternary Period - quartzite pebbles
KwaZulu-Natal	• Natal Group - quartzite, sandstone • Karoo Sequence - tillite of the Dwyka Formation
Gauteng and Free State	• Witwatersrand Super Group - quartzite, shale • Dolomite Series - more than 20% chert
Mpumalanga	• Archaean granite and gneiss

2.3.2. Environmental Conditions

Temperature

The normal seasonal movements of an arch dam are usually governed mainly by ambient temperatures. These ambient temperatures also affect the rate of AAR - temperature rises tend to accelerate AAR and according to Oberholster (2009: 192) the rate of expansion can be expected to double for each 10°C increase in the mean annual ambient temperature. Interestingly, the viscosity of the silica gel will decrease with rises in temperature and the gel will be more able to escape into cracks and voids in the concrete (ICOLD, 1991: 55). Saouma & Perotti (2006: 195) demonstrated the temperature dependence of AAR expansion by comparing

a laboratory specimen at 38°C with a dam at the average temperature of 7°C. Figure 2-5 contains the two different expansion curves.

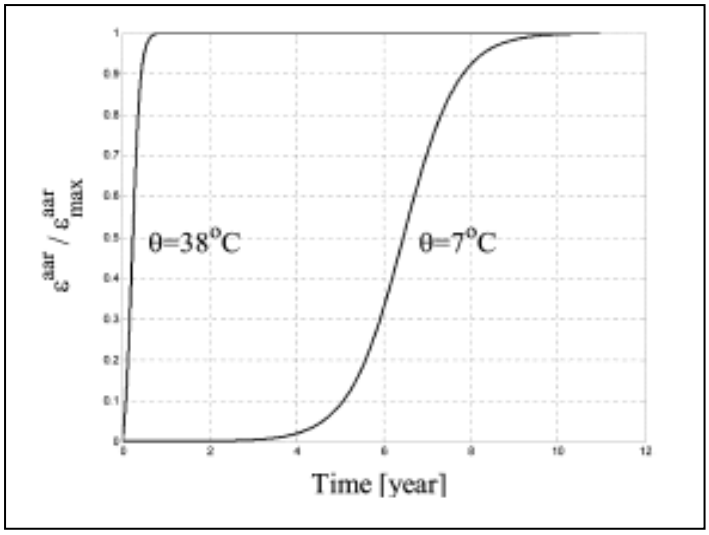

Figure 2-5: Differences in AAR expansion due to temperature (Saouma & Perotti, 2006: 195)

Moisture

The internal relative humidity of concrete is the major driving force of expansion due to AAR. The moisture acts as a transportation medium of alkalis and is also absorbed by the hygroscopic silica gel which leads to the expansion phenomenon. The moisture that is present in the concrete from the mixing water is generally deemed as sufficient to initiate and, to a certain extent, sustain AAR (Martin *et al.*, 2013). The upstream water level in dams will provide additional moisture to sustain AAR for very long periods of time.

The presence or continuation of AAR is unlikely when the relative internal humidity of the concrete is below about 80% (Oberholster, 2009: 192). In the case of dams, the fluctuation of the water level can lead to a worse case of AAR deterioration than a continuous exposure to saturated conditions that would be the case if the dam remained full for long periods of time (ICOLD, 1991: 53). Oberholster (2009: 192) states that fluctuations in temperature and moisture conditions tend to increase the width and number of cracks caused by AAR expansion.

2.3.3. Time

The onset and rate of AAR are governed by many factors as previously highlighted. Swelling of concrete may occur gradually and subside after a certain period or it may occur suddenly at a later stage. Similarly, cracks will appear after variable periods of time (ICOLD, 1991: 27). Oberholster (2009: 210) mentions that in South Africa, the earliest signs of expansion due to AAR have been observed three to four years after construction completion.

Charlwood (2011) argues that the long-term chemical expansion of concrete dams is an issue of increasing concern, especially because in many cases the expansion behaviour shows no signs of slowing down. Charlwood *et al.* (2013) have identified alkali recycling and re-supply as the probable cause of this continuous expansive behaviour.

There is usually a certain period of normal behaviour before swelling starts. There are various reasons for the delay of the onset of swelling, including the fact that there is always an initiation

period. Macroscopic swelling only becomes visible after a certain period as the porous structure of the concrete could absorb much of the initial expanding gel, creep occurs, thermal cooling could occur, and shrinkage occurs at early age.

Larive (1998) proposed a numerical model for the time expansion of concrete based on thermodynamic principles involving τ_L, which is the latency time, and τ_C, which is the characteristic time. The latency time corresponds with the inflection point and the characteristic time is defined in terms of the intersection of the tangent at τ_L with the asymptotic unit value of ξ (see Figure 2-6) (Saouma & Perotti, 2006: 195). Ulm *et al.* (2000) determined expressions for the latency and characteristic times in terms of the absolute temperature and the corresponding activation energies. The activation energy is the minimum energy required to trigger the reaction. Figure 2.6 and equations 2.5 - 2.9 explain the findings of Larive (1998) and Ulm *et al.* (2000).

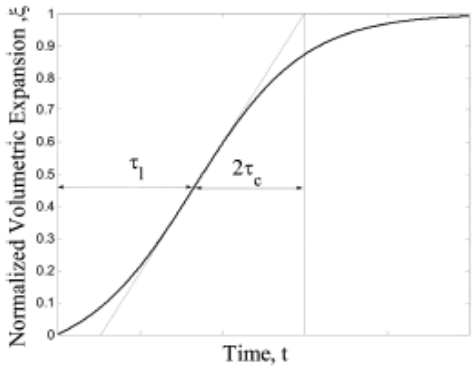

Figure 2-6: Normalized expansion curve with time (Saouma & Perotti, 2006)

$$\xi(t,\theta) = \frac{1 - e^{-\frac{t}{\tau_C(\theta)}}}{1 + e^{\frac{t - \tau_L(\theta, I_\sigma, f'_C)}{\tau_C(\theta)}}} \quad (2.5)$$ (Larive, 1998)

$$\tau_C(\theta) = \tau_C(\theta_0)\exp\left[U_C\left(\frac{1}{\theta} - \frac{1}{\theta_0}\right)\right] \quad (2.6)$$ (Ulm *et al.*, 2000)

$$\tau(\theta, I_\sigma, f'_c) = f(I_\sigma, f'_c)\tau_L(\theta_0)exp\left[U_L\left(\frac{1}{\theta} - \frac{1}{\theta_0}\right)\right] \quad (2.7)$$ (Ulm *et al.*, 2000)

$$U_c = 5400 \pm 500K \quad (2.8)$$ (Larive, 1998)

$$U_L = 9400 \pm 500K \quad (2.9)$$ (Larive, 1998)

Figure 2-7 portrays Charlwood's (2016: 33) interpretation of the typical development of expansion strain with time.

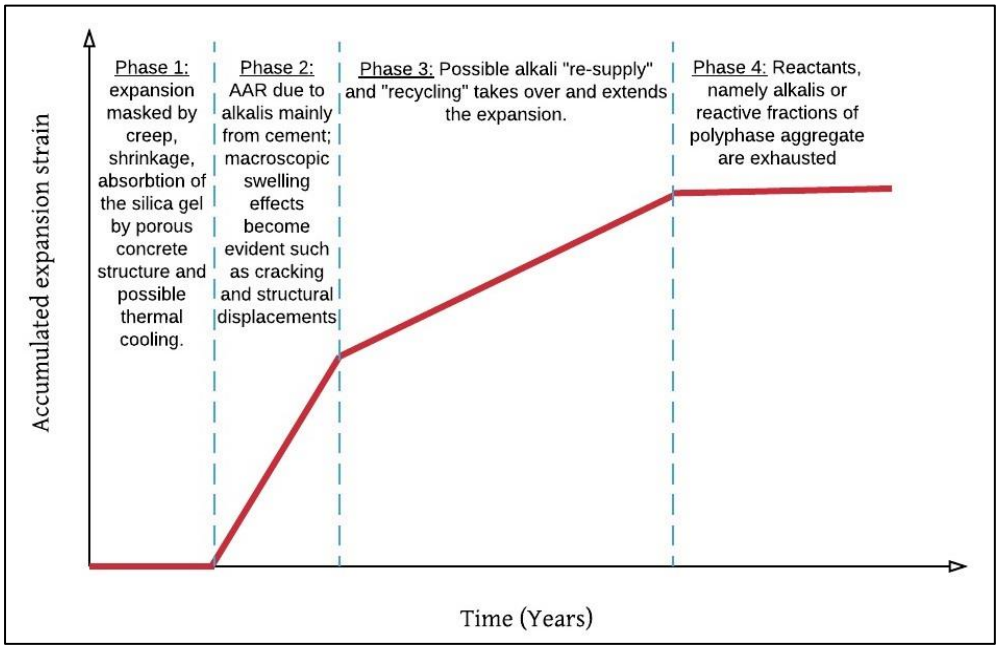

Figure 2-7: Typical accumulated expansion strain trend versus time for concrete dam walls adapted from Charlwood (2016: 33)

2.4. Concrete Arch Dams

2.4.1. Construction

An arch dam relies on sound foundations that can withstand the loads that are transferred to it by the concrete arch structure. During excavation of the foundation, weak areas are removed while avoiding sharp breaks and irregularities - a smooth foundation contact is the desired result. Dental concrete can be used to create a smooth foundation profile, while symmetry of the dam site may be achieved by using additional concrete pads and thrust blocks. In addition to dental concrete, consolidation grouting is performed to fill voids, fracture zones and cracks slightly below the excavated foundation. Consolidation grouting usually precedes any other grouting and is performed from the excavated surface using low pressures (USACE, 1994: 13-5).

A grout curtain's function is to control seepage from the dam basin through the foundation. The grouting is performed at higher pressures than consolidation grouting to reach greater depths. The depth of the grout curtain usually varies between 30 to 70 percent of the upstream hydrostatic head (full supply water level in the dam) (USACE, 1994: 13-7).

An arch dam is constructed as a sequence of monolithic blocks separated by vertical joints. Shear resistance between the monoliths are provided by shear keys for which there are various designs such as vertical shear keys, dimple shear keys and waffle shear keys. These different shear keys are mainly distinguished by their shape. The construction sequence of an arch dam is illustrated in Figure 2-8 and Figure 2-9 (note also the waffle shear keys in Figure 2.9) (USACE, 1994: 13-13 & 13-14).

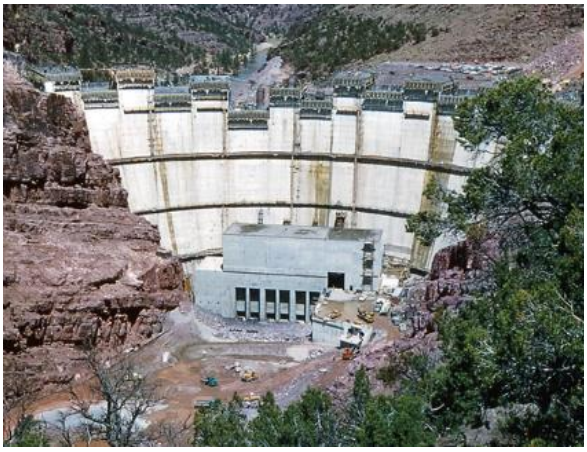

Figure 2-8: The construction of Flaming Gorge Dam in the United States of America (USA) (USBR, 2017)

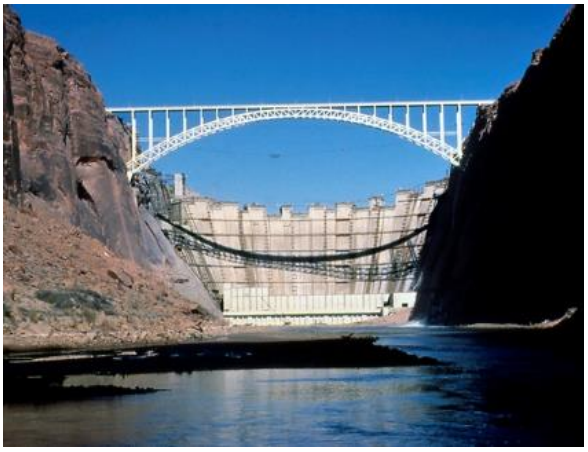

Figure 2-9: The construction of Glen Canyon Dam in the USA (USBR, 2017)

Controlling the heat of hydration of the concrete during construction is very important as a lack of such control may lead to excessive thermal cracking and unfavourable internal stress distributions within the dam wall. There are several ways in which the temperature of the concrete can be controlled during construction such as pre-cooling, post-cooling, reducing the cement content of the concrete, limiting the height of construction lifts and restricting placement to night times, cooler seasons or warmer seasons (depending on the climate of the region) (USACE, 1994: 8-15 to 8-18).

Monolith joint grouting is usually performed after construction has been completed to provide a complete monolithic structure. Grout is injected at high pressures into the vertical joints between the monoliths though a network of embedded pipes (USACE, 1994: 13-17; USBR, 1977: 258). United States Army Corps of Engineers (USACE) (1994: 13-17) proposes that grout lifts be limited to 18 metres to ensure proper filling of the joints and to prevent excessive pressure on the seals and concrete blocks. Shaw (2015: 28-29) argues that performing joint grouting at an appropriate temperature, also referred to as the closure temperature, may limit the development of large stresses during future temperature drops.

2.4.2. General Arch Function

It is important to develop a clear understanding of the normal or intended structural function of concrete arch dams to easily distinguish when there are deviations in its behaviour that may jeopardise the safety of the structure. Arch dams are designed to carry static and dynamic loads in three-dimensions (3D) into the abutments and foundations in a smooth manner. This is achieved by shaping the arch to find the optimal geometry that would require the least amount of concrete while ensuring that the structure would only experience compressive stresses as far as possible. The loads in an arch dam are transferred to the abutments by shear forces on the horizontal planes between arch units and by thrust on the vertical planes between the cantilever units (Shaw, 2015: 324; USBR, 1977:1). These forces translate to hoop stresses in the horizontal plane and cantilever stresses in the vertical plane. The resulting principal compressive stresses are illustrated in Figure 2-10 and Figure 2-11. Typical deflection patterns of an arch dam are shown in Figure 2-12 and Figure 2-12.

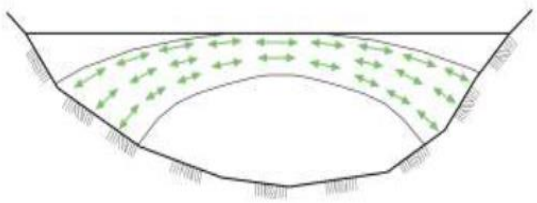

Figure 2-10: The typical principal compression stress vectors on a developed arch elevation (Shaw, 2015: 324)

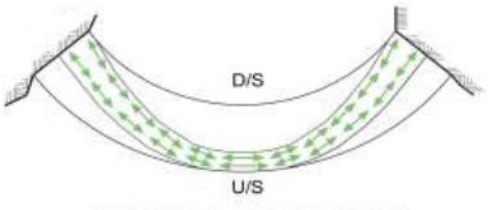

Figure 2-11: The typical principal compression stress vectors on a horizontal arch section (Shaw, 2015: 324)

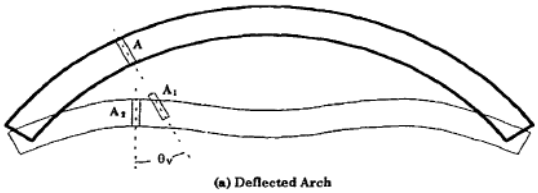

Figure 2-12: Typical deflected arch unit (Ghanaat, 1993: 2-4)

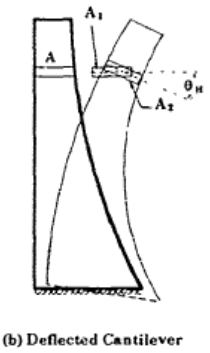

Figure 2-13: Typical deflected cantilever unit (Ghanaat, 1993: 2-4)

The different static and dynamic loads that act on arch dams are summarized in Table 2-2. Some of the static loads follow a cyclic pattern, such as the hydrostatic load, uplift load, and pore pressure which varies with the water level. Temperature loads are cyclic due to the ambient climate which varies with the seasons.

Table 2-2: Different static and dynamic loads that act on arch dams as adapted from Vezi (2014: 6-10), Kroon (1984: 5-1 to 5-8) and Prins (2014: 154)

Type of load		Description
Static & Cyclic static	Gravity loading	This load constitutes the self-weight of the concrete and the weight of appurtenances such as gates and bridges
	Hydrostatic loading (cyclic)	The linearly distributed water pressure acting on the wetted upstream surface of the dam wall; increases linearly with depth
	Temperature loading (cyclic)	Variations in temperature result in thermal stresses especially as the foundation rock does not permit the associated volumetric changes
	Silt loading	Similar to hydrostatic load; the density of the silt dictates the magnitude; increases linearly with depth
	Uplift loading (cyclic)	Joints, interstitial spaces and cracks in the foundation and concrete cause uplift pressures as water enters them
	Pore pressure (cyclic)	Water pressures under the phreatic surface in the pores present in the foundation rock
Dynamic	Earthquake loading	Earthquakes cause acceleration of the earth crust leading to intensified water and silt loads

	Ambient loading	Caused by waves, wind, traffic, machinery and other atmospheric phenomena
	Other	Impacts such as explosions, lightning and collisions. Landslides resulting in direct impact or wave action in the basin

Site selection is an important aspect when designing an arch dam. According to Shaw (2015: 323) sites are often classified as U-shaped, narrow V-shaped, wide V-shaped, composite U-V-shaped or just wide. The canyon shape factor (K) represents the total developed length of the foundation surface / maximum dam height and is an important factor to consider during the design. A site that would promote an arch dam wall that relies mainly on arch effects as opposed to cantilever effects, is desirable - which will in most cases be a V-shaped valley with a low canyon shape factor. Such valleys are perfectly suited for thin-sectioned double-curvature arch dams. The wider the valley becomes (K-values exceeding 5) the more the arch structure will rely on cantilever action resulting in much thicker-sectioned structures (Shaw, 2015: 324).

2.4.3. Different Types of Arch Dams

Arch dams are designed to best fit the valley geometry and distribute the forces into the abutments. The condition and orientation of the foundation rock plays a big role in the choice of arch dam for a specific site. Table 2-3 summarizes the different types of pure arch dams.

Table 2-3: The different types of arch dams according to its thickness as adapted from Shaw (2015: 323)

Type of arch dam	Classification
Thick arch dam	Base width/height ratio > 0.3
Medium-thick arch dam	0.2 ≤ Base width/height ratio ≤ 0.3
Thin arch dam	Base width/height ratio < 0.2

Arch-gravity dam walls may be best suited for wider valleys and where more sliding resistance is required due to the condition of the foundation rock. These structures rely on a combination of arch action and cantilever action (Shaw, 2015: 323-324).

2.5. Concrete Arch Dams Experiencing Expansion due to Chemical Reaction

2.5.1. Surveillance of Arch Dams

The dam safety surveillance of arch dams includes manual and automated monitoring systems that gather information on the load response of the dam. Regular monitoring of the dam's behaviour along with its foundations and any appurtenant structures plays a big role in helping to guarantee the long-term safety of the structure. The instrumentation used as part of the monitoring system should be selected on the principle of answering a specific question - if there is no question, there should be nothing to measure. Visual inspections and proper analysis and evaluation of the monitoring results also form part of dam safety surveillance (Oosthuizen, 2015). Table 2-4 summarizes the typical instrumentation that may be used to monitor arch dams.

Table 2-4: Typical instrumentation used for measuring an arch dam's load response as adapted from Oosthuizen (2015)

Parameter	Instrument
Foundation deformation	Pendulums, extensometers, trivec installations, inclinometers
Arch dam deformation	Crack width gauges, pendulums, geodetic surveys, trivec installations
Seepage and leakage	Pipes (jug measurements) or weirs (such as a V-notch weir)
Pore water pressure	Piezometers (vibrating wire, pneumatic, hydraulic, electrical resistance etc.)
Stress and strain	Strain rosettes, stress cells
Temperature	Thermometers, thermistors
Pressure	Pressure gauges (vibrating wire or piezo-electric)

ICOLD Bulletin 138 (2009: 33) describes the monitoring of the behaviour of a dam as an activity that involves periodical analysis of inspection results, monitoring data, special studies and maintenance records. This bulletin also proposes that a properly qualified engineer conducts the analysis of the monitoring results so as to appraise the observed behaviour of the dam compared to its expected behaviour. In many cases, unusual behavioural patterns caused by expansion can be detected before they become visible to the naked eye (Amberg, 2011).

2.5.2. Expansion Phenomena in Arch Dams

Arch dams respond to expansion in a unique way when compared to other types of concrete dams. Essentially, the overall volume change caused by AAR will influence the stress distribution and deformation of the dam. Expansion phenomena in arch dams have been confirmed by various case studies around the world that are either picked up by monitoring systems or are clearly visible during inspections. Amberg (2011) mentions that the most common phenomena include permanent rises in crest elevations, permanent upstream displacements and cracks in the galleries due to non-uniform expansion in the dam wall body which can, in some cases, be attributed to the higher temperatures at the surface of the concrete that increases expansion rates. Charlwood and Sims (2013: 3) mention additional phenomena such as separation or slips on horizontal construction lift joints and excessive leakage and seepage through joints. Peripheral cracks along the abutments and foundations of an arch dam on the downstream face are also typical indicators of expansion and are mainly caused by tensile stresses that develop due to permanent upstream displacements (Amberg, 2011; Charlwood & Sims, 2013: 4). Figure 2-14 and Figure 2-15 are good examples of horizontal joint separation and peripheral cracks near an abutment.

Figure 2-14: Typical separation of a horizontal construction lift joint at Poortjieskloof Dam in South Africa

Figure 2-15: Typical peripheral cracks at Poortjieskloof Dam in South Africa

When loads cannot be supported in certain directions due to significant structural discontinuities, local problems in the form of structural cracks and even rupture of the concrete may occur. These structural discontinuities include spillway openings, abutment blocks and sudden changes in elevation and geometry (Amberg, 2011; Charlwood & Sims, 2013: 3-4).

2.5.3. The Role of Creep

Creep is a characteristic of concrete which allows it to absorb some of the swelling effect (Giorla *et al.*, 2014: 197). Creep is the time-dependent increase of strain of a solid body under constant or controlled stress or a relaxation of stress under constant strain (Addis, 1998: 41) (see Figure 2-16 and Figure 2-17).

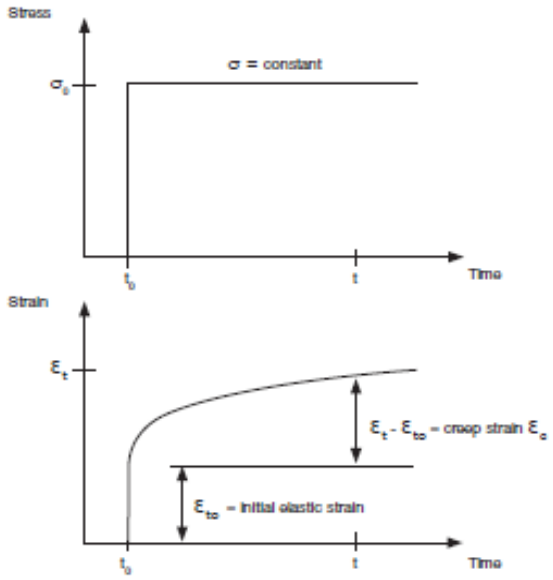

Figure 2-16: Time-dependent increase in strain under constant stress (Alexander & Beushausen, 2009: 119)

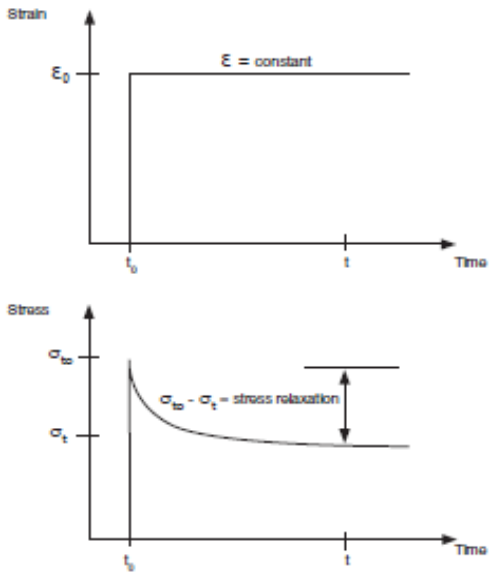

Figure 2-17: Time-dependent decrease in stress under constant strain (Alexander & Beushausen, 2009: 119)

In terms of swelling in arch dams, creep has mostly beneficial effects. Since expansion is a slow loading condition, creep plays an important role structurally in that the ductility provided increases the ability of the concrete to absorb some of the swelling effect (Amberg, 2011).

2.6. Case Studies

2.6.1. Cahora Bassa Dam (Mozambique)

Cahora Bassa Dam is a 170 m high double-curvature arch dam located in the Zambezi River in Mozambique. The dam was completed in 1976 and relatively soon after its completion, in the early 1980s, signs of AAR expansion were picked up by the extensive monitoring system present at the dam. The monitoring system at the dam is especially useful as it provides sufficient redundancy for most of the responses of the dam, e.g strains in the concrete are measured by precision levelling, rod extensometers, deformeters, Carlson strain gauges and convergence meters (Hattingh *et al.*, 2014: 498-499).

Figure 2-18: Cahora Bassa Dam (Carvalho *et al.*, 2016: 6-87)

Figure 2-19: Close-up view of Cahora Bassa Dam from the downstream side (Botha *et al.*, 2016: 2a-210)

Hattingh *et al.* (2014: 507) conclude that strain results from different monitoring systems provide comprehensive evidence of the expansion that the dam wall is experiencing due to AAR. Strain rates of the different systems correlate extremely well, and the results do not indicate any decrease in the rate of the AAR.

The expansion in the dam wall contributed to the need for rehabilitation of the radial gates. The lateral function gap between the gate leaf and the fixed sealing parts had decreased and Boulat *et al.* (2015) ascribed this to the permanent deformations that were observed in the concrete.

Cahora Bassa Dam is an interesting case study as much research and analyses have been performed on the effects of the expansion on the structure. Hattingh *et al.* (2014: 498) states that it is important to interpret monitoring results to fully understand the effects of confinement, the extent of expansion in different directions, and the effect of expansion of concrete around galleries.

2.6.2. Kouga Dam (South Africa)

Kouga Dam is a double-curvature thin arch dam which was completed in 1969. It was the first of its kind constructed in South Africa and the design and construction was done by the South African National Department of Water and Sanitation. Extensive contact, consolidation and curtain grouting of the foundation was done during construction.

Figure 2-20: Kouga Dam as viewed from the downstream side (Mahlabela & Oosthuizen, 2012: 233)

Figure 2-21: Kouga Dam as viewed from the right flank (Hattingh, 2011)

During the first three years after its construction, the dam behaved in a normal manner. Measurements of strain rates started in 1972 and in 1976 the first pronounced signs of expansion due to AAR were observed (Mahlabela & Oosthuizen, 2012: 233; Elges *et al.*, 1995: 3). Elges *et al.* (1995: 3) further mentioned a continuous swelling trend that was picked up by geodetic surveys and strain measurements since 1976, especially rising crest levels of the spillway ranging between 25 mm and 45 mm. Furthermore Hattingh (2011) reported that the vertical expansion stopped in 2000, but that the horizontal expansion has continued and that maximum horizontal displacements are evident at the quarter points of the arch with the right flank showing more permanent displacements than the left flank.

In 2006 the trivec measurements provided evidence of a deep-seated foundation movement in the right flank foundation. In 2010, ambient vibration measurements picked up on unusual natural frequency modes, the cause of which was suspected to be the right flank blocks not being in direct contact with each other during low water levels. The 3D crack width measurement results also confirmed the independent movement of the upper parts of the arch (Mahlabela & Oosthuizen, 2012: 233).

All the previously-mentioned phenomena, including the AAR problem, led to a decision to initiate the rehabilitation of the dam wall. Mainly, the rehabilitation would focus on restoring the structural integrity of the upper parts of the arch whilst also improving the force distribution to the abutments of the dam (Mahlabela & Oosthuizen, 2012: 233).

3. Methodology

3.1. Introduction

The South African National Department of Water and Sanitation is responsible for installing instrumentation that measures the structural behavioural patterns of major dams in the country. Such instrumentation includes geodetic survey measuring points, trivec installations, crack width gauges, stress measuring cells and piezometers. For the purpose of this study, instrumentation data for three separate dams were collected and analysed.

3.2. Systematic Approach

A systematic approach was followed for each of the case studies. First, a visual inspection was conducted in order to identify distinct deterioration of ASR related swelling in the concrete. Good quality photographs are important to document the findings. Subsequent to the visual inspections, in-depth studies of the instrumentation results for each dam were conducted. A brief description of the different techniques and instruments that are used during the monitoring of these dams is included below.

3.2.1. Visual Inspections

The Regulations Regarding the Safety of Dams (NWA, No. 36 of 1998. Reg 139, 2012) prescribe certain procedures for the design, construction, maintenance and operation of dams. Visual inspections are included among these procedures and form an integral part of evaluating the safety of an existing dam wall structure. Van Den Berg (2008: 8-9) argues that it is important to identify any visual signs of distress or disorder on or around the structure. Often, visual inspections reveal structural defects or signs of changes in behavioural patterns of a structure that would not otherwise have been detected.

Visual inspections play an important role in the detection and monitoring of AAR-related swelling trends in arch dams. For the purpose of this study, thorough visual inspections were carried out.

3.2.2. Geodetic Surveys

According to Pretorius (2008: 30) a geodetic survey system comprises a triangulation network consisting of reference beacons and targets. It involves the precise levelling from fixed benchmarks in the surrounding area of the structure to determine the absolute displacements of certain points/targets located on and inside the structure. The target intersection method is used to determine the positions of points on the exterior of the structure while the precise traverse method is used to determine the positions of points within the galleries of a dam wall. The Department of Water and Sanitation (DWS) carries out geodetic surveys twice a year, once during the summer and once during the winter, and the raw data is then adjusted, and final three-dimensional displacements of the targets are generated.

For the purpose of this study, geodetic survey results as generated by the DWS were used to investigate the deformation trends of the arch dams.

3.2.3. Three-Dimensional Crack Width Gauges

3-D crack gauges have the distinct advantage of being able to measure changes in crack widths (translations) in 3 directions (x, y and z) and, in the case of certain gauges, relative rotations (tilt) across specific cracks or joints in concrete.

Vinchon 3-D crack gauges which are of French origin, were installed in South African dams mostly during the 1970s and early 1980s. In many instances, these gauges were replaced by *Sinco* 3-D crack gauges during the latter 1980s due to inconsistencies and inaccuracies with the readings. Problems were also experienced with the *Sinco* gauges due to galvanic corrosion producing false trends (Oosthuizen *et al.*, 2003: 600).

In-house 3-D crack gauges were developed by the then Department of Water Affairs and Forestry (DWAF) in the early 1990's and were installed at dams throughout the country. Electronic digital indicator gauges, similar to those used for *Sinco* gauges, are used to take readings manually. The relative accuracy of the different crack gauges is shown in Table 3-1. Figure 3-1 shows a typical DWAF2001 3-D crack gauge.

Table 3-1: Relative accuracies of different crack gauges used in South Africa as adapted from Oosthuizen *et al.* (2003: 604)

Type of Gauge or readout unit	3-D Parameter					
	X (mm)	Y (mm)	Z (mm)	θ_x (deg)	θ_y (deg)	θ_z (deg)
Vinchon	0.03	0.03	0.03			
Sinco	0.02	0.02	0.02			
DWAF94/96/2000	0.02	0.02	0.02			
DWAF98	0.05	0.05	0.05			
DWAF95	0.02	0.02	0.02	0.03	0.03	0.03
DWAF2001	0.02	0.02	0.02	0.03	0.03	0.03

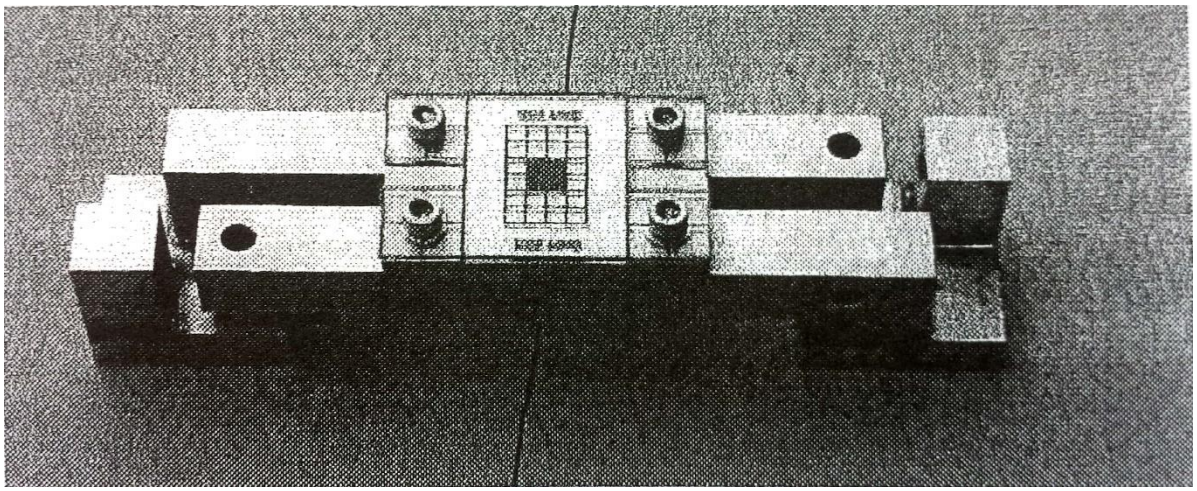

Figure 3-1: A typical DWAF2001 3-D crack-width-tilt gauge with assembly unit (Dorfling, 2008: 45)

For the purpose of this study, selected crack gauge results obtained from the DWS are considered and discussed.

3.2.4. Trivec Installations

A Trivec installation is a high-precision measuring set to determine the spatial displacement components x, y and z in a vertical borehole. The z component is identical with the borehole axis. The other two components x and y lie in two mutually perpendicular planes, the intersection of which is also the borehole axis. Un-plasticized polyvinyl chloride (uPVC) measuring tubes which

are connected with stainless steel measuring couplings at 1 m intervals are inserted in the borehole. The measuring marks are firmly bonded to the surrounding medium by injecting a suitable mortar. After the mortar has set, a zero measurement is performed by bracing the Trivec probe in the measuring tube and measuring the zero values of components x, y and z at the various measuring points. From subsequent measurements, the relative changes x, y and z are determined with respect to the zero measurement. By summation of these differences the spatial displacements along the borehole(s) are obtained. Figure 3-2 shows the typical equipment used for the system.

Figure 3-2: The typical components of the Trivec system used in South Africa (Naude, 2002: 4)

3.2.5. In Situ Stress Measurements

There are several ways of monitoring the stress situation (whether an area is experiencing compressive or tensile stresses and in which directions) at a certain point in a structure. These include in situ, real-time stress measurements which are achieved by the over-coring method using the Commonwealth Scientific and Industrial Research Organisation (CSIRO) Hollow Inclusion (HI) stress measurement cells. These cells are very sensitive to temperature changes and they may exhibit results that imply a radial biaxial compression due to moisture absorption of the epoxy (Oosthuizen *et al.* 2003: 64). Figure 3-3 shows the typical procedure followed during the over-coring method.

In situ stress measuring cells that measure the stress over time can also be installed and these will provide information on how the stress situation changes over time.

For the purpose of this study, in situ stress measurement results for tests that were conducted on the Hartebeeskuil Dam (over-coring), were considered and are discussed further in the following chapter.

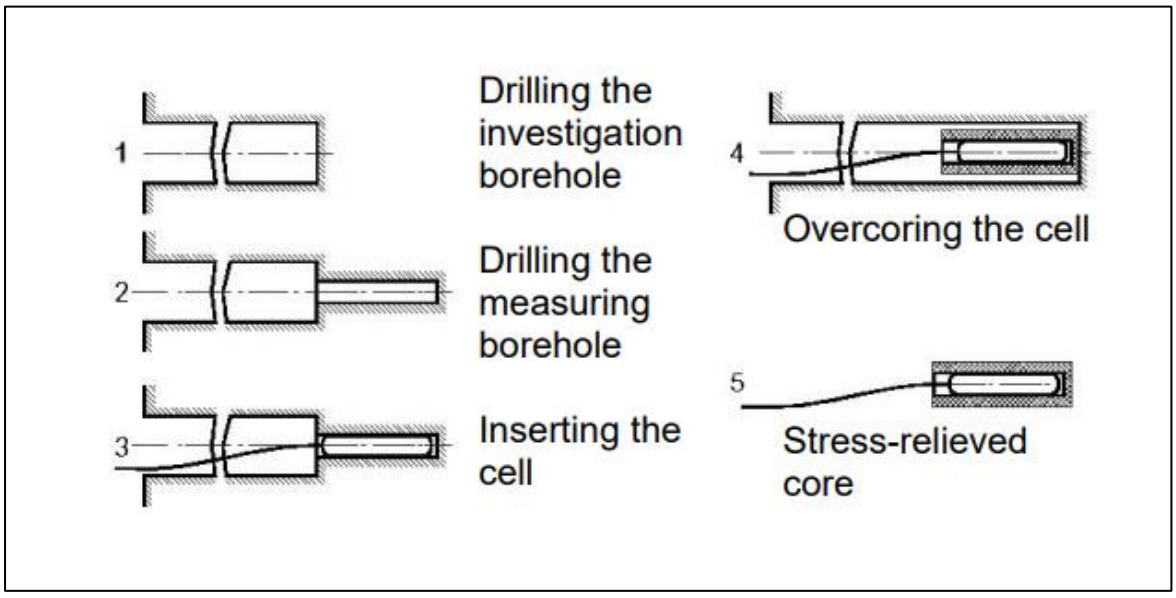

Figure 3-3: The over-coring method for in situ stress measurement (Geotechnisches Ingenieurbüro, 2004)

4. Hartebeeskuil Dam

4.1. Introduction

The Hartebeeskuil Dam is situated in the Hartenbos River 16 km north west of Mossel Bay and 10 km west of Hartenbos in the Western Cape. The dam was designed and constructed between 1965 and 1969 by the DWS, the current owner and operator of the dam. The dam wall is a cylindrical arch structure with a maximum wall height of 27 m, a crest length of 82 m and a constant radius of 35 m. The wall thickness varies from 1.5 m at spillway level to 2.7 m just above the foundation (Van Den Berg, 1994). The dam has been classified as a Category III dam in terms of Government Notice R.139, as published in Government Gazette No. 15062 of 24 February 2012.

Hartebeeskuil Dam

Figure 4-1: Hartebeeskuil Dam as viewed from the downstream side

Structure type:	Cylindrical arch
Age of dam:	48 years
Wall height:	27 m
Climate region:	Mediterranean maritime climate; Average maximum temperature of 22°C; Average minimum temperature of 14°C; Average annual precipitation of 440 mm (based on 8 years' weather data provided by SA Weather Services).
Structure orientation:	The downstream face of the dam wall faces east (this implies that the downstream face is generally exposed to direct sunlight in the morning whilst the upstream face is generally exposed to direct sunlight in the afternoon)
Construction materials:	Limited information available. Conventional mass concrete was used and Van Den Berg (1994) reports that the sand and coarse aggregate used in the concrete mix design was of quarzitic origin. A water: cement ratio of 0.5 was specified.

Hartebeeskuil Dam is situated in an area which has a Meditarranean maritime climate. A Mediterranean maritime climate is distinguished by warm, wet winters under prevailing westerly winds and calm, hot and dry summers. The average annual rainfall ranges from 300 to 500 mm.

First mention of possible AAR was made by Van den Berg (1994), specifically the presence of a set of fine cracks just above and parallel to the "pulvino" or cushion line. Van Den Berg (1994) also mentions that the aggregate used in the construction of the dam is of quarzitic origin and thus alkali reactive to a degree and recommended that the dam be monitored to record the long-term effects of the AAR.

Goldie (2002) also makes mention of the cracking pattern and calcite staining on the downstream face of the dam wall that was reported by Van den Berg (1994). Goldie (2002) further argues that AAR occurs primarily on the upstream face of the structure, an assumption which is supported by the un-cracked appearance of the upstream face and in situ stress measurements which were conducted in 1999. The swelling of the upstream portion of the arch structure has resulted in tensile stresses on the downstream face, an assumption which is supported by the presence of cracks and the in-situ stress measurements.

Beukes (2008) confirms similar observations than Goldie (2002). Prins (2013) confirmed the crack patterns that suggest the swelling of the concrete due to AAR. Prins (2013) further mentioned that the effective arch thickness has possibly been reduced due to the AAR. Cracks on the upstream face of the right flank were reported by Prins (2013).

No documented evidence could be found of a clear diagnosis of AAR at Hartebeeskuil Dam. However, during 1999, a major grouting operation was conducted at the dam and several cores were drilled and inspected. No formal documentation of the core sample inspections could be found, but clearly these convinced the DWS to earmark this dam as being affected by AAR (based on discussions with the late Dr Chris Oosthuizen who was a Senior Specialist Engineer in the DWS).

4.2. Visual Inspection

A visual inspection was carried out on the 30th of July 2016. The objective was to look for typical evidence of AAR in the concrete.

4.2.1. Right Flank

The upstream face of the right flank mostly displayed horizontally orientated cracks (see Figure 4-2 and Figure 4-3).

Figure 4-2: Hartebeeskuil Dam: The upstream concrete face of the right flank displaying horizontal cracks

Figure 4-3: Hartebeeskuil Dam: The upstream concrete face viewed towards the inlet tower

The crest of the right flank displayed one significant tangential crack that spans across two adjacent blocks (Blocks 7 and 8) and a few smaller cracks with both tangential and radial

orientations (see Figure 4-4 and Figure 4-5). The smaller cracks are possibly only shrinkage cracks due to the small crack widths and random orientation. A core sample of the significant tangential crack was drilled in 1999 and it revealed that the crack was only approximately 0.4 m deep.

Figure 4-4: Hartebeeskuil Dam: A major tangential crack on the right flank crest

Figure 4-5: Hartebeeskuil Dam: An indication of the crack width and previous core drill hole that determined the depth of the crack

There are steps on the far-right flank that provide access to a survey beacon on the right abutment. These steps showed signs of possible AAR-related cracking. This was especially evident from the crack width, crack orientation and staining around the cracks (see Figure 4-6 and Figure 4-7).

Figure 4-6: Hartebeeskuil Dam: AAR cracking pattern on the far-right abutment steps

Figure 4-7: Hartebeeskuil Dam: Crack width and typical ASR crack staining

The right flank downstream face displayed peripheral cracks that are orientated approximately parallel to the abutments (see Figure 4-8 to Figure 4-11). These peripheral cracks give evidence of a principal stress distribution that is not ideal for an arch dam which is similar to that typically caused by AAR-related swelling.

Figure 4-8: Hartebeeskuil Dam: Typical parallel peripheral cracks in the vicinity of the right flank "pulvino"

Figure 4-9: Hartebeeskuil Dam: Parallel cracks evident on the right flank downstream face

Figure 4-10: Hartebeeskuil Dam: Close-up view of one of the peripheral cracks on the right flank downstream face

Figure 4-11: Hartebeeskuil Dam: Parallel cracks in the vicinity of the "pulvino"

4.2.2. Spillway Section

The upstream face of the spillway could not be inspected due to restricted access and the fairly high water level. The crest of the spillway displayed one significant tangential crack.

Figure 4-12: Hartebeeskuil Dam: Tangential crack between two radial cracks on the spillway crest

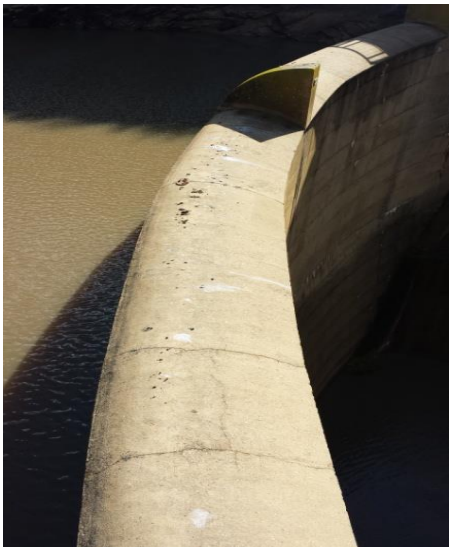

Figure 4-13: Hartebeeskuil Dam: General view of the spillway crest

The spillway downstream face was generally in a good condition. No prominent cracking patterns were visible. One horizontal lift joint (the lift joint where the vertical profile of the concrete above and the slightly sloped concrete below, meet) displayed evidence of calcite staining which is indicative of an open joint (see Figure 4-14).

Figure 4-14: Hartebeeskuil Dam: Calcite staining visible on the downstream face of the spillway section

4.2.3. Left Flank

The left flank upstream face and non-overspill crest (NOC) could not be accessed. The left flank downstream face displayed more of the same cracks as were evident on the right flank downstream face though slightly less prominent (see Figure 4-15 to Figure 4-17).

Figure 4-15: Hartebeeskuil Dam: Spillway and left flank downstream face

Figure 4-16: Hartebeeskuil Dam: Close-up view of left flank downstream face

Figure 4-17: Hartebeeskuil Dam: Typical peripheral cracks on the left flank

4.3. Geodetic Survey Results

Geodetic surveys are valuable in terms of monitoring the behavioural patterns of a dam wall. Any permanent displacements or unusual behavioural patterns can be easily picked up due to the accuracy of the system (Pretorius, 2008). The first geodetic survey of Hartebeeskuil Dam was conducted by the DWS in 1995. There are 10 survey targets on the crest of the dam (Figure 4-18 provides the layout of the targets). A geodetic survey was performed twice a year - once in the summer and once in the winter. Data up until July 2015 was available for this study. "T" is short for "Target".

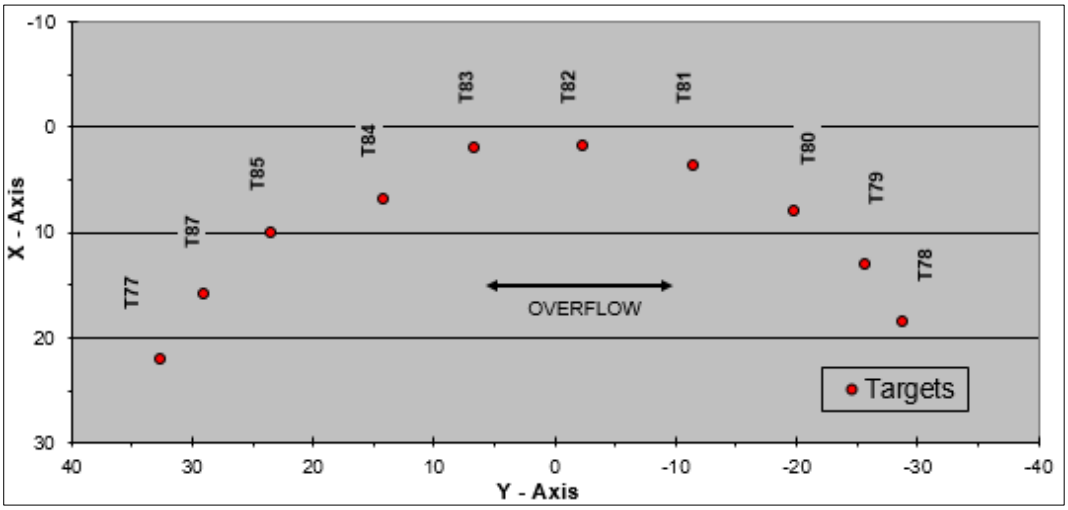

Figure 4-18: Plan layout of the crest geodetic survey targets at Hartebeeskuil Dam

4.3.1. Tangential Movements

The tangential movements are movements toward or away from the flanks. Figure 4-19 to Figure 4-24 provide the tangential movements for all the targets since 1995 and positive values indicate movement toward the right flank.

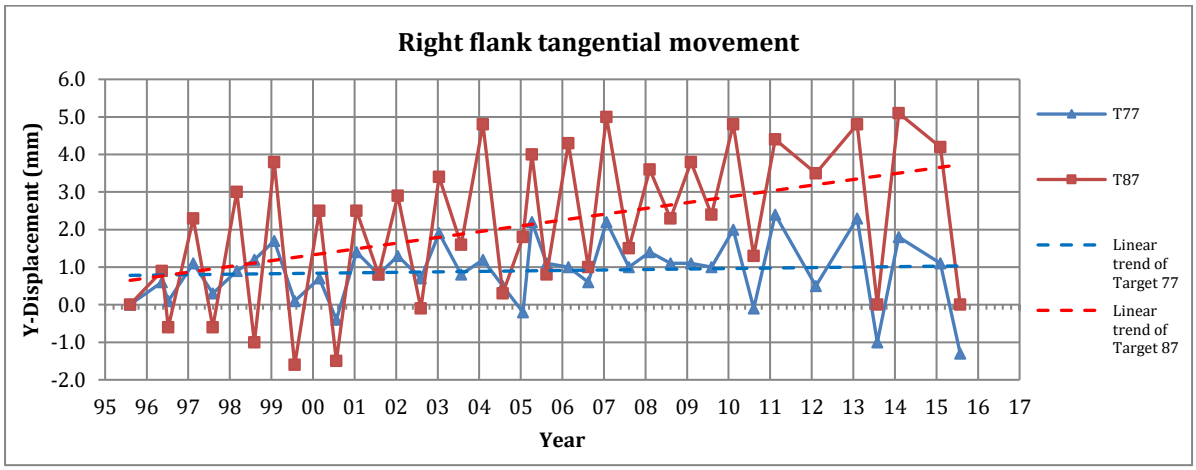

Figure 4-19: Tangential movements of T77 and T87 at Hartebeeskuil Dam

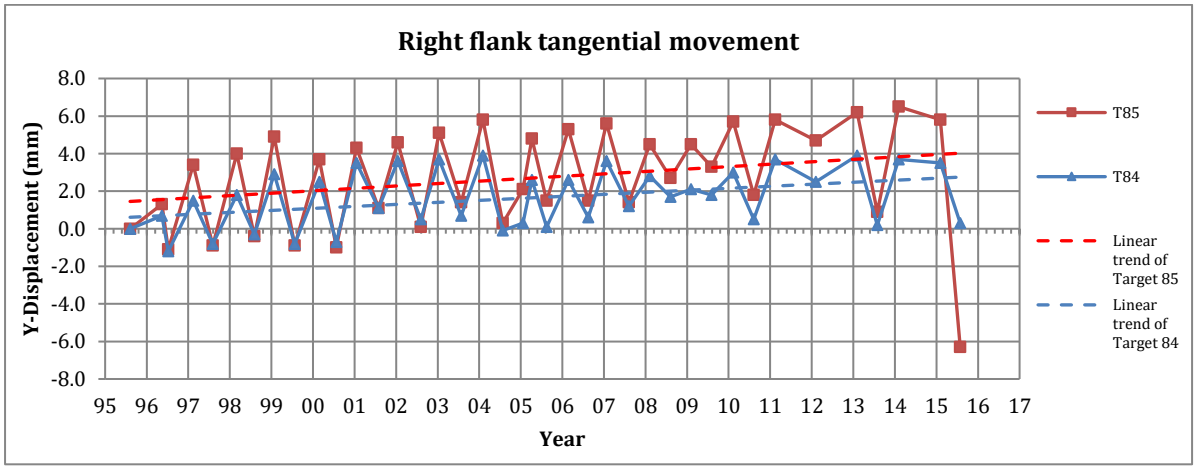

Figure 4-20: Tangential movements of T85 and T84 at Hartebeeskuil Dam

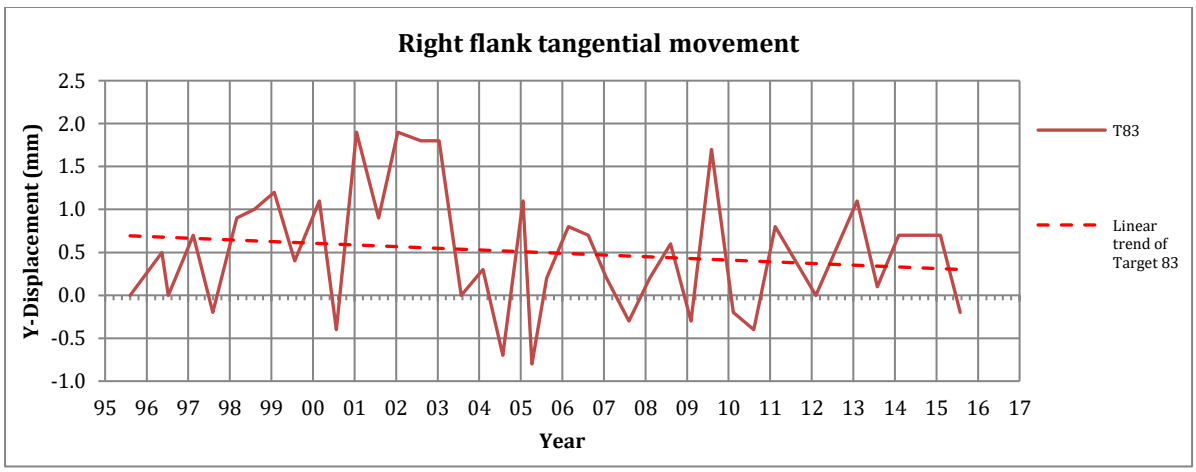

Figure 4-21: Tangential movements of T83 at Hartebeeskuil Dam

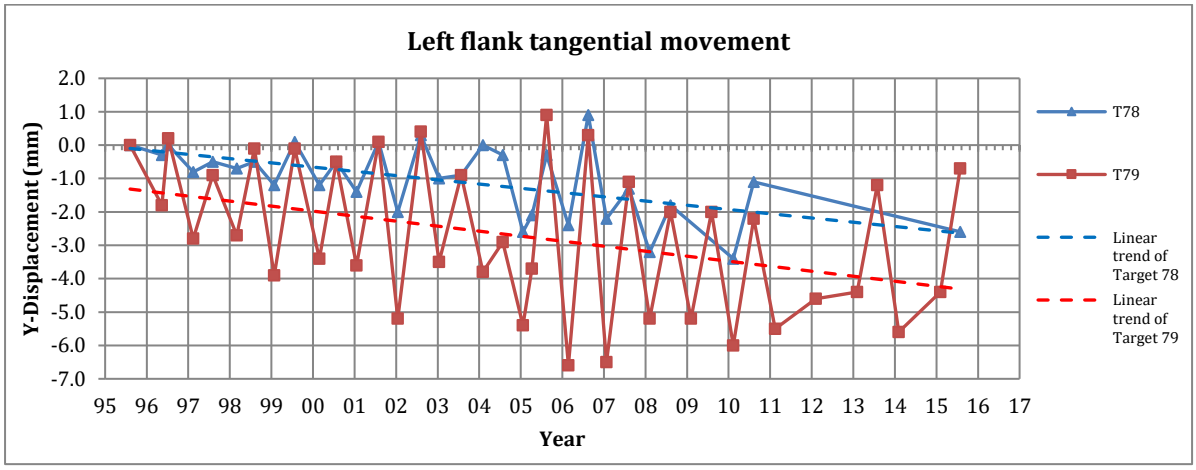

Figure 4-22: Tangential movements of T78 and T79 at Hartebeeskuil Dam

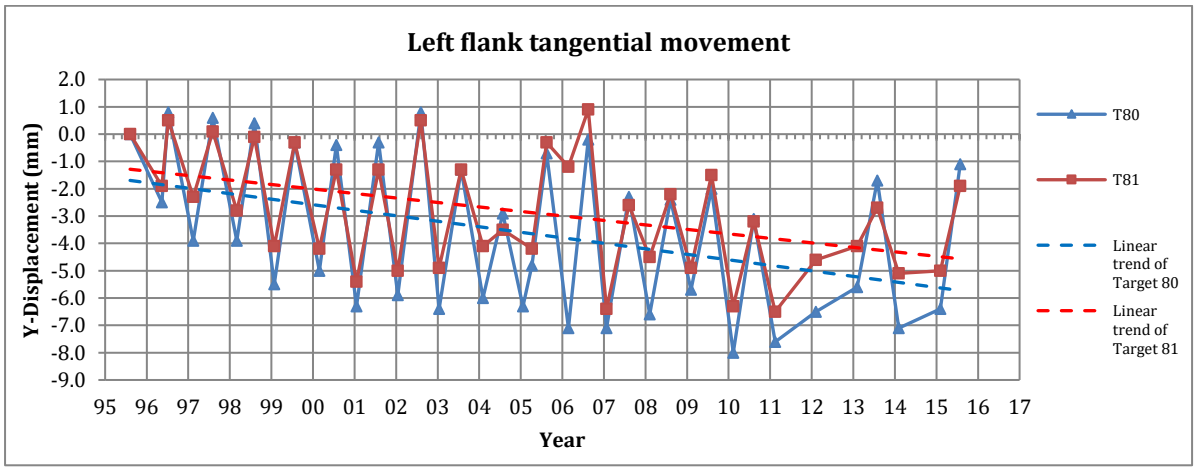

Figure 4-23: Tangential movements of T80 and T81 at Hartebeeskuil Dam

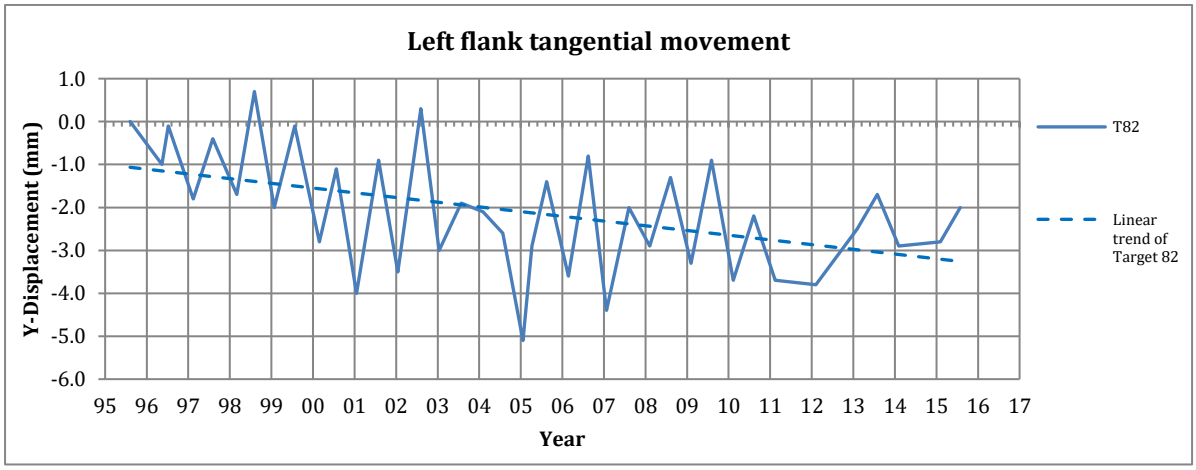

Figure 4-24: Tangential movements of T82 at Hartebeeskuil Dam

The far-right flank (T77) shows small permanent trends of approximately 1 mm towards the right abutment (see Figure 4-19). The middle-right flank (T84, T85 and T87) shows more significant permanent trends of approximately 3 mm towards the right abutment (see Figure 4-19 and Figure 4-20). The spillway crest (T82 and T83) show permanent trends of approximately 1-2.5 mm towards the left abutment. The far-left flank (T78) shows permanent trends of approximately 2.5 mm towards the left abutment. The middle-left flank (T79, T80 and T81) shows more significant permanent trends of approximately 3-4 mm towards the left

abutment. In summary, these results prove that there is a permanent swelling action toward both abutments, with the middle-third of each flank showing the biggest permanent trends.

4.3.2. Radial Movements

The radial movements are movements that are measured in an upstream and downstream direction. Figure 4-25 to Figure 4-30 provide the radial movements for all the targets since 1995 and positive values indicate movement in a downstream direction.

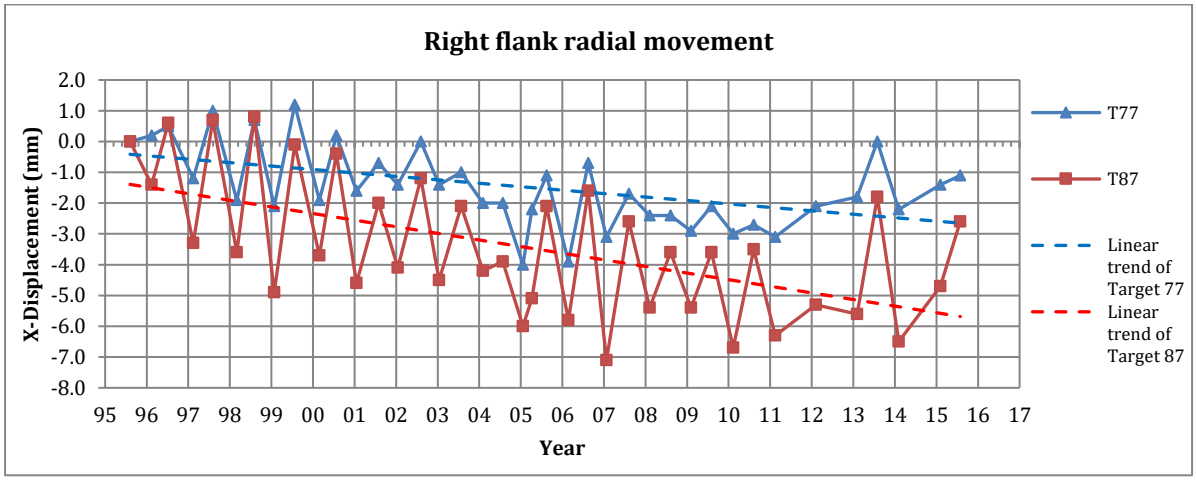

Figure 4-25: Radial movements of T77 and T87 at Hartebeeskuil Dam

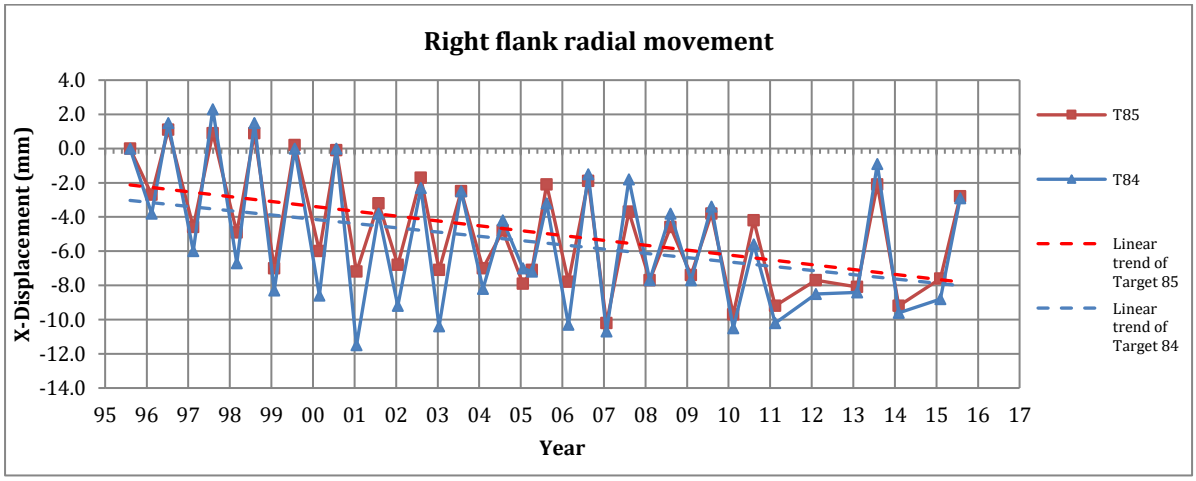

Figure 4-26: Radial movements of T85 and T84 at Hartebeeskuil Dam

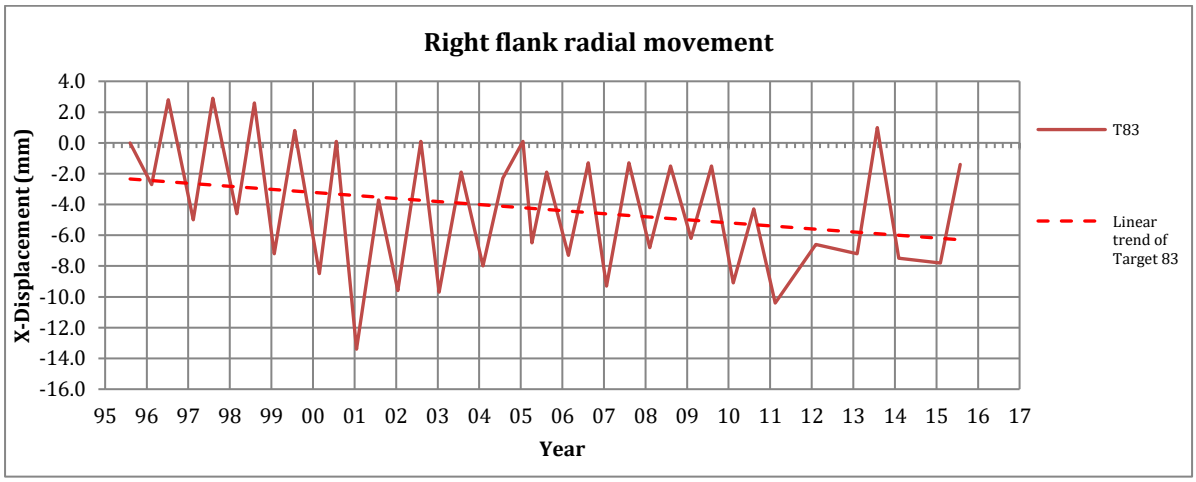

Figure 4-27: Radial movements of T83 at Hartebeeskuil Dam

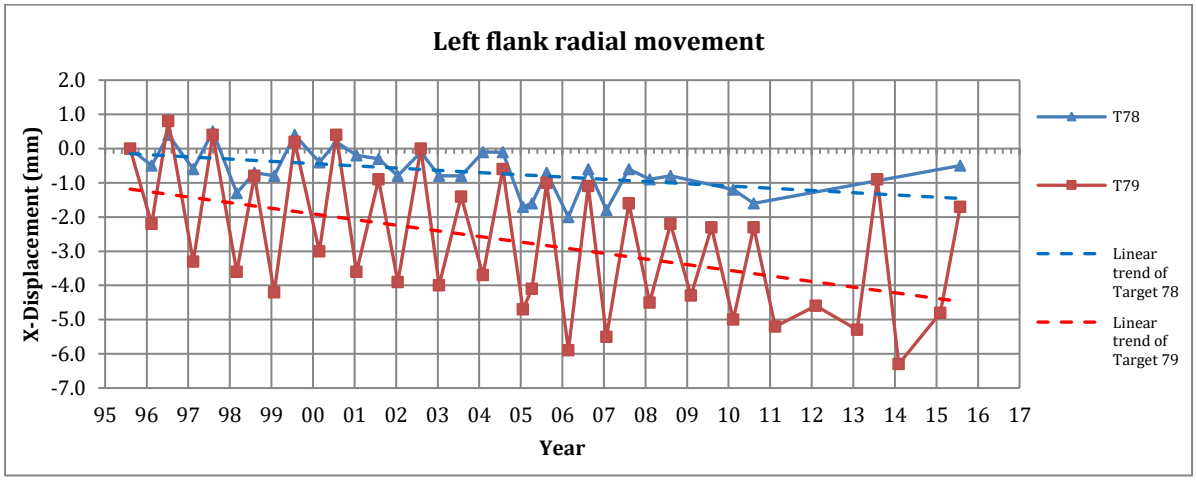

Figure 4-28: Radial movements of T78 and T79 at Hartebeeskuil Dam

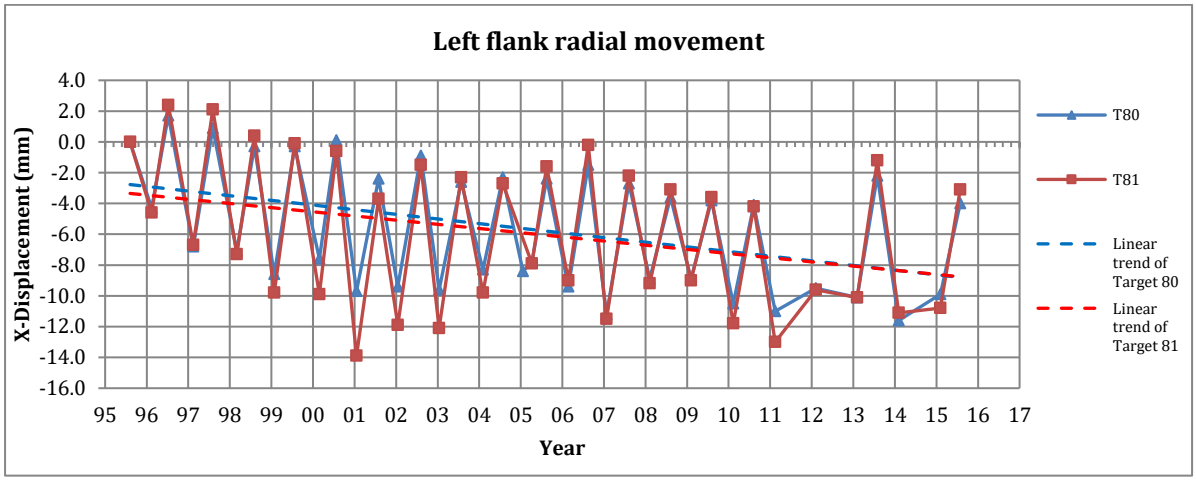

Figure 4-29: Radial movements of T80 and T81 at Hartebeeskuil Dam

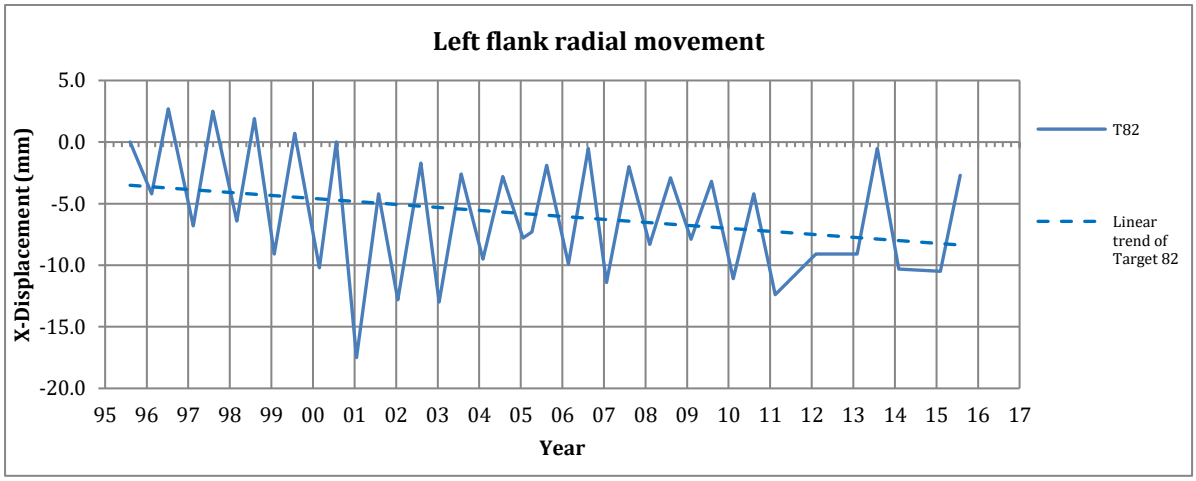

Figure 4-30: Radial movements of T82 at Hartebeeskuil Dam

The right flank, left flank and spillway show permanent trends toward the upstream side of approximately 1-6 mm. The smallest upstream trends occur on the far-right and far-left flanks. The biggest trends occur more toward the centre of the arch structure. In summary, these results prove that there is a permanent swelling action in an upstream direction.

4.3.3. Vertical Movements

The vertical movements are movements that show trends of increasing or decreasing elevations. Figure 4-31 to Figure 4-36 provide the vertical movements for all the targets since 1995 and positive values indicate rising crest elevations.

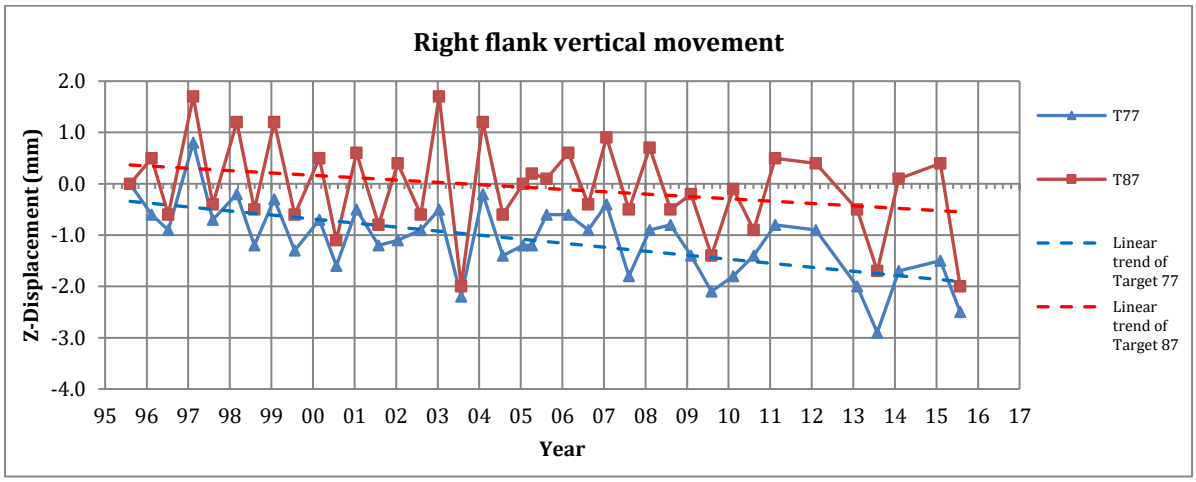

Figure 4-31: Vertical movements of T77 and T87 at Hartebeeskuil Dam

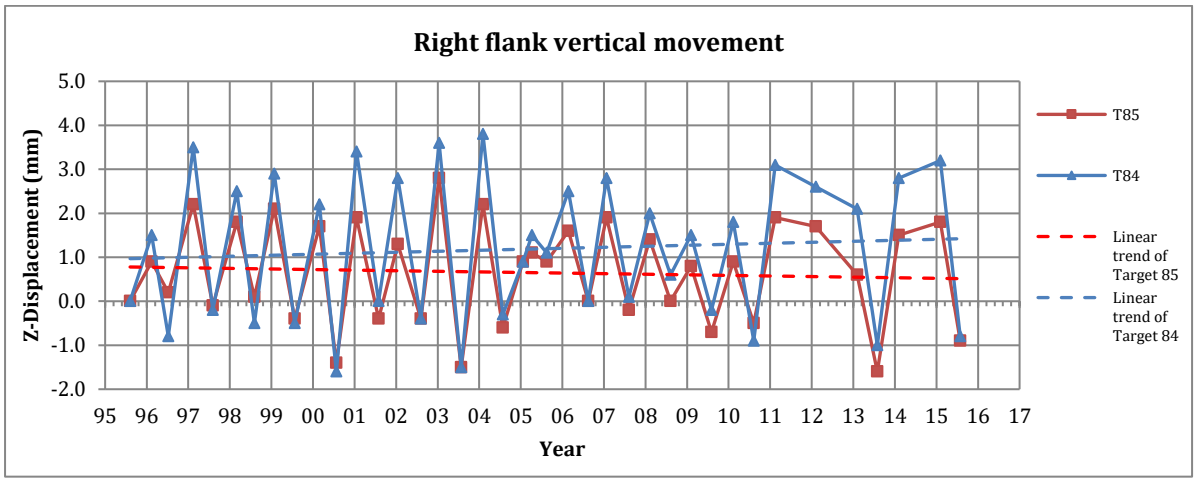

Figure 4-32: Vertical movements of T85 and T84 at Hartebeeskuil Dam

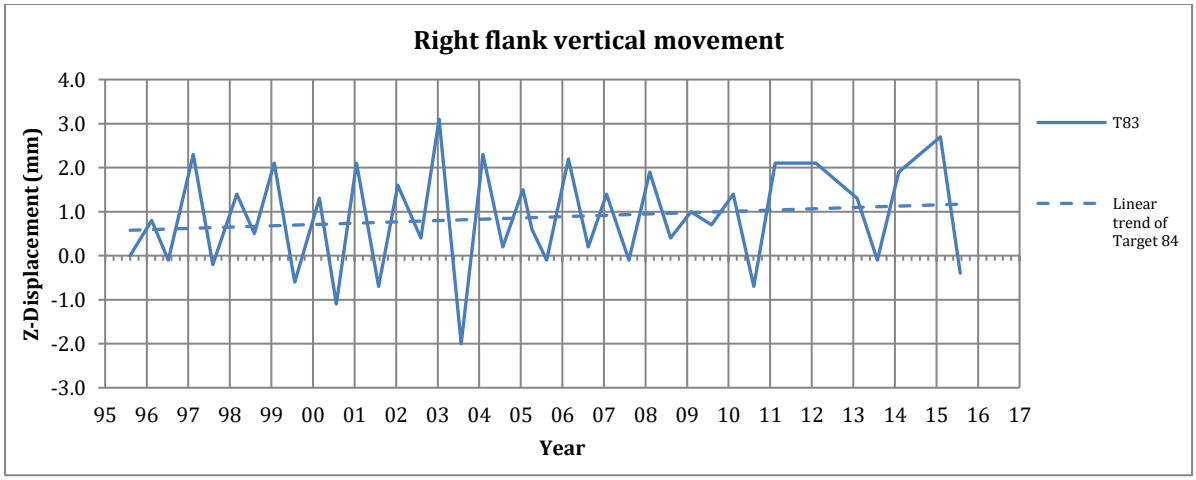

Figure 4-33: Vertical movements of T83 at Hartebeeskuil Dam

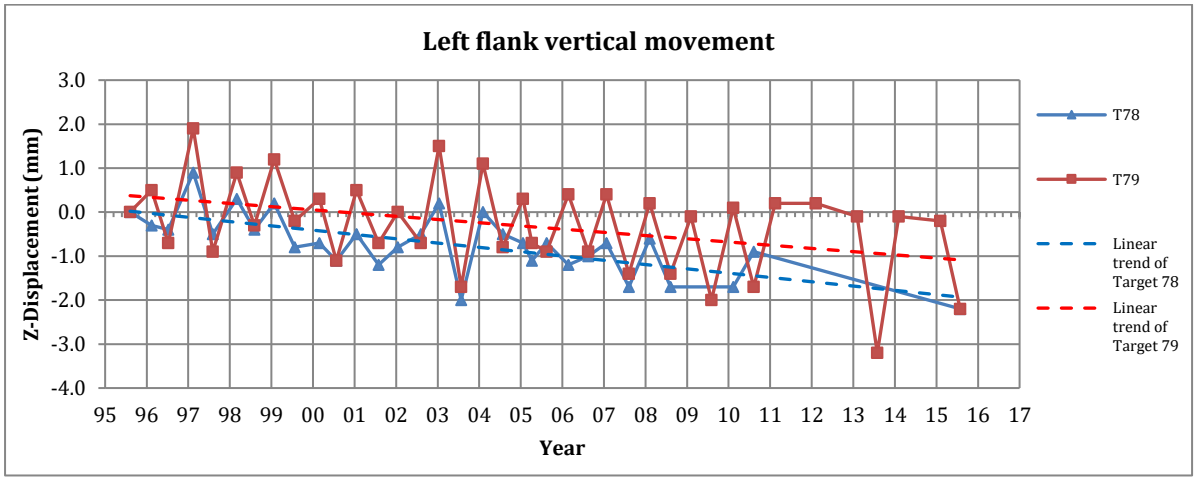

Figure 4-34: Vertical movements of T78 and T 79 at Hartebeeskuil Dam

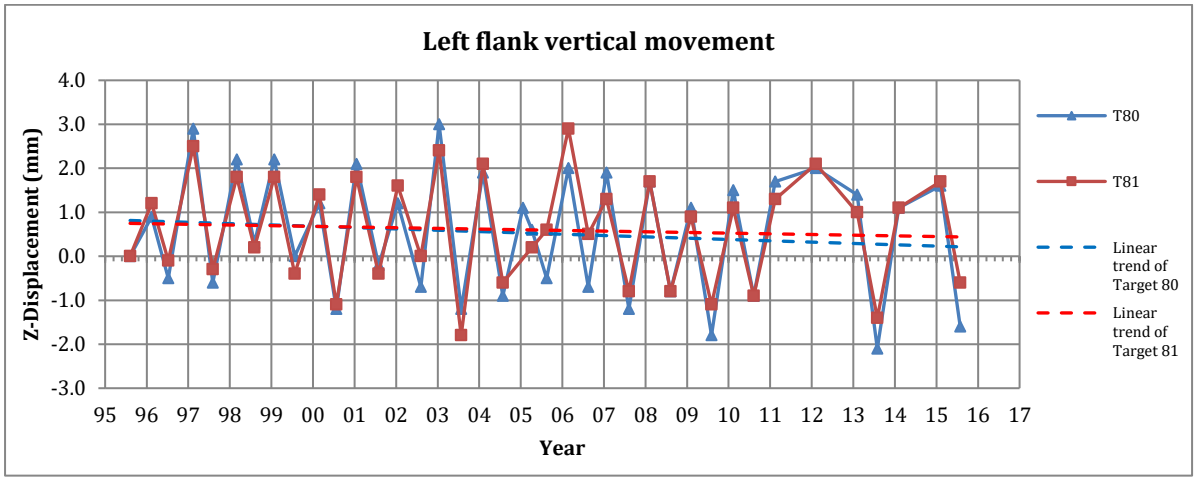

Figure 4-35: Vertical movements of T80 and T81 at Hartebeeskuil Dam

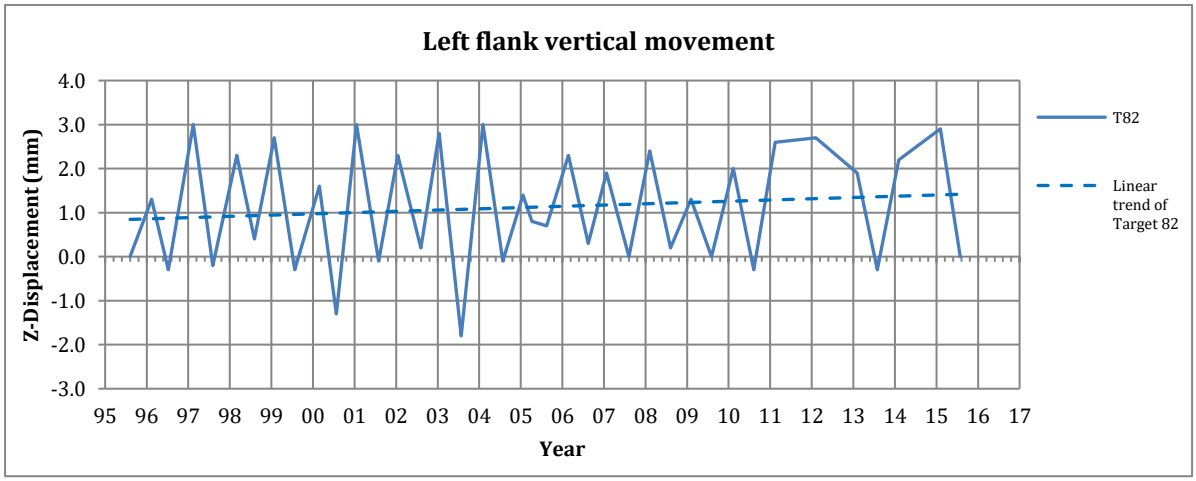

Figure 4-36: Radial movements of T82 at Hartebeeskuil Dam

The far-right flank and far-left flank show permanent settlement trends of approximately 1-2 mm. The targets toward the middle of the dam wall show very stable trends, with some signs of rising crest elevation at the spillway (T82 and T83); the permanent trends are very small and do not exceed 2 mm. In summary, these results prove that both the flanks are settling, and the middle of the dam is rising slightly.

4.4. Crack Width Gauges

Vinchon-type crack width gauges were installed at the Hartebeeskuil Dam during the mid-1980s, which were replaced by *Sinco* gauges during the early 1990s due to inconsistencies and inaccuracies with the readings. Problems were also experienced with the *Sinco* gauges due to galvanic corrosion producing false trends. Consequently, these gauges were replaced by seventeen 3-D DWAF98-type gauges in 1998. These gauges were again replaced in 2002 by DWAF2001-type gauges to ensure better accuracy in readings. The DWAF2001-type gauges can be read with an electronic dial gauge to an accuracy of 0.001 mm (Beukes, 2008).

4.4.1. Tangential Crack on Crest

The tangential crack on the right flank NOC is monitored by crack width gauges K15 and K16 which are both located on block number 8 (one gauge on each side of the block). Generally, the movements show trends that do not exceed 1mm. However, from about middle 2010 to about middle 2012, erratic measurements were recorded that exceeded 3mm for all three directions. This could be the result of an erroneous read-out unit since all three directions and both gauges display the same spikes in the readings. The radial movement results are shown in Figure 4-37, the tangential movement results in Figure 4-38 and the vertical movement results in Figure 4-39.

Legend for positive directions (left and right as viewed from the upstream side):
- Radial = the crack opening increases
- Tangential = the upstream part moves to the right relative to the downstream side
- Vertical = the upstream part moves upwards relative to the downstream part

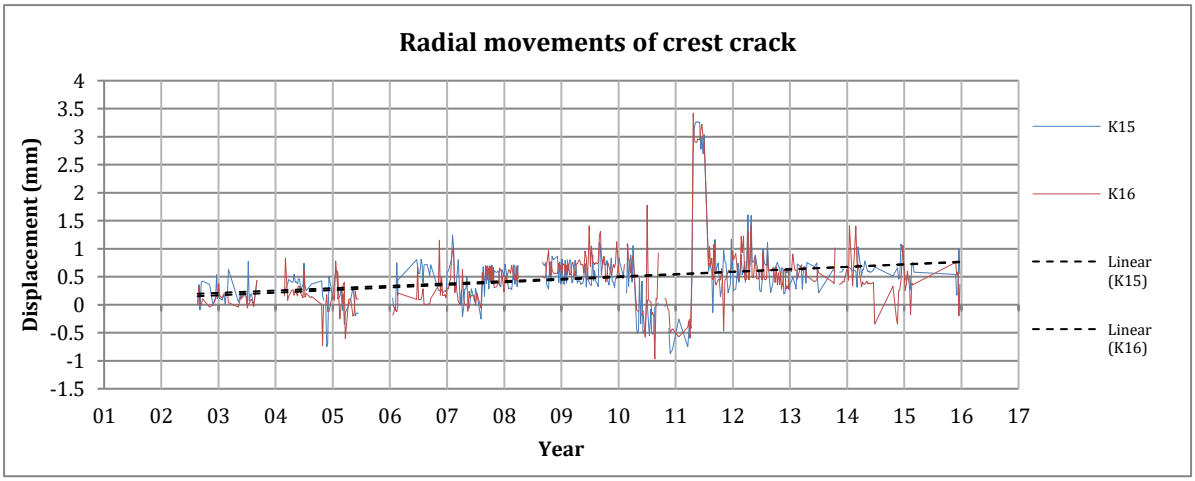

Figure 4-37: Radial movements of the tangential crest crack at Hartebeeskuil Dam

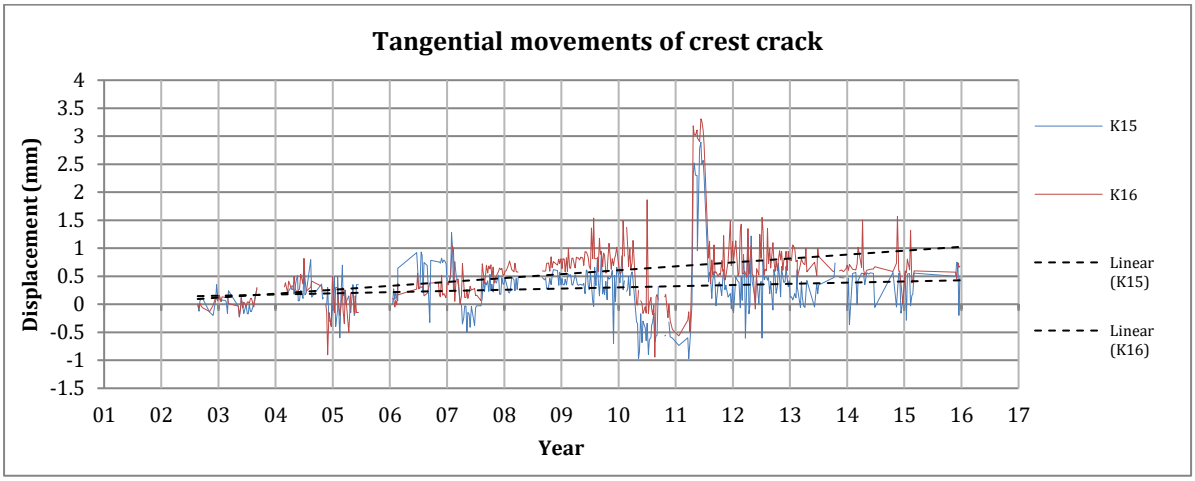

Figure 4-38: Tangential movements of the tangential crest crack at Hartebeeskuil Dam

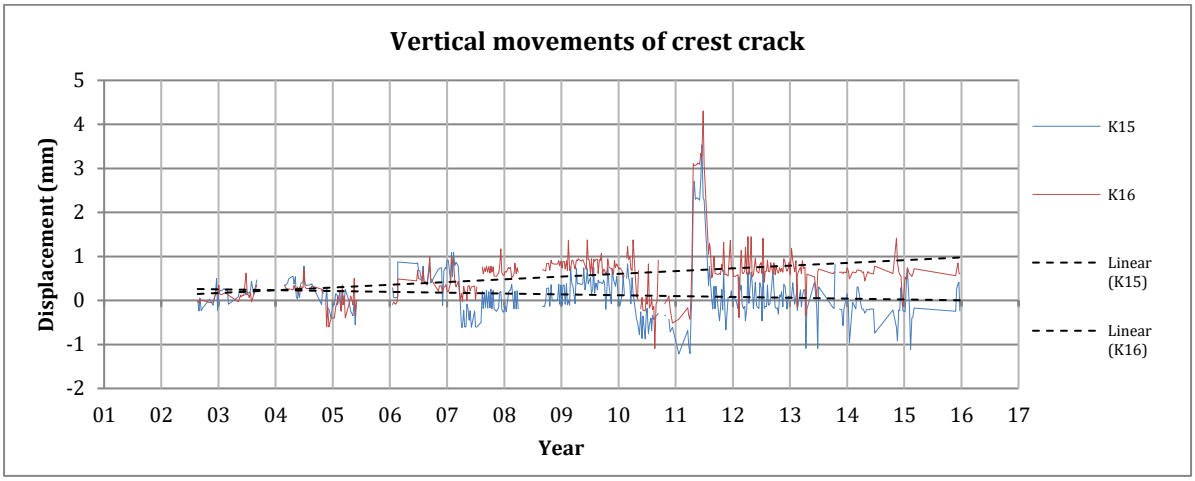

Figure 4-39: Vertical movements of the tangential crest crack at Hartebeeskuil Dam

The radial measurements show that the crack has opened slightly - less than 1 mm (see Figure 4-37). The tangential measurements show that the upstream section of the crack has moved in the direction of the right flank relative to the downstream section - less than 1 mm (see Figure 4-38). Gauge K16 shows that the upstream section moved slightly upward relative to the downstream section of the crack - less than 1 mm. Gauge K15 shows a stable trend, but the movements hint at a swelling trend of the upstream section of the arch dam (see Figure 4-39).

4.4.2. Vertical Joints on Right Flank Crest

There are three crack width gauges that are installed to measure movements of the vertical joints between blocks 8 and 9, between blocks 7 and 8 and between blocks 6 and 7 (see the layout of the blocks in Figure 4-40). These are gauges K11, K12 and K13 respectively. Due to problems experienced with gauge K13, only measurements for K11 and K12 were available and up to date.

Generally, the movements show trends that do not exceed 1.5 mm. However, from about middle 2010 to about middle 2012, erratic measurements were recorded that exceeded 3 mm for all three directions. This could be the result of an erroneous read-out unit since all three directions and both gauges display the same spikes in the readings. The radial movement results are shown in Figure 4-41, the tangential movement results in Figure 4-42 and the vertical movement results in Figure 4-43.

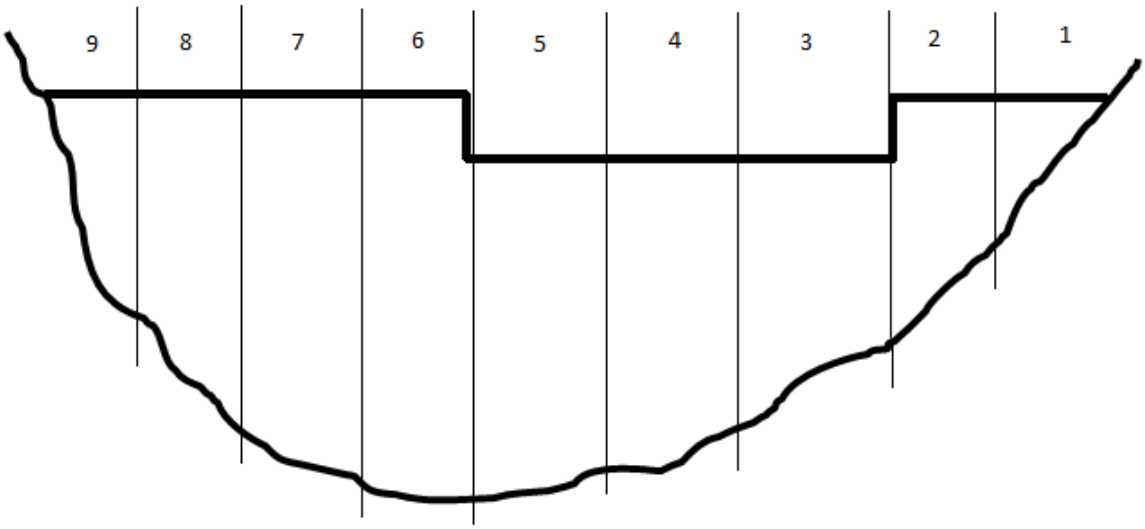

Figure 4-40: Hartebeeskuil Dam: The positions of the vertical joints and block numbers

Legend for positive directions (left and right as viewed from the upstream side):

- Radial = the block on the right side moves downstream relative to the block on the left side
- Tangential = the joint opening increases
- Vertical = the block on the right side moves upward relative to the block on the left side

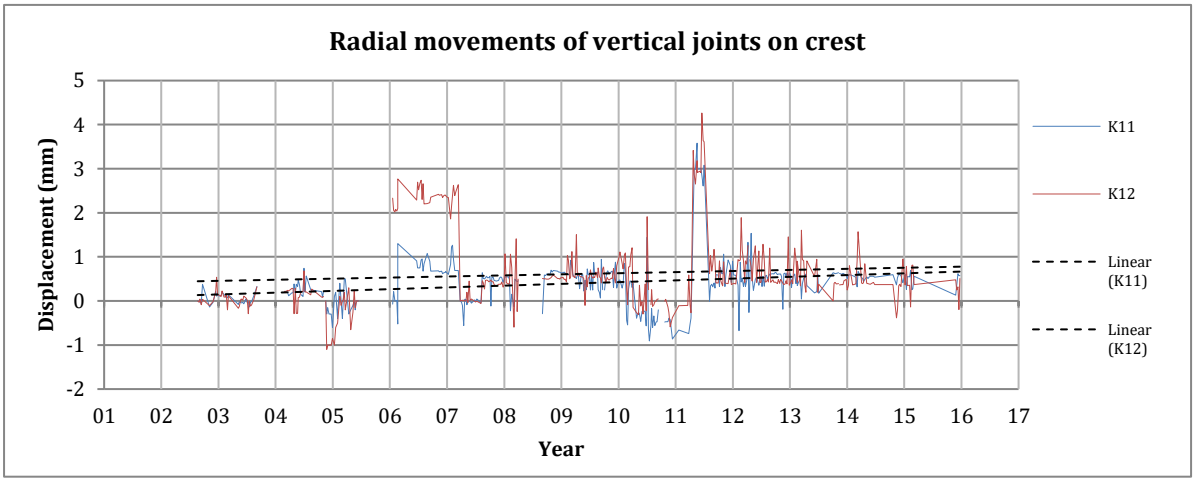

Figure 4-41: Radial movements of crest vertical joints at Hartebeeskuil Dam

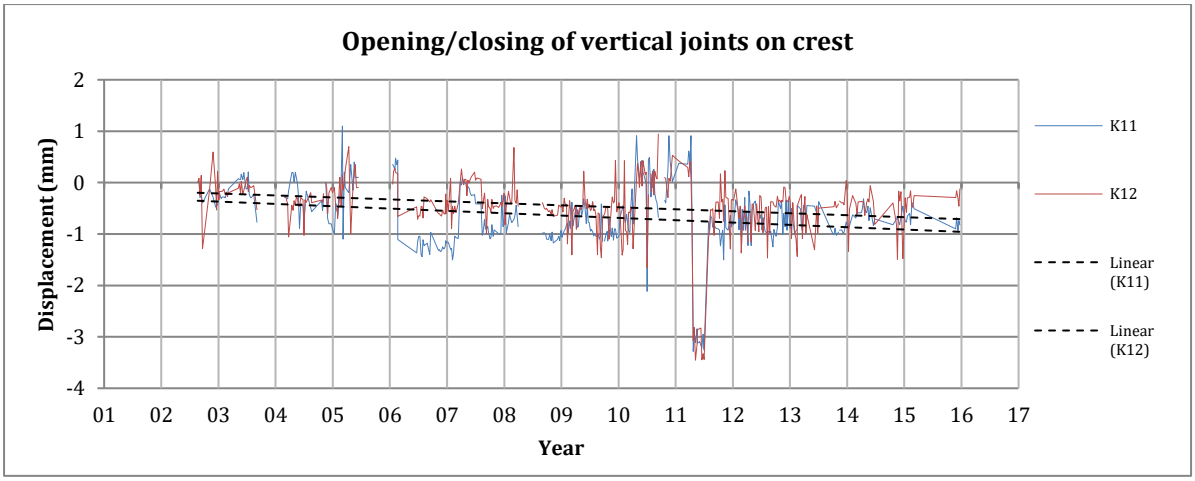

Figure 4-42: The opening/closing of crest vertical joints at Hartebeeskuil Dam

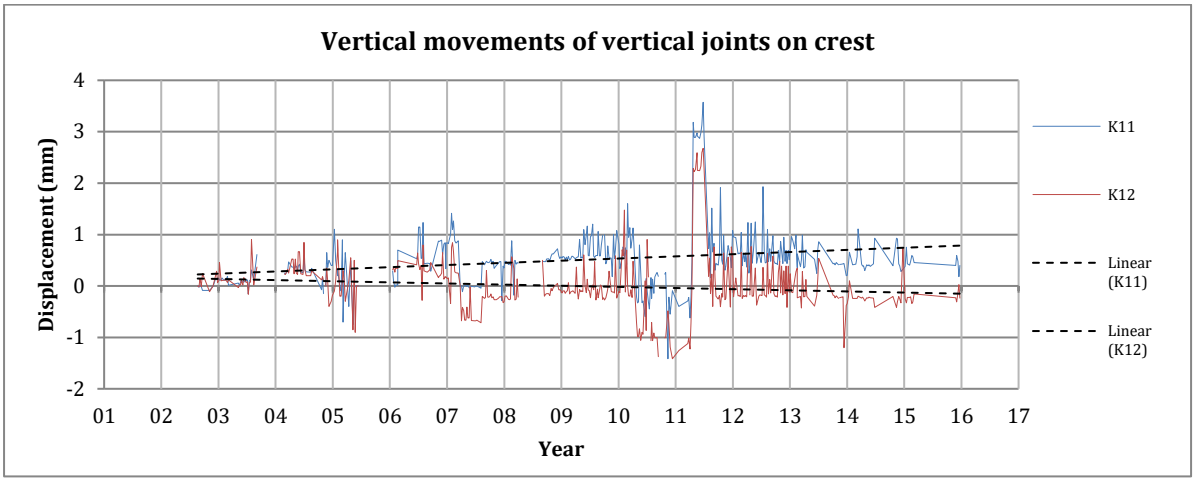

Figure 4-43: The vertical movements of crest vertical joints at Hartebeeskuil Dam

The radial movements show that Block 9 moved slightly downstream relative to Block 8 and that block 8 moved downstream relative to Block 7 with permanent trends of less than 1 mm (see Figure 4-41). The tangential movements show that the joints are closing slightly with permanent trends of less than 1 mm (see Figure 4-42). The vertical movements show that Block 9 moved upwards relative to Block 8. Block 8 moved downwards relative to Block 7 with permanent trends of less than 1 mm (see Figure 4-43). No clear swelling trends are evident from these results.

4.4.3. Vertical Joints on Right Flank Base

The vertical joints on the base of the right flank are monitored at two locations, namely between block 8 and 9 on the "pulvino" and between block 6 and 7 near the toe of the wall (gauges K6 and K3 respectively). From about middle 2010 to about middle 2012, erratic measurements were recorded that exceeded 3 mm for all three directions. This could be the result of an erroneous read-out unit since all three directions and both gauges display the same spikes in the readings. The radial movement results are shown in Figure 4-44, the tangential movement results in Figure 4-45 and the vertical movement results in Figure 4-46.

Legend for positive directions (left and right as viewed from the upstream side):

- Radial = the block on the right side moves downstream relative to the block on the left side
- Tangential = the joint opening increases
- Vertical = the block on the right side moves upward relative to the block on the left side

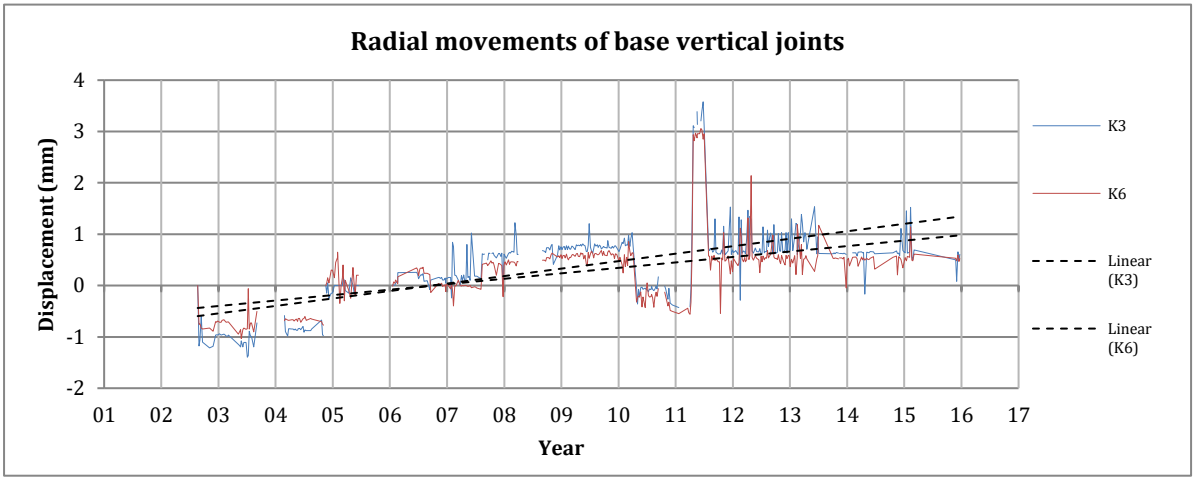

Figure 4-44: Radial movements of base vertical joints at Hartebeeskuil Dam

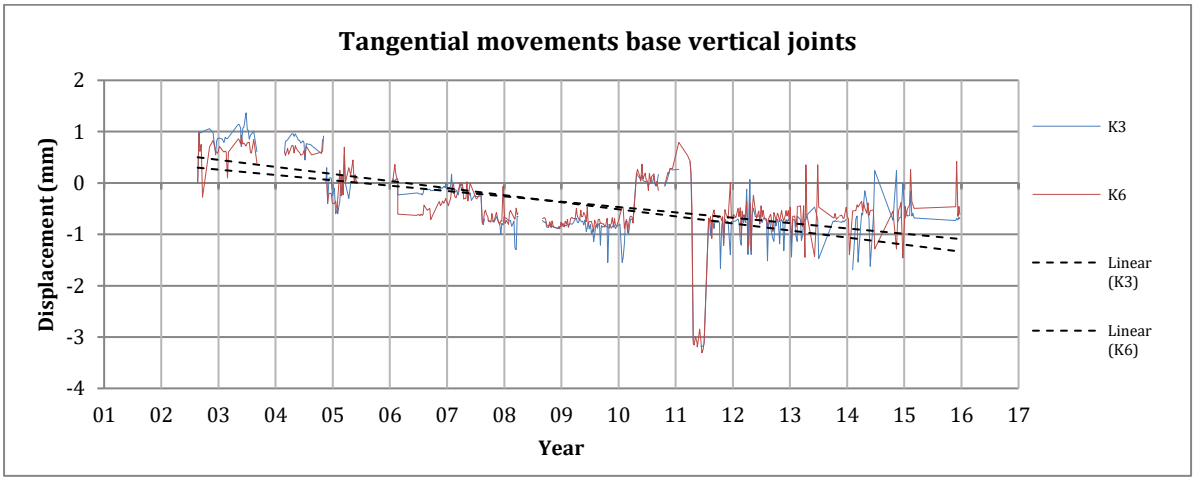

Figure 4-45: The opening/closing of base vertical joints at Hartebeeskuil Dam

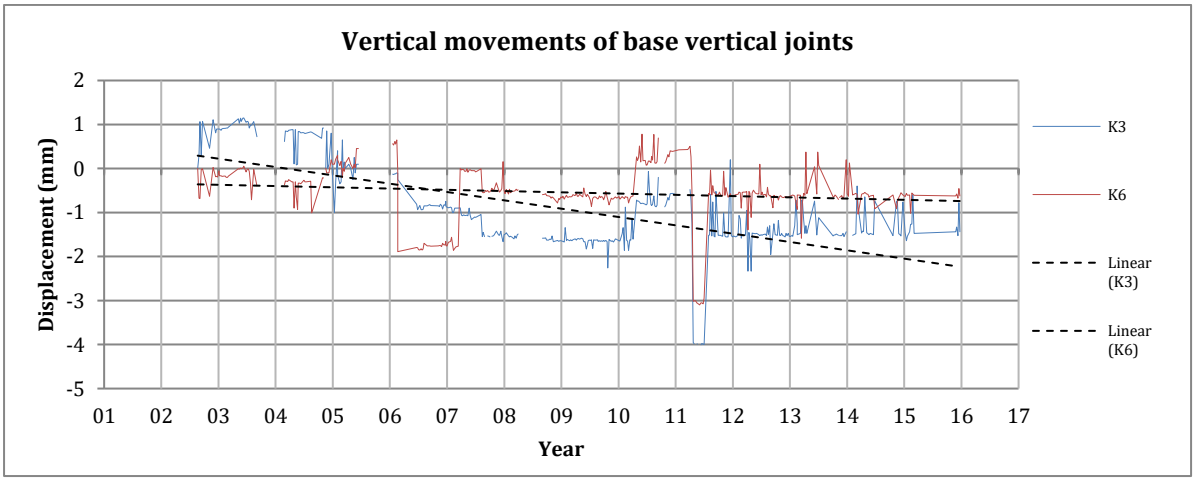

Figure 4-46: The vertical movements of base vertical joints at Hartebeeskuil Dam

Block 9 has moved downstream relative to block 8 and Block 7 has moved downstream relative to block 6 with permanent trends of less than 2 mm (see Figure 4-44). Both K3 and K6 show closing of the joints with permanent trends of less than 2 mm (see Figure 4-45). Blocks 8 and 9 have remained more or less even with regards to permanent vertical trends. Block 6 has moved up relative to block 7 with permanent trends of less than 3 mm (see Figure 4-46). Due to the erratic nature of some of the readings, it is hard to draw any certain conclusions on the crack width results.

4.4.4. Horizontal Lift Joints on Right Flank

There are only two crack width gauges measuring the movements of horizontal construction lift joints, namely K4 and K5. Both are located on the "pulvino" within block 8. The same erratic readings were recorded as was the case with the previous results. This could be the result of an erroneous read-out unit since all three directions and both gauges display the same spikes in the readings. The radial movement results are shown in Figure 4-47, the tangential movement results in Figure 4-48 and the vertical movement results in Figure 4-49.

Legend for positive directions (left and right as viewed from the upstream side):

- Radial = the top lift moves downstream relative to the bottom lift
- Tangential = the top lift moves to the right relative to the bottom lift
- Vertical = the joint opening increases

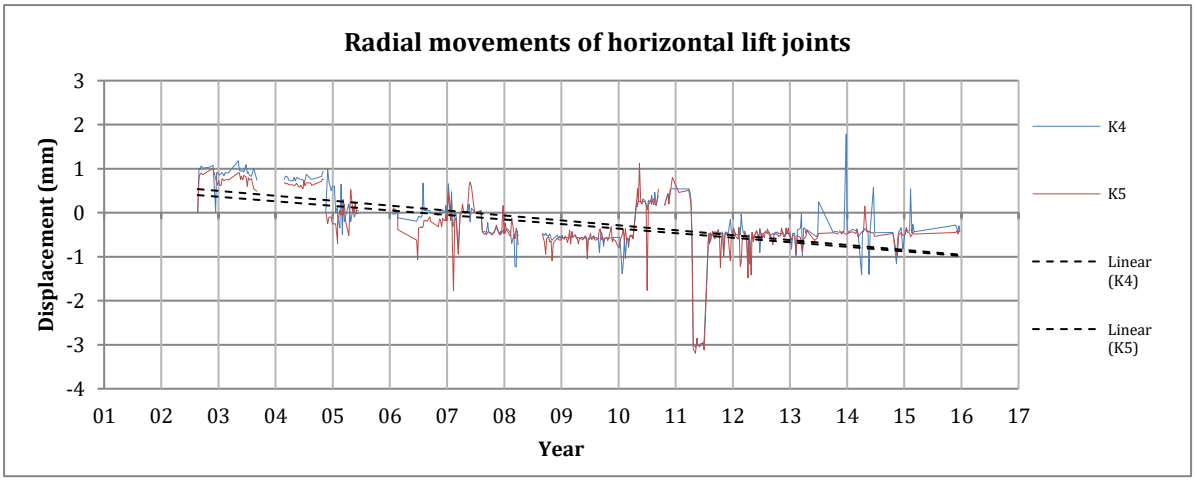

Figure 4-47: Radial movements of horizontal lift joints at Hartebeeskuil Dam

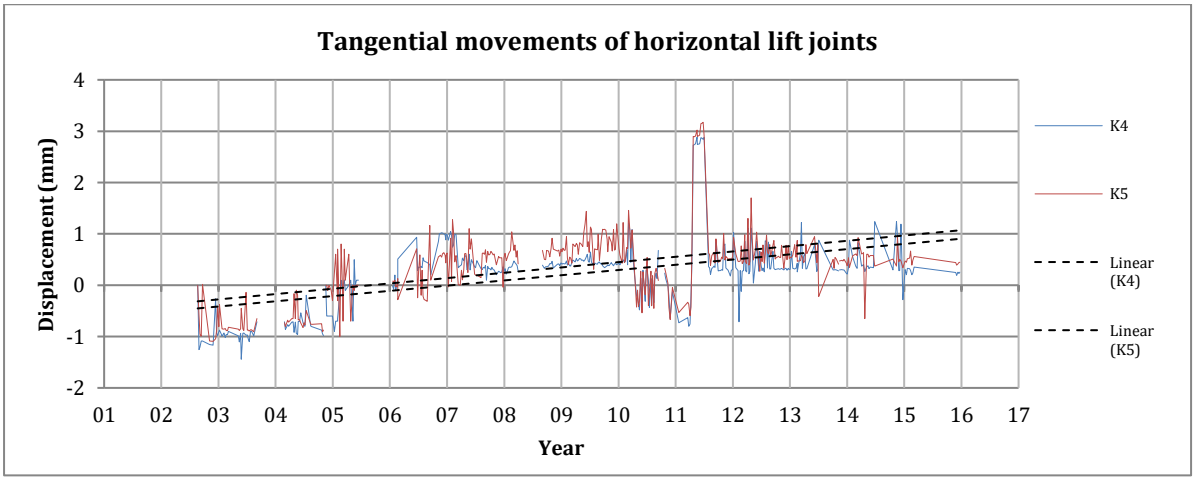

Figure 4-48: Tangential movements of horizontal lift joints at Hartebeeskuil Dam

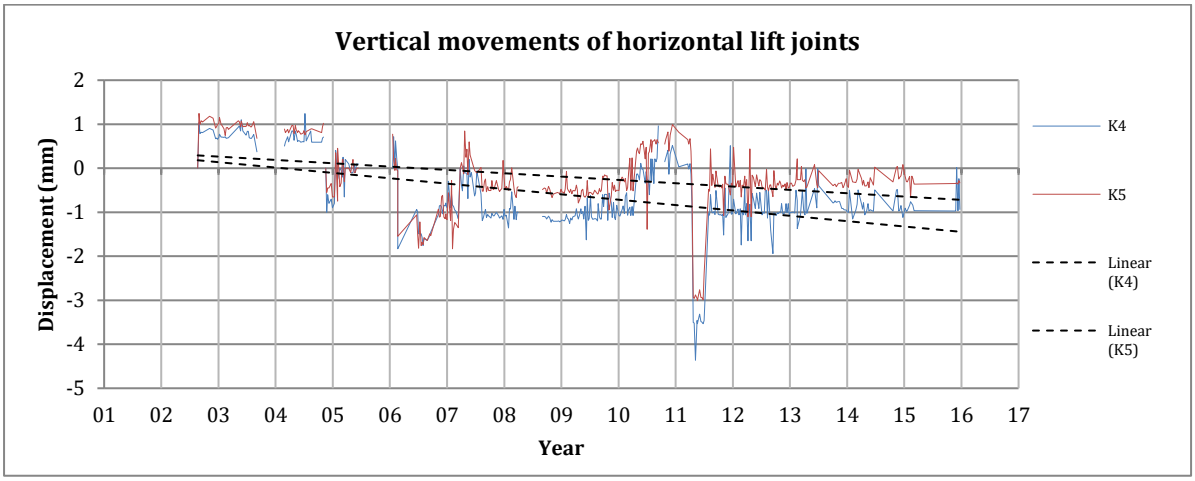

Figure 4-49: Vertical movements of horizontal lift joints at Hartebeeskuil Dam

The radial movements show that the top lifts on the joints generally move upstream relative to the bottom lifts with permanent trends of less than 2 mm (see Figure 4-47). The tangential movements show that the top lifts on the joints generally move to the right relative to the bottom lifts with permanent trends of less than 2 mm (see Figure 4-48). The vertical movements show that the joints have generally closed with permanent trends of less than 2 mm (see Figure 4-49). Due to the erratic nature of some of the readings, it is hard to draw any certain conclusions on the crack width results.

4.5. In Situ Stress Measurements

The over-coring method was used during three in situ stress measurement exercises in 1999. CSIRO Hollow Inclusion stress measurement cells were used. Oosthuizen *et al.* (2003) mentioned that these cells are very sensitive to temperature changes and that radial biaxial compression due to moisture absorption of the epoxy may have an influence on the results. The tests aimed at determining the in-situ stress distribution throughout the thickness of the arch. Two of the tests were conducted on the downstream side of the wall and one test was conducted on the upstream side. The results are summarized in Table 4-1.

Table 4-1: Results gained from the in-situ stress measurements conducted in 1999

Test number	Location	Direction	Magnitude (MPa)	Stress state
1	1 m above the apron in the horizontal centre of the downstream face of block 5 at a depth of 0.5 m	Radial (upstream/downstream)	1.35	Tension
		Tangential (right flank/left flank)	1.21	Tension
		Vertical	1.6	Tension
2	Same as above but at a depth of 1 m	Radial	0.02	Tension
		Tangential	2.71	Compression
		Vertical	0.49	Tension
3		Radial	0.76	Tension

	In the horizontal centre of block 7 on the upstream face at a depth of 150 mm and 7.5 m below the NOC	Tangential	2.07	Compression
		Vertical	0.56	Compression

The results showed that the swelling of the upstream portion of the arch structure has resulted in tensile stresses on the down-stream face. This is supported by visual observation (cracks and joint openings) and the 1999 grouting records. The cracking pattern on the downstream face is typically the result of the tensile strength of the concrete being exceeded by the tensile forces that are present in this area.

The upstream face is mostly in compression and this is consistent with the appearance of the upstream face (mostly horizontal cracks are visible). Test number 2 indicates that there is a transition between a tension zone on the downstream and a compression zone on the upstream part of the arch. Effectively, the arch has become thinner (the active arch is the section where compressive stresses are present).

4.6. Chapter Summary

This chapter looked at the typical behaviour of Hartebeeskuil Dam in order to gain evidence of the effects of possible AAR-related expansion. The behaviour of Hartebeeskuil Dam is monitored by geodetic surveys, crack width gauges and 5-yearly visual inspections. In situ stress measurements and grouting of the dam were conducted in 1999 which provided valuable insight into the behaviour of the structure.

Visual inspection:

The upstream face mainly displayed horizontal cracks. The downstream face displayed peripheral cracks which run approximately parallel to the pulvino. The crack patterns in general reveal a structure that swells mostly on the upstream side causing the downstream side to be in tension.

Geodetic surveys:

The geodetic surveys revealed that the dam moved permanently in an upstream direction since 1995. It also revealed that the right and left flanks have moved permanently towards the abutments since 1995. The flanks of the dam wall showed trends of slight permanent settlement while the centre of the dam seems to have increased in elevation slightly since 1995.

Crack width gauges:

The crack width gauges did not reveal any major permanent trends and most of the trends did not exceed 2.5 mm. The results reveal that the joints are moving within acceptable limits and remain quite tight. The tangential crack on the crest seems to be opening up slightly.

In situ stress measurements:

The measurements revealed that the downstream face is in tension and the upstream face in compression. The effective arch has become thinner - this is due to a decrease in the compression area (arch dams are designed to act in compression only).

5. Poortjieskloof Dam

5.1. Introduction

The Poortjieskloof Dam was constructed in the Groot River and is situated 27 km east of Montagu in the Western Cape. The dam was designed and constructed by the DWS, the current owner and operator. The dam wall is a double-curvature arch ("Pregnant Mary" type) which had an initial wall height of 33.5 m after construction completion in 1955. In 1968 the wall was raised by 4.57 m. The total crest length is 143.25 m.

Poortjieskloof Dam	
	
Figure 5-1: Poortjieskloof Dam	
Structure type:	Double-curvature arch ("Pregnant Mary" type)
Age of dam:	62 years
Wall height:	38 m
Climate region:	Local steppe climate region; average maximum temperature of 26°C (based on temperature data gained from three online resources*); average minimum temperature of 11.5 °C (based on temperature data gained from three online resources*); average annual precipitation of 440 mm (based on 8 years' rainfall data provided by the DWS)
Structure orientation:	The downstream face of the dam wall faces north (this implies that the downstream face will generally be more exposed to direct sunlight than the upstream face)
Construction materials:	Limited information available. Quartzite from the Table Mountain Group was used as coarse and fine aggregate for both the old (prior to raising of the dam wall) and new concrete (Van Der Spuy, 1987).

*climatedata.eu; meteoblue.com; worldweatheronline.com

Poortjieskloof Dam is situated in an area which has a local steppe climate. A local steppe climate can be described as semi-arid with fairly low average annual rainfall ranging between 200 and 500 mm per annum. The summers are fairly warm, and the winter are fairly cold in contrast. The low average annual rainfall is only sufficient to support the growth of grass and small shrubs and trees.

Van Der Spuy (1987) first mentioned the presence of AAR at Poortjieskloof Dam. Cores had been drilled before and although it is not clear which tests were performed on the cores, Van Der Spuy (1987) was satisfied that these had confirmed the presence of AAR. Specific mention was made of cracks along the construction lift joints which Van Der Spuy (1987) also attributed toward AAR.

Hagen (1996) mentioned that the crack patterns visible on the dam wall are typical of those caused by AAR. He summarized the results from the cores that were drilled during the 1980s as follows:

- The vertically drilled cores showed evidence that the vertical construction joints are open at the top and closed at the bottom.
- The horizontally drilled cores showed that to a depth (into the dam wall from the downstream side) of about 1 m the horizontal lift joints are completely open; between depths of 1 m and 2 m the crack was visible but was completely closed.

Observations made by Muller (2006) are very much in agreement with previous findings. He mentioned that the instrumentation results confirm inelastic behaviour of the concrete due to AAR.

Sibanda (2011) mentioned that the presence of AAR was evident from the crack patterns present especially on the old concrete. He also mentioned the opening of construction lift joints on the downstream side of the dam wall. The instrumentation results from the trivec system and the crack width gauges seemed to indicate a swelling mechanism in the dam that could possibly be attributed to AAR.

5.2. Visual Inspection

A visual inspection was carried out on the 30th of July 2016. The objective was to look for typical evidence of AAR.

5.2.1. Left Flank

The upstream face of the left flank was in a fairly good condition with no major cracks visible (see Figure 5-2 and Figure 5-3).

Figure 5-2: Poortjieskloof Dam: General view of left flank upstream face

Figure 5-3: Poortjieskloof Dam: Close-up view of left flank upstream face

The left flank NOC was in a good condition (see Figure 5-5). The concrete structure to the left of the NOC (which include the steps from the parking area) displayed AAR cracking patterns as shown in Figure 5-4 and Figure 5-6.

Figure 5-4: Poortjieskloof Dam: Map cracking on concrete step structure left of the NOC

Figure 5-6: Poortjieskloof Dam: Some more map cracking on the concrete step structure

Figure 5-5: Poortjieskloof Dam: The left flank NOC

The left flank downstream face displayed fairly severe cracking patterns. The staining around the cracks and the orientation of the cracks provide clear evidence of AAR-related swelling and a principal stress distribution that is not ideal for an arch dam (see Figure 5-7 to Figure 5-9).

The area around the outlet structure displayed excessive map pattern cracking. This area also displayed evidence of seepage and staining around the cracks. The stiffness of the outlet structure clearly has an influence on the immediate surrounding arch structure as more severe cracking was present in the vicinity of this structure (see Figure 5-10 and Figure 5-13).

Figure 5-7: Poortjieskloof Dam: Clear parallel peripheral cracking patterns visible on the left flank downstream face

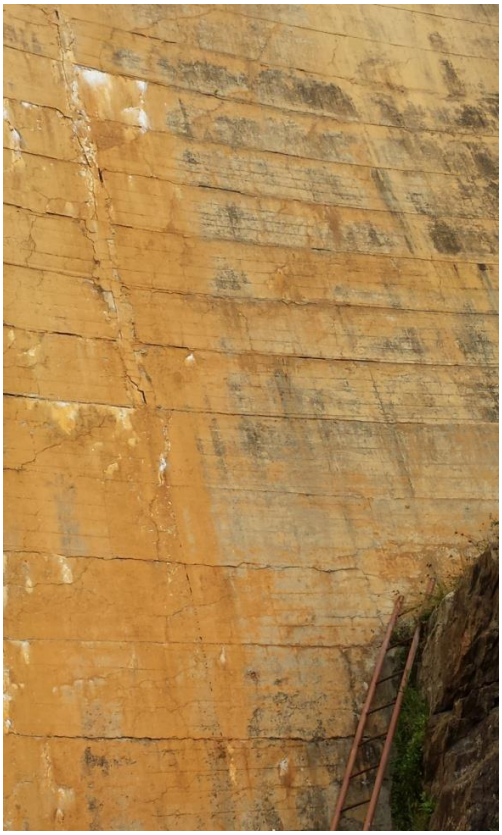

Figure 5-8: Poortjieskloof Dam: Close-up view of the cracking patterns on left flank downstream face

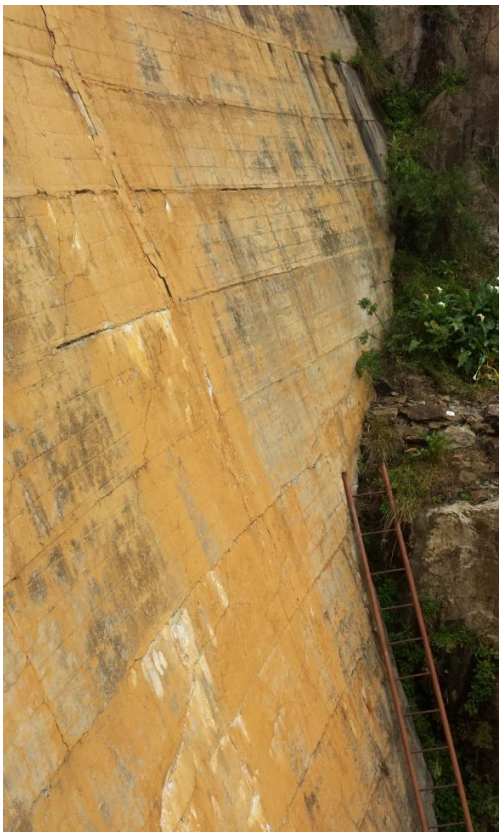

Figure 5-9: Poortjieskloof Dam: Some seepage through horizontal lift joints bordering the left abutment

Figure 5-10: Poortjieskloof Dam: Excessive map cracking patterns surrounding the outlet structure; also, note the staining

5.2.2. Spillway Section

The upstream face of the spillway could not be inspected due to restricted access. The crest of the spillway generally displayed no real signs of distress or cracking as shown in Figure 5-11.

Figure 5-11: Poortjieskloof Dam: View of spillway crest

The downstream face of the spillway displayed excessive seepage through the horizontal construction lift joints, which is characterised by calcite staining and moist areas (see Figure 5-12). The first major lift joint above the apron showed clear separation on the downstream side (see Figure 5-14). The separation and excessive leakage of the horizontal construction lift joints are typical AAR expansion phenomena.

Figure 5-12: Poortjieskloof Dam: General view of spillway downstream face

Figure 5-14: Poortjieskloof Dam: Clear separation of first horizontal construction lift joint above apron

Figure 5-13: Poortjieskloof Dam: Increased cracking in the area surrounding the outlet structure

5.2.3. Right Flank

The right flank upstream face and NOC could not be accessed. The downstream face displayed some significant cracking patterns similar to those on the left flank downstream face (see Figure 5-15 to Figure 5-18).

Figure 5-15: Poortjieskloof Dam: Unfavourable cracking patterns on the right flank

Figure 5-16: Poortjieskloof Dam: General view of the right flank downstream face

Figure 5-17: Poortjieskloof Dam: A prominent crack parallel to the abutment

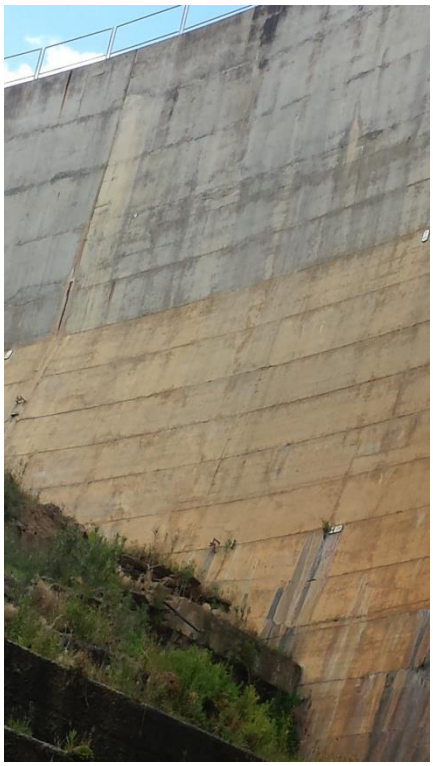

Figure 5-18: Poortjieskloof Dam: Close-up view of the far-right flank downstream face

5.3. Geodetic Survey Results

The geodetic survey network at Poortjieskloof consists of 6 network pillars and 25 targets at several locations and relative levels (RL) on the downstream face of the dam wall (see Figure 5-19 and Figure 5-20). A geodetic survey was performed twice a year, once in the summer and once in the winter. Data up until February 2015 was available for this research.

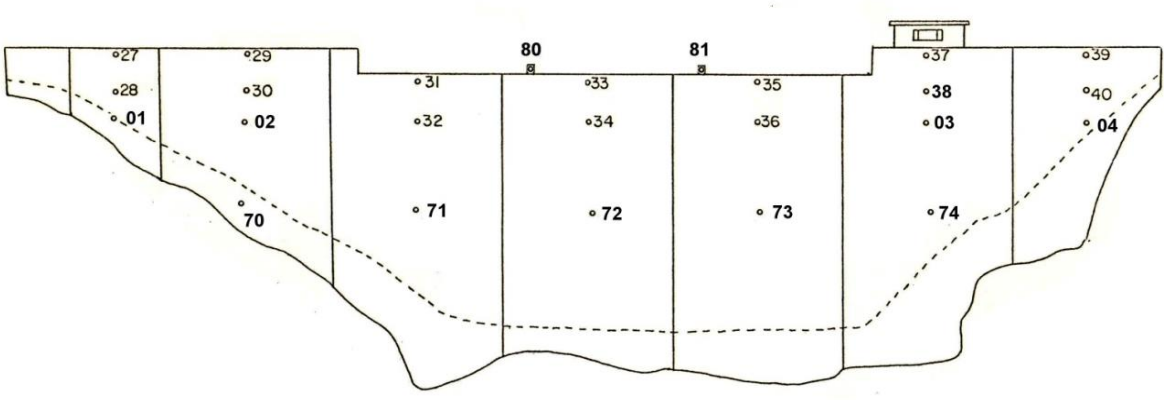

Figure 5-19: Upstream elevation of the geodetic survey targets at Poortjieskloof Dam

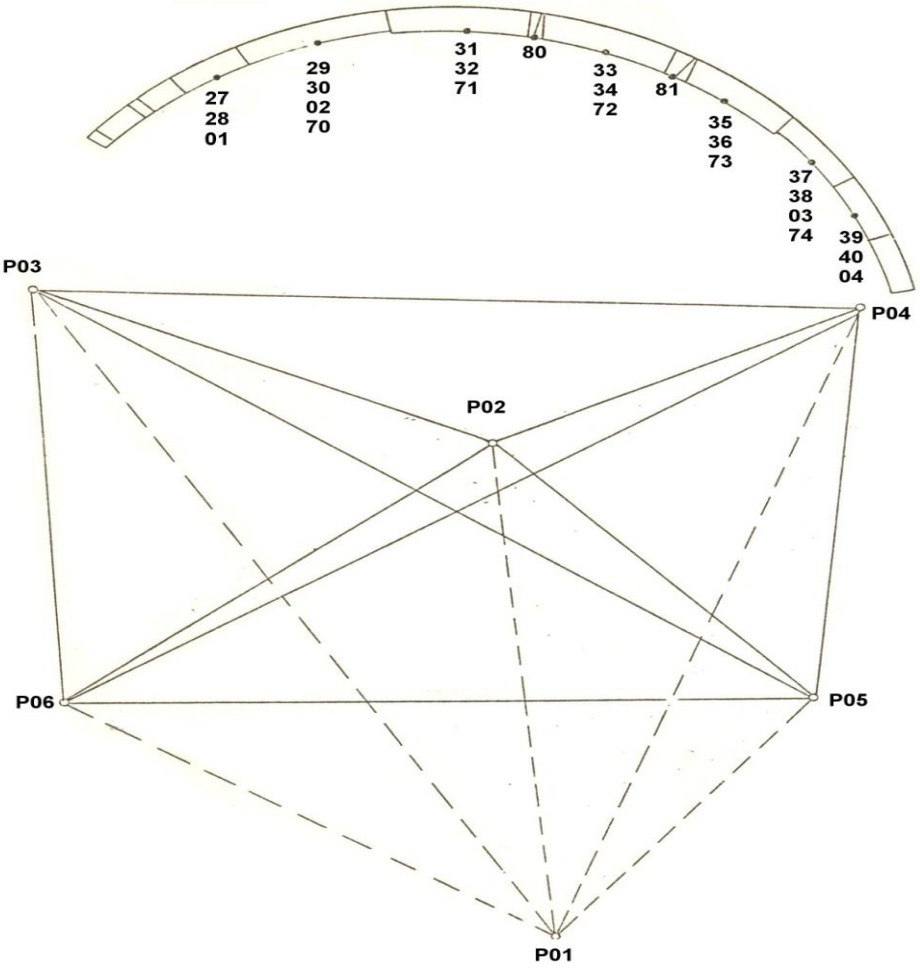

Figure 5-20: Plan view of the geodetic survey network at Poortjieskloof Dam

5.3.1. Tangential Movements

The tangential movements are movements toward or away from the flanks. Figure 5-21 to Figure 5-31 provide the tangential movements for all the targets since 1998. Positive values indicate movement toward the right flank. "T" is short for "Target".

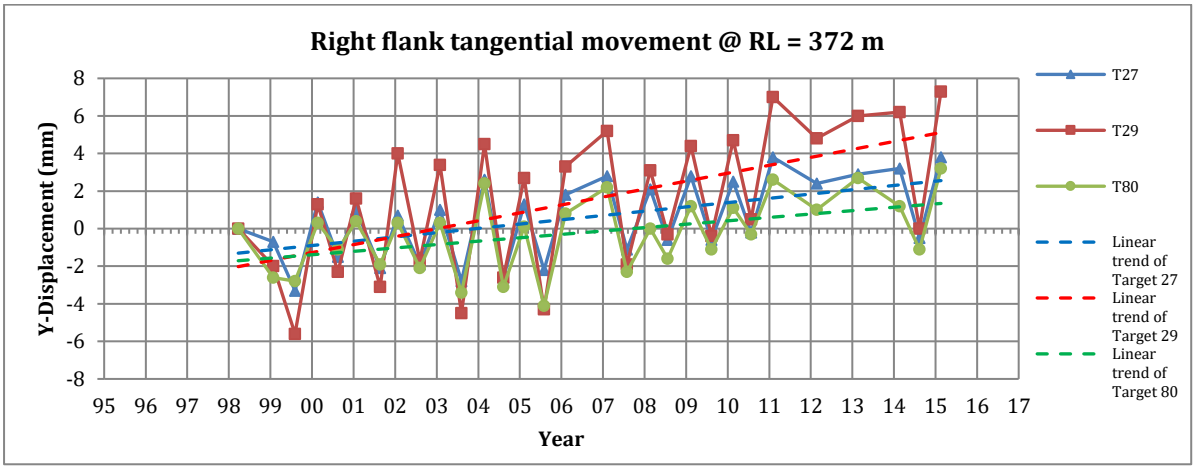

Figure 5-21: Tangential movements of T27, T29 and T80 at Poortjieskloof Dam

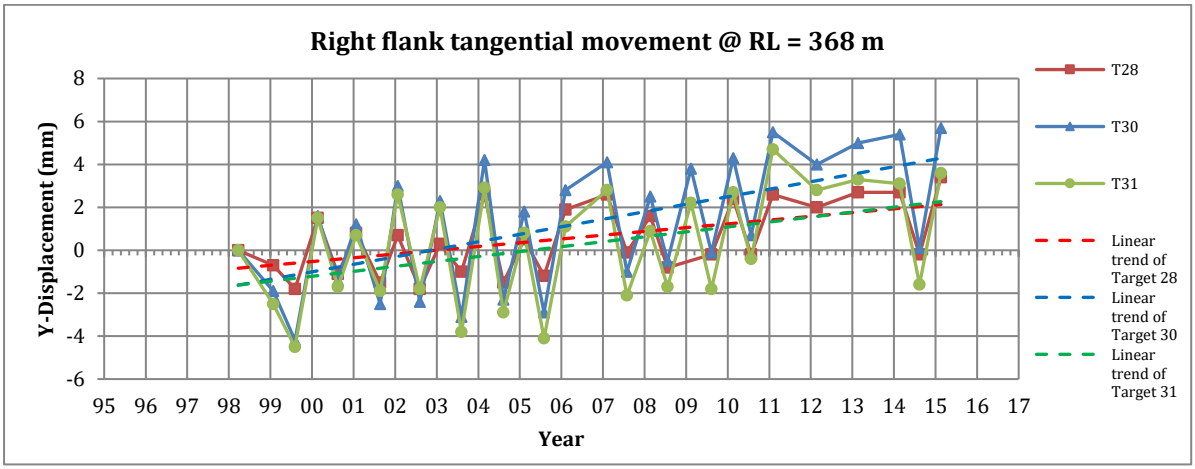

Figure 5-22: Tangential movements of T28, T30 and T31 at Poortjieskloof Dam

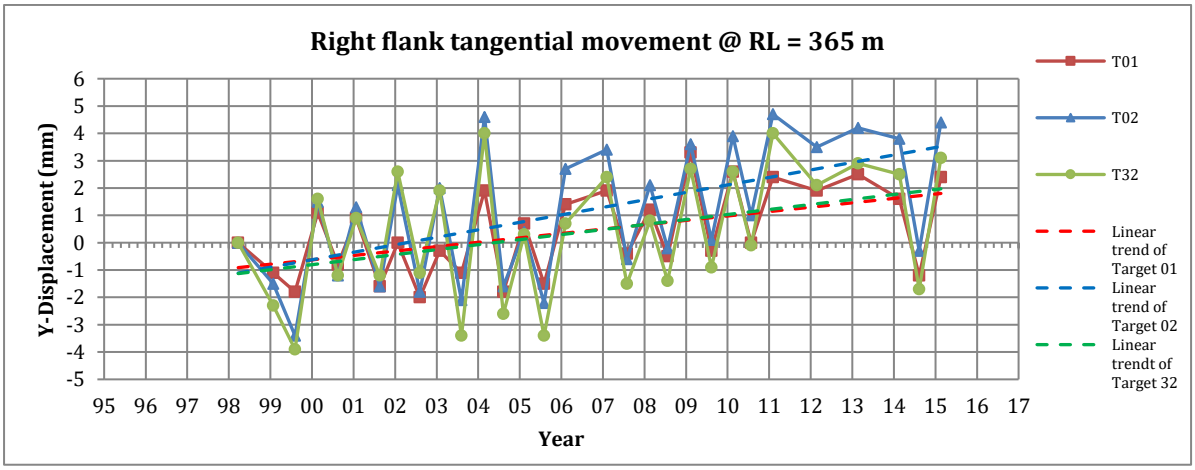

Figure 5-23: Tangential movements of T01, T02 and T32 at Poortjieskloof Dam

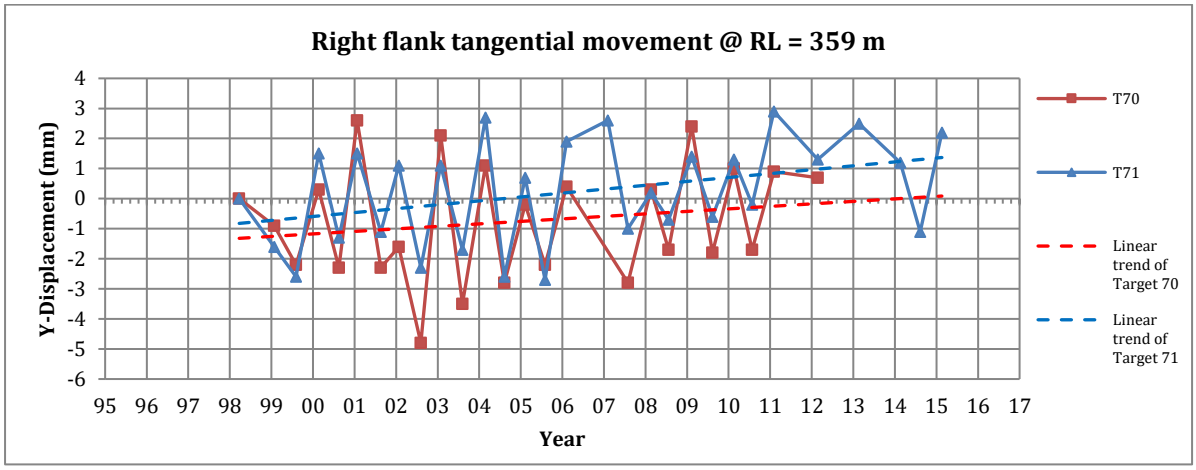

Figure 5-24: Tangential movements of T70 and T71 at Poortjieskloof Dam

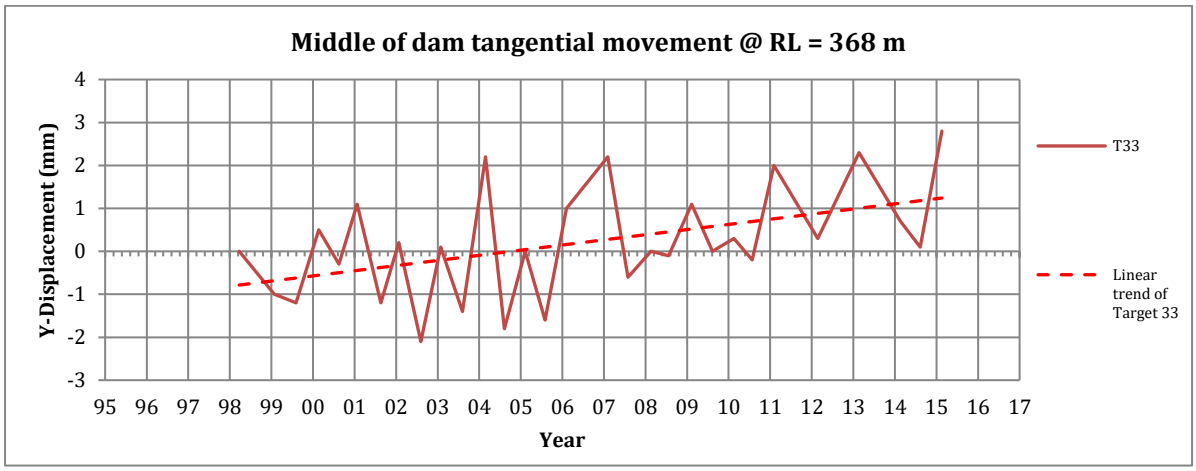

Figure 5-25: Tangential movements of T33 at Poortjieskloof Dam

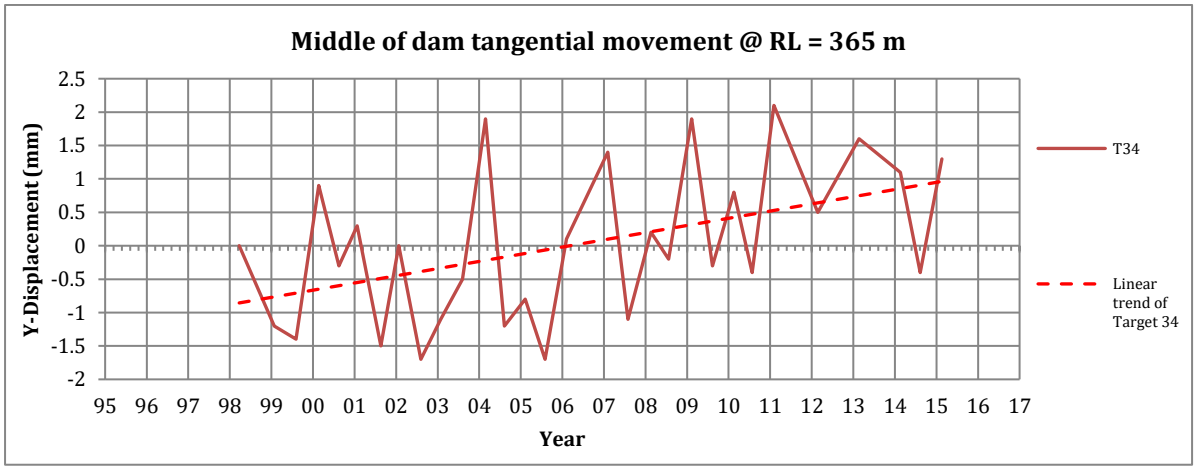

Figure 5-26: Tangential movements of T34 at Poortjieskloof Dam

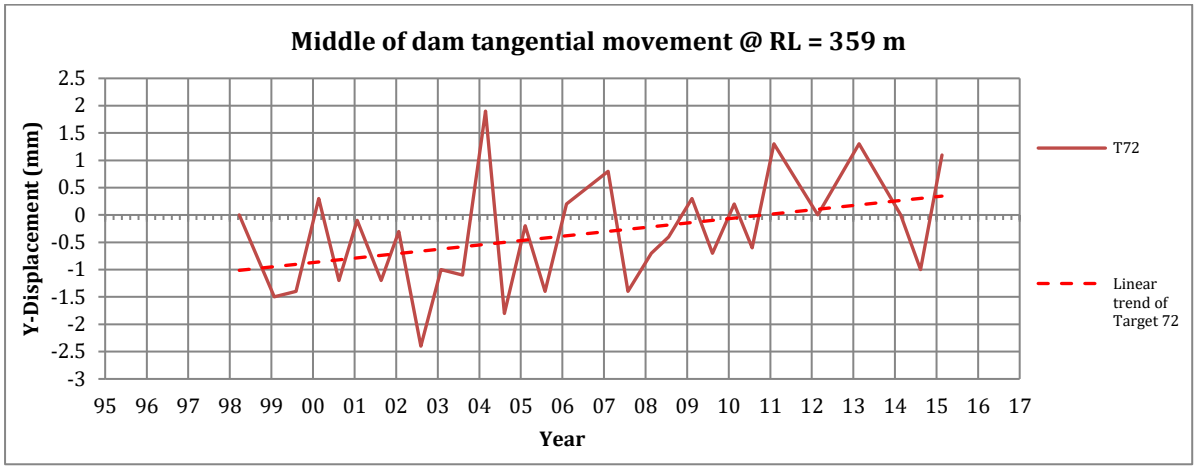

Figure 5-27: Tangential movements of T72 at Poortjieskloof Dam

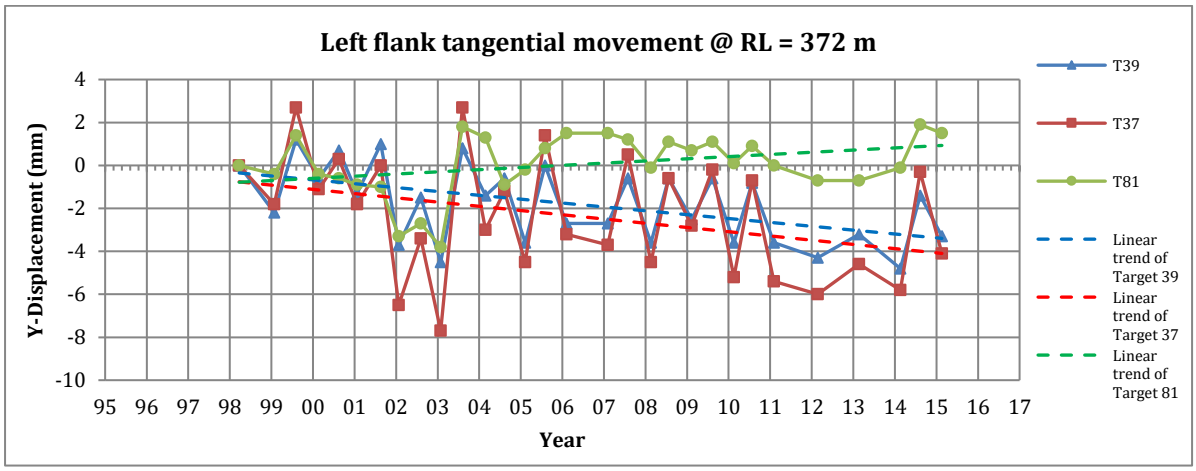

Figure 5-28: Tangential movements of T39, T37 and T81 at Poortjieskloof Dam

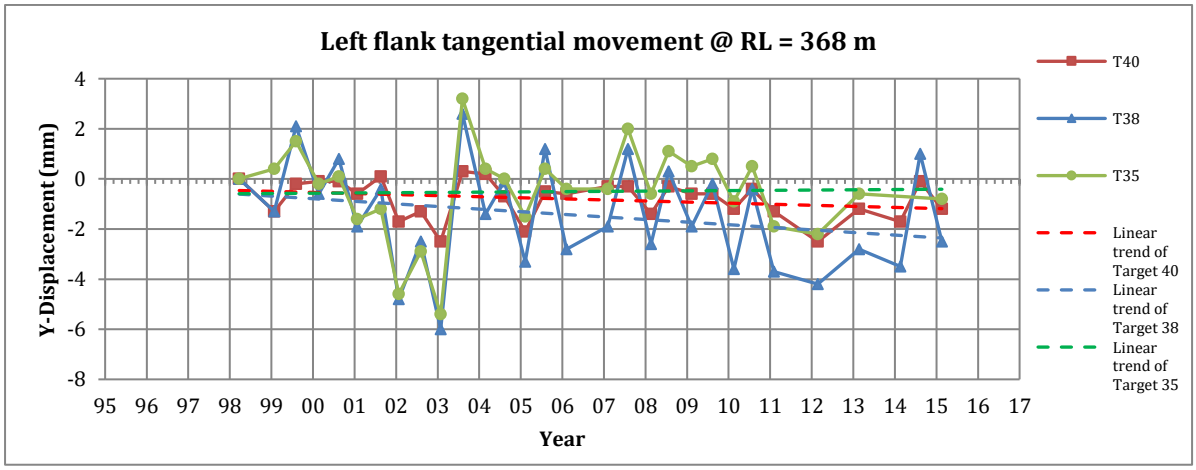

Figure 5-29: Tangential movements of T40, T38 and T35 at Poortjieskloof Dam

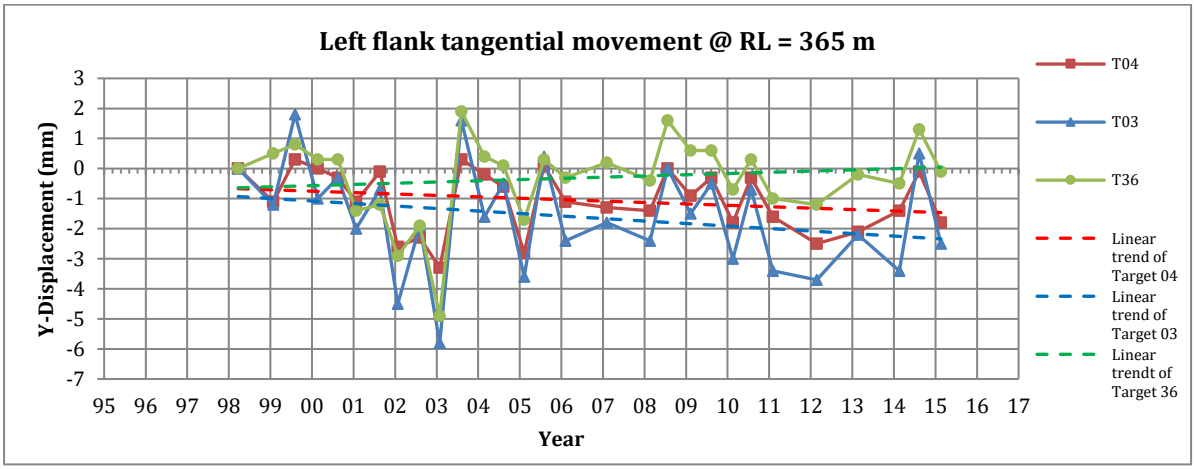

Figure 5-30: Tangential movements of T04, T03 and T36 at Poortjieskloof Dam

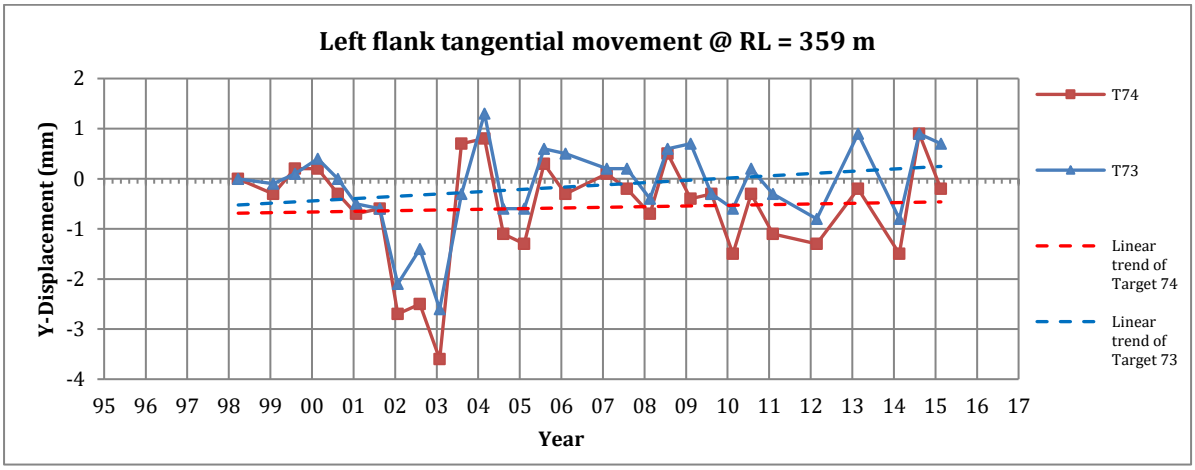

Figure 5-31: Tangential movements of T74 and T73 at Poortjieskloof Dam

The right flank targets display a definite trend of permanent displacement towards the right flank. T29 (RL = 372 m), T30 (RL = 368 m) and T02 (RL = 365 m) which are all located on Block 7 (the approximate quarter point of the arch from the right flank), display the biggest permanent trends - permanent trends do not exceed 7 mm. (Refer Figure 5-21 to Figure 5-24).

The targets located in the middle of the arch dam display a slight trend of permanent movement in the direction of the right flank. Permanent trends are very small and do not exceed 2 mm. (Refer Figure 5-25 to Figure 5-27).

Some of the left flank targets display a definite trend of permanent displacement towards the left flank - although less prominent than the right flank. T37, T38 and T03 which are all located on Block 3 (the approximate quarter point of the arch from the left flank), display the biggest permanent trends toward the left flank - permanent trends do not exceed 4 mm.

In summary, these results prove that there is a permanent swelling action toward both abutments, with the quarter points of each flank showing the biggest permanent trends.

5.3.2. Radial Movements

The radial movements are movements that are measured in an upstream or downstream direction. Figure 5-32 to Figure 5-42 provide the radial movements for all the targets since 1998 and positive values indicate movement in a downstream direction. “T” is short for “Target”.

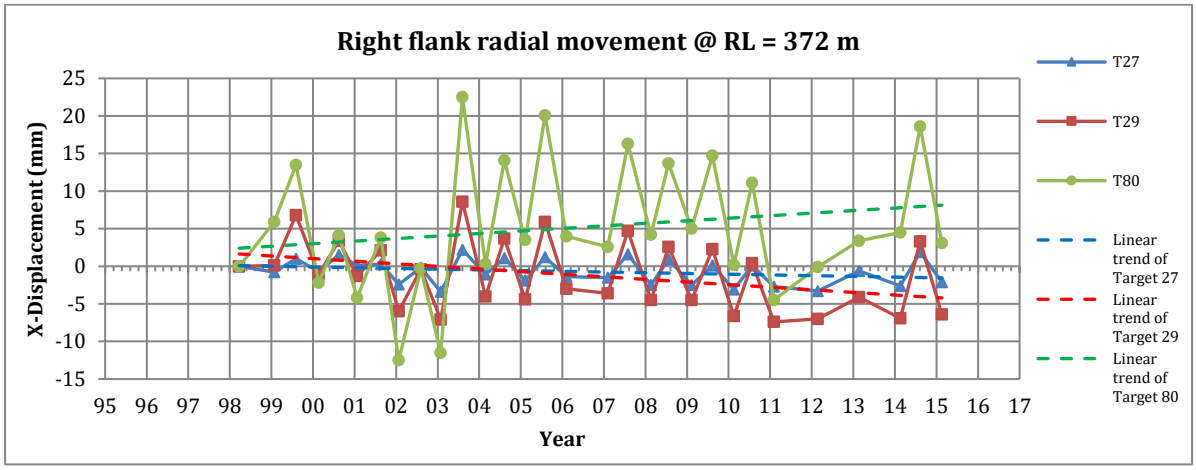

Figure 5-32: Radial movements of T27, T29 and T80 at Poortjieskloof Dam

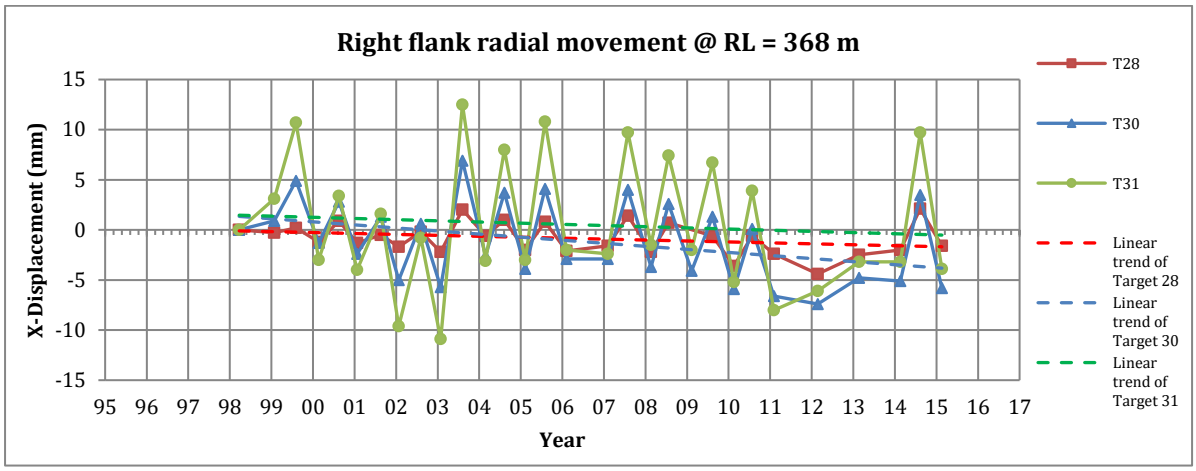

Figure 5-33: Radial movements of T28, T30 and T31 at Poortjieskloof Dam

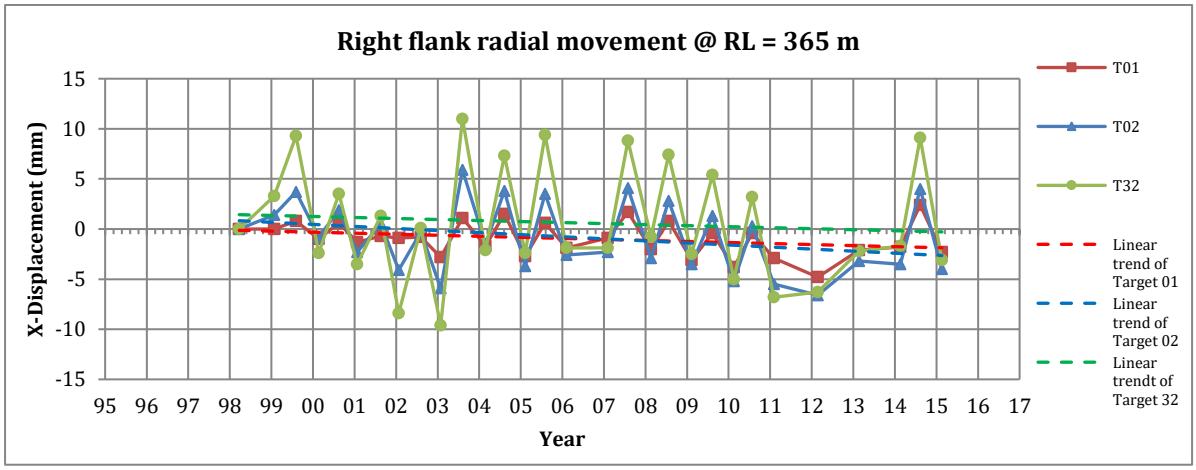

Figure 5-34: Radial movements of T01, T02 and T32 at Poortjieskloof Dam

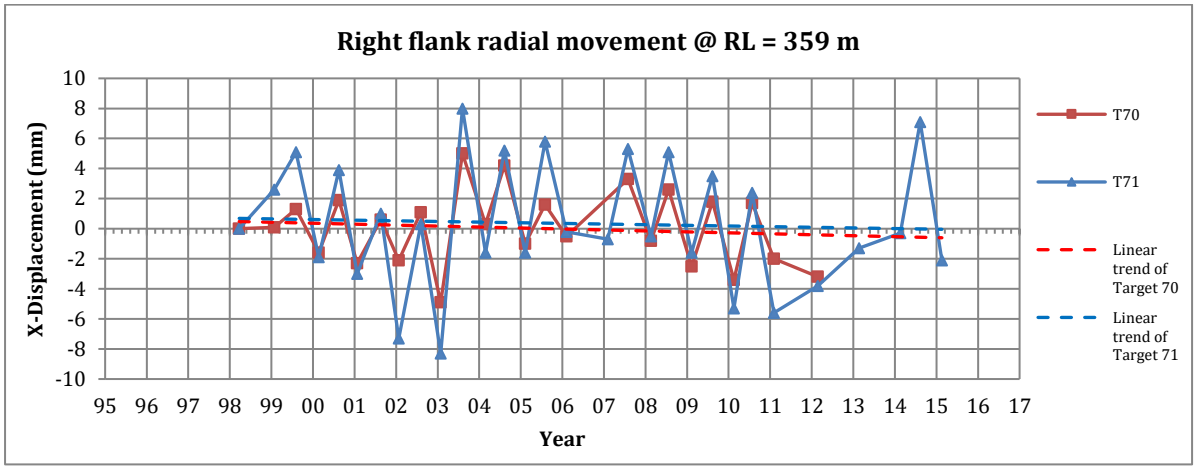

Figure 5-35: Radial movements of T70 and T71 at Poortjieskloof Dam

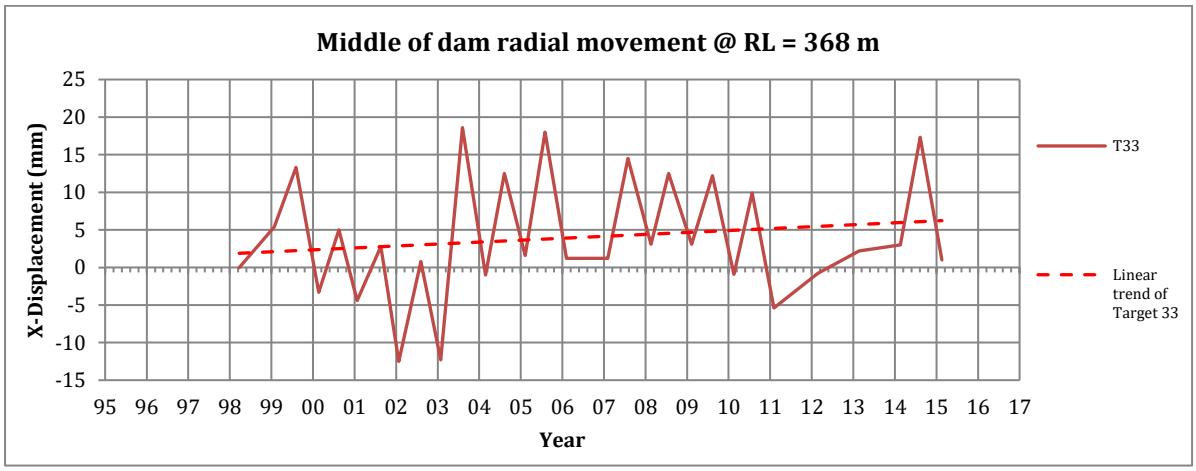

Figure 5-36: Radial movements of T33 at Poortjieskloof Dam

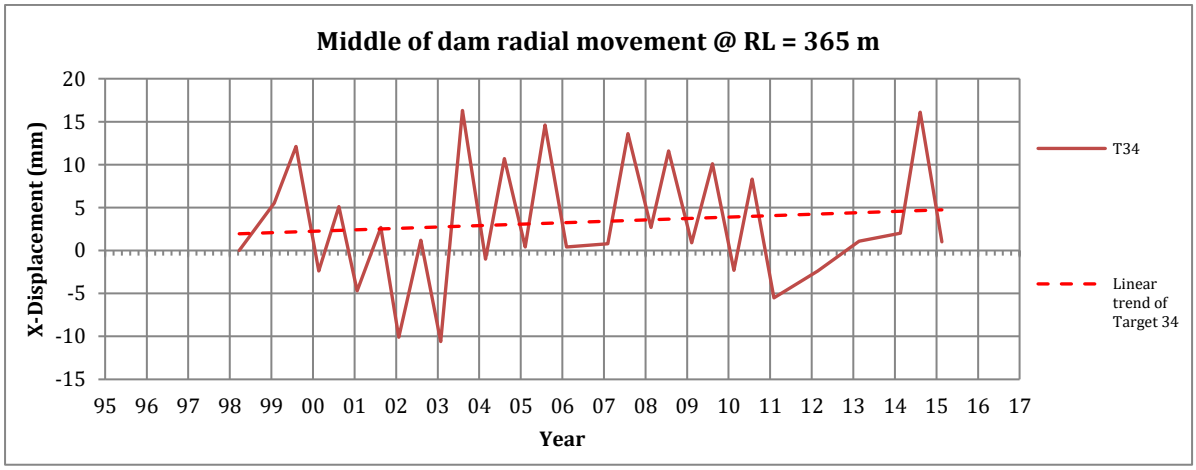

Figure 5-37: Radial movements of T34 at Poortjieskloof Dam

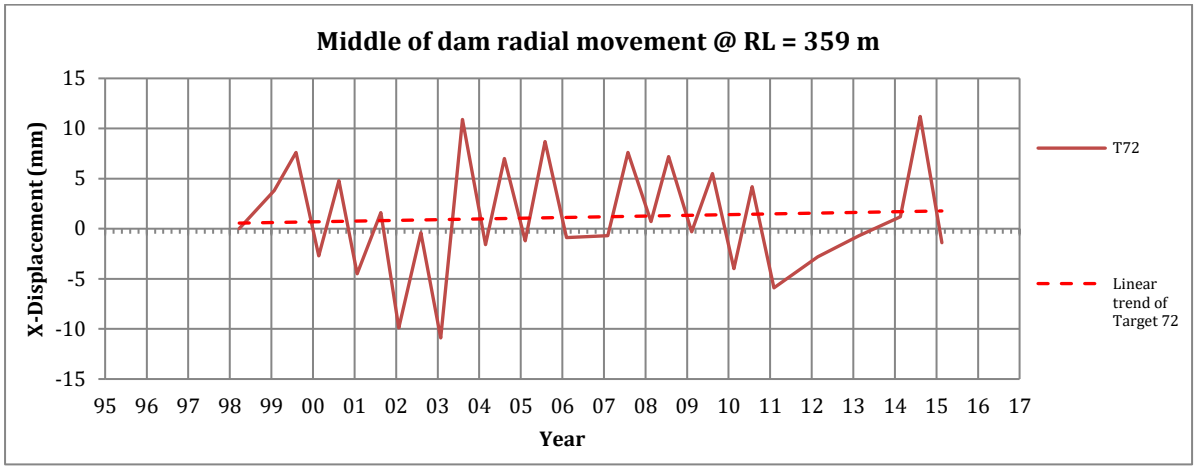

Figure 5-38: Radial movements of T72 at Poortjieskloof Dam

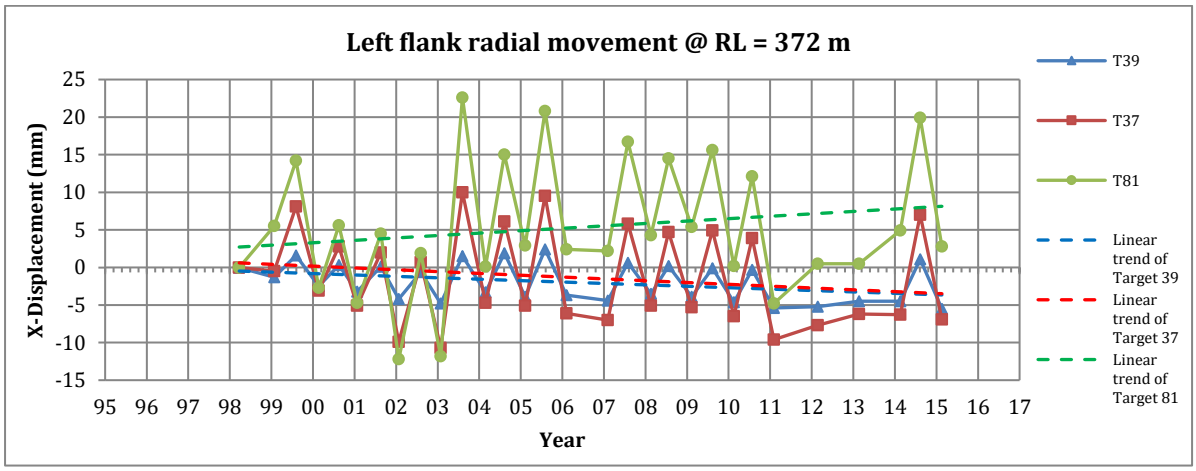

Figure 5-39: Radial movements of T39, T37 and T81 at Poortjieskloof Dam

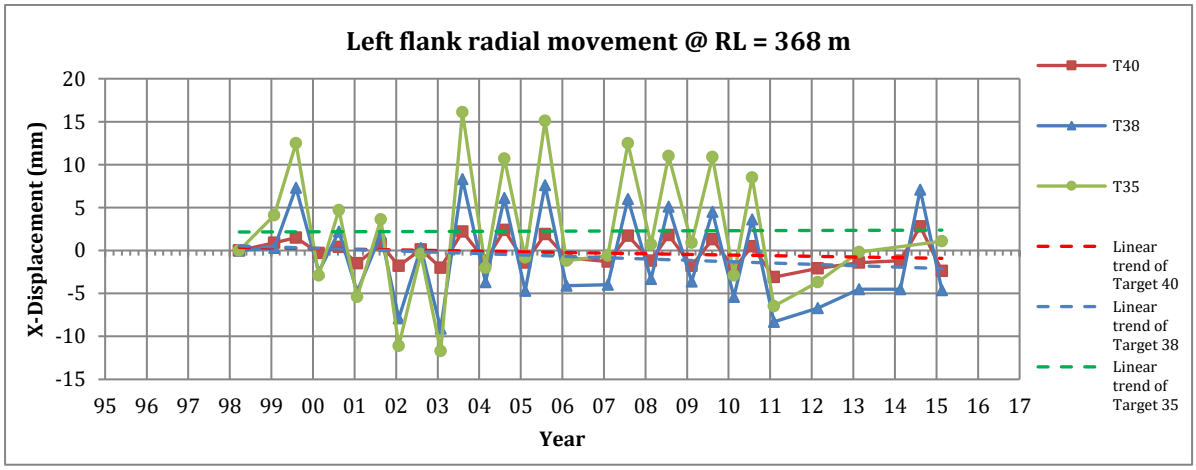

Figure 5-40: Radial movements of T40, T38 and T35 at Poortjieskloof Dam

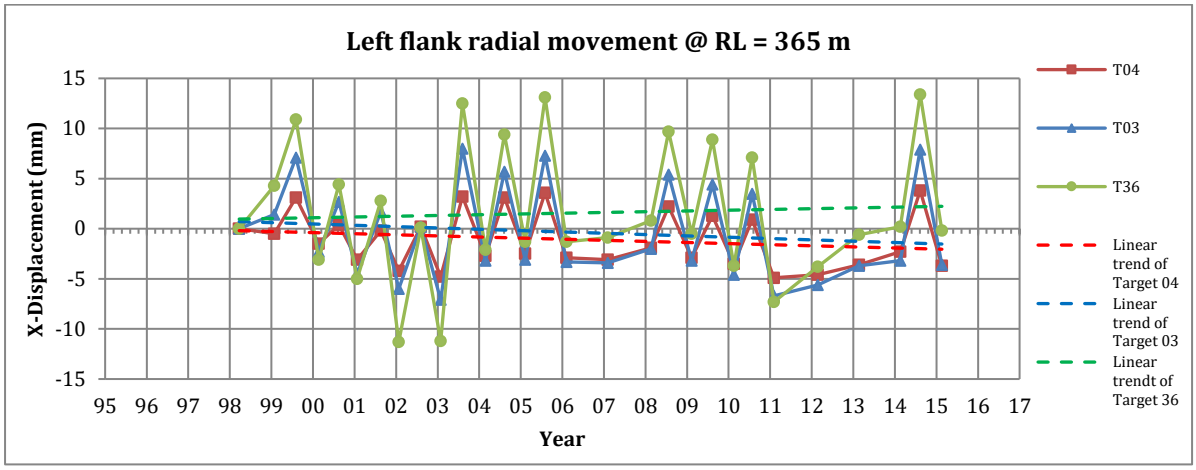

Figure 5-41: Radial movements of T04, T03 and T36 at Poortjieskloof Dam

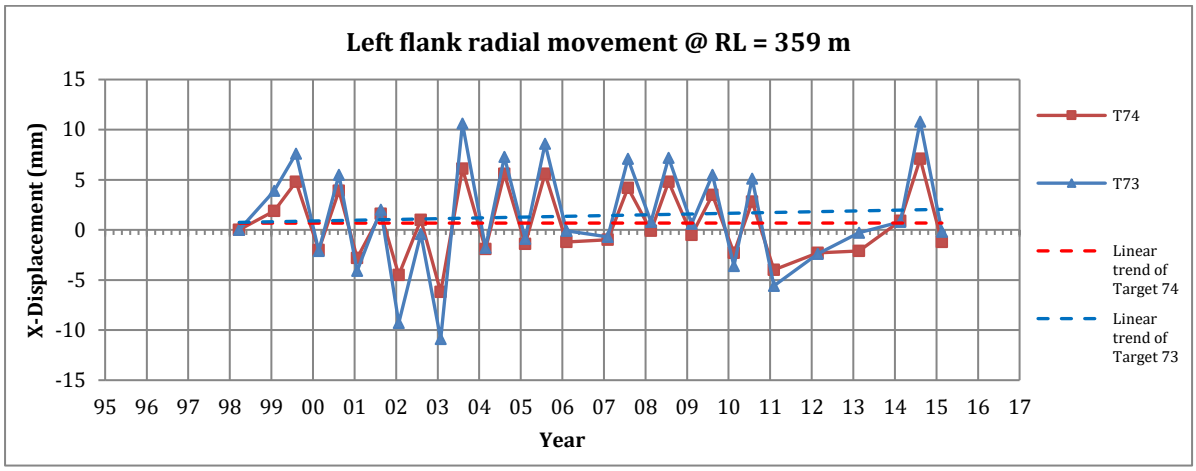

Figure 5-42: Radial movements of T74 and T73 at Poortjieskloof Dam

The right flank targets generally show a permanent upstream displacement trend, except for T80, which is located on the spillway splitter. T80 displays a downstream trend which does not exceed 5 mm. The targets on the upper sections (T27, T28, T29, and T30) located on Blocks 7 and 8 display the biggest permanent upstream trends. Trends do not exceed 5 mm. The targets on the lower sections display very small upstream trends that do not exceed 2 mm. The targets that are located closer to the middle (T31, T32, and T71) of the arch dam on Block 6 display much smaller upstream trends. (Refer Figure 5-32 to Figure 5-35).

The targets located in the middle of the arch dam (T33, T34, and T72) display a downstream trend. The largest downstream trends are higher up on the dam wall and the trend decreases with decreasing elevations. The largest trend (T33) does not exceed 5 mm and the smallest trend (T72) does not exceed 2 mm. (Refer Figure 5-36 to Figure 5-38).

The left flank targets generally show a permanent upstream displacement trend, except for T81, which is located on the spillway splitter. T81 displays a downstream trend which does not exceed 5 mm. The targets on the upper sections (T37, T38, T39, and T40) located on Blocks 2 and 3 display the biggest permanent upstream trends. Trends do not exceed 5 mm. The targets on the lower sections display very small trends that do not exceed 2 mm. The targets that are located closer to the middle (T35, T36, and T73) of the arch dam on Block 4 display very small downstream trends. Trends smaller than 2 mm. (Refer Figure 5-39 to Figure 5-42).

In summary these results suggest that both flanks are moving permanently in an upstream direction with the quarter points of each flank showing the biggest permanent trends. The middle of the arch dam is however showing permanent downstream trends. These movements suggest the ongoing presence of AAR-related swelling.

5.3.3. Vertical Movements

The measurements of vertical movements show trends of increasing or decreasing elevation. Figure 5-43 to Figure 5-53 provide the vertical movements for all the targets since 1998. Positive values indicate rising crest elevations. "T" is short for "Target".

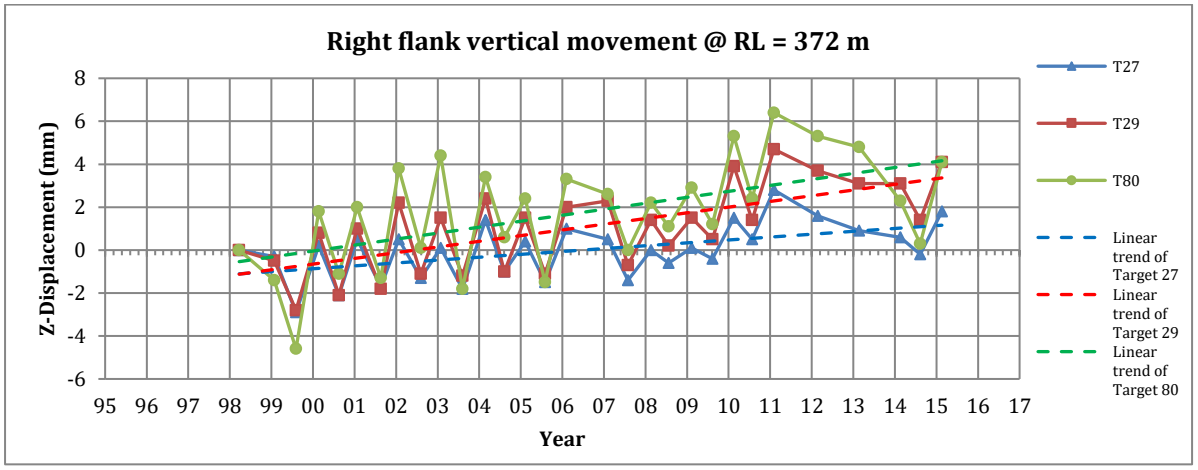

Figure 5-43: Vertical movements of T27, T29 and T80 at Poortjieskloof Dam

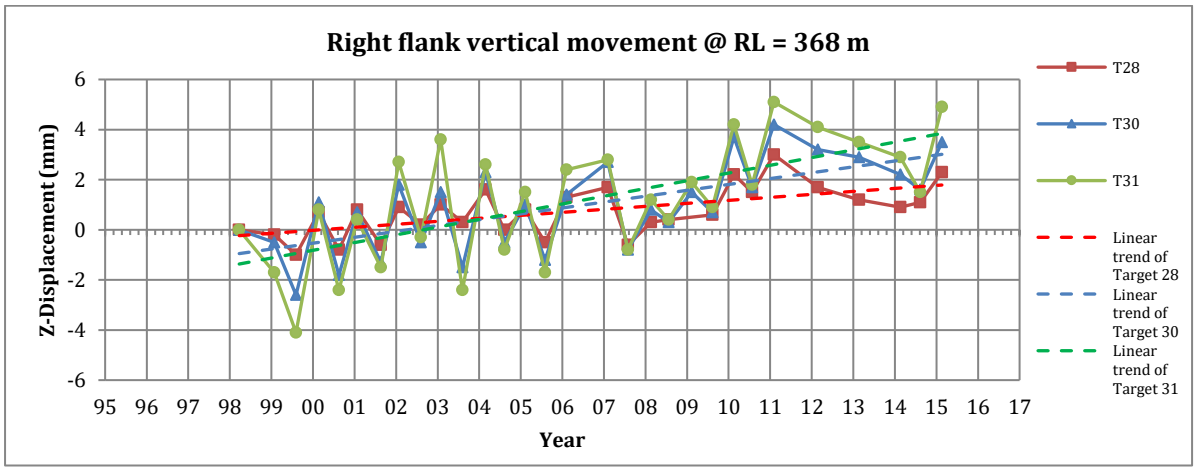

Figure 5-44: Vertical movements of T28, T30 and T31 at Poortjieskloof Dam

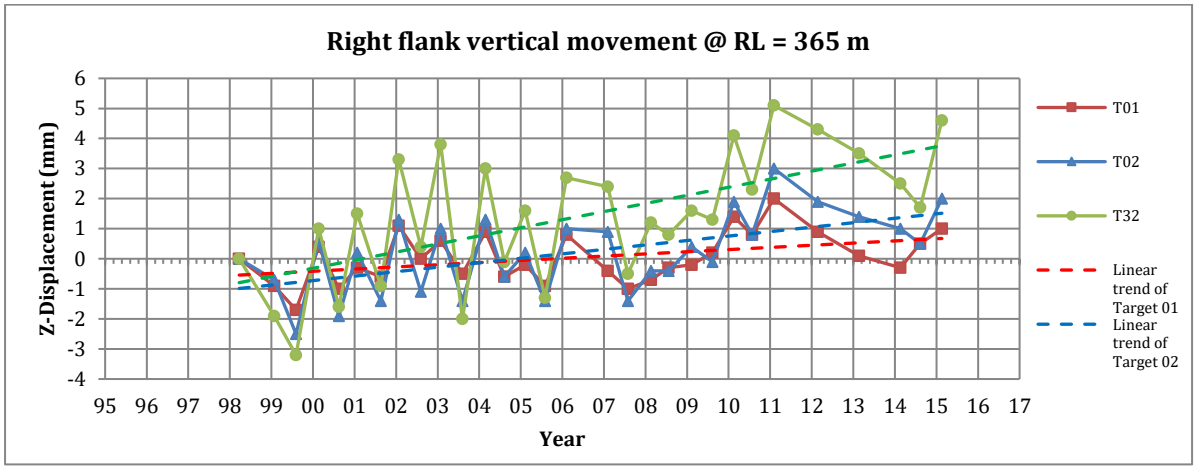

Figure 5-45: Vertical movements of T01, T02 and T32 at Poortjieskloof Dam

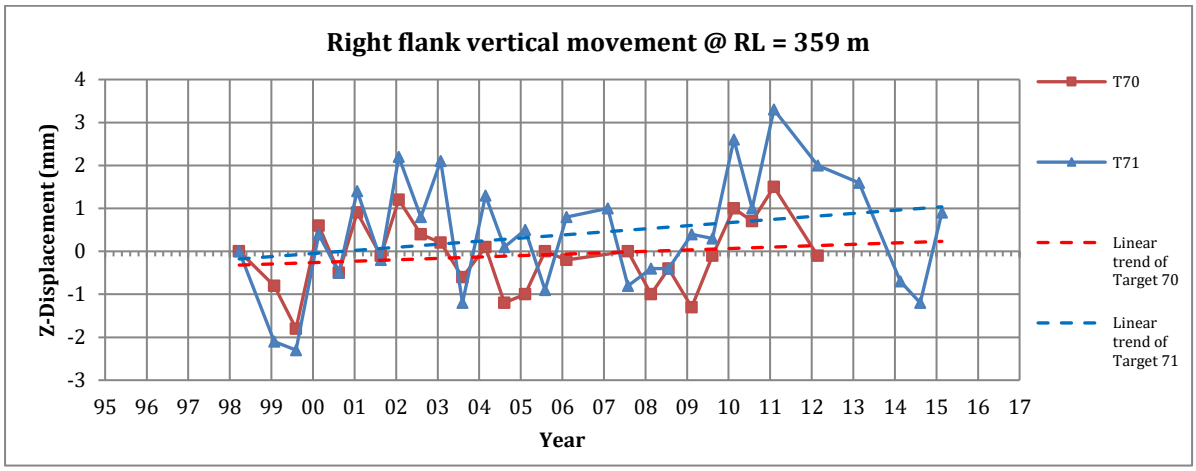

Figure 5-46: Vertical movements of T70 and T71 at Poortjieskloof Dam

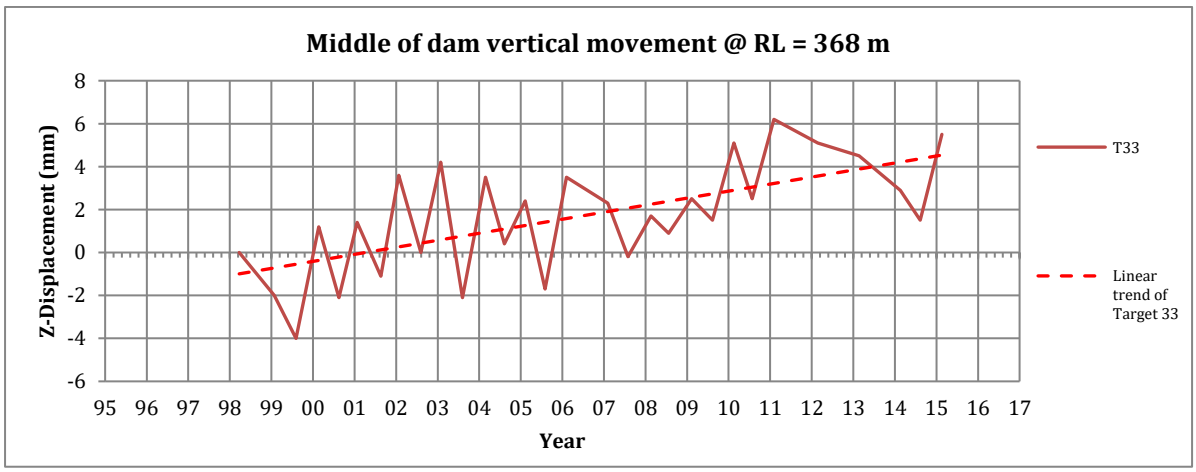

Figure 5-47: Vertical movements of T33 at Poortjieskloof Dam

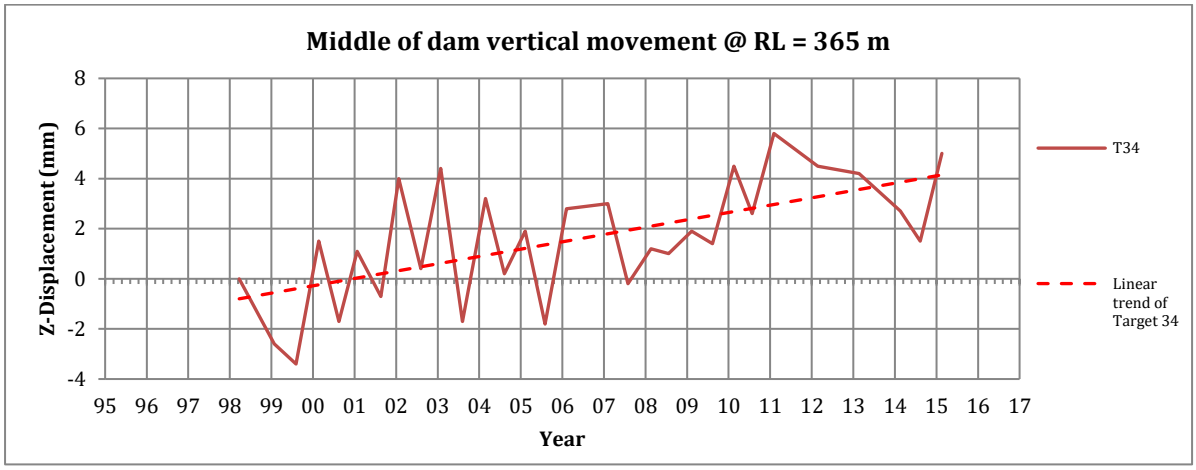

Figure 5-48: Vertical movements of T34 at Poortjieskloof Dam

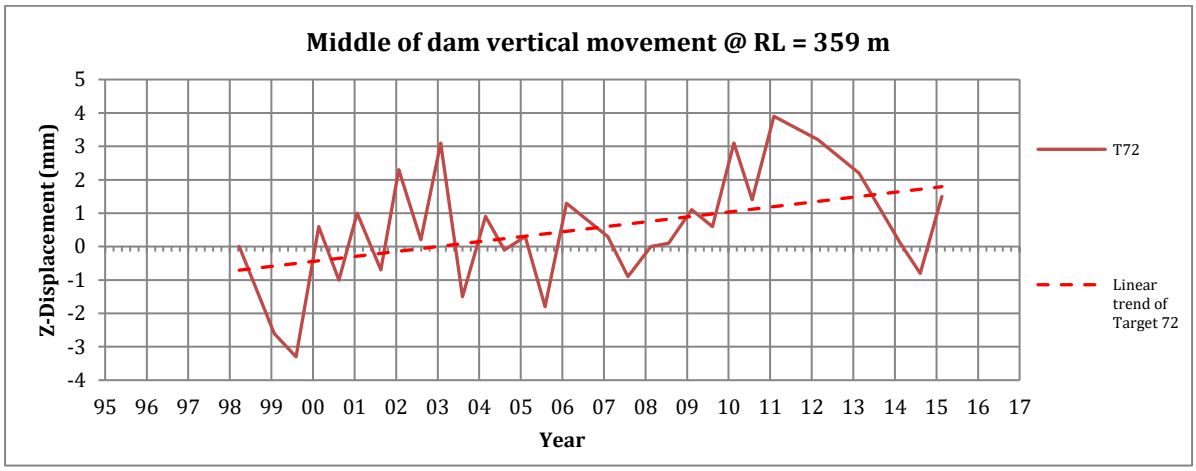

Figure 5-49: Vertical movements of T72 at Poortjieskloof Dam

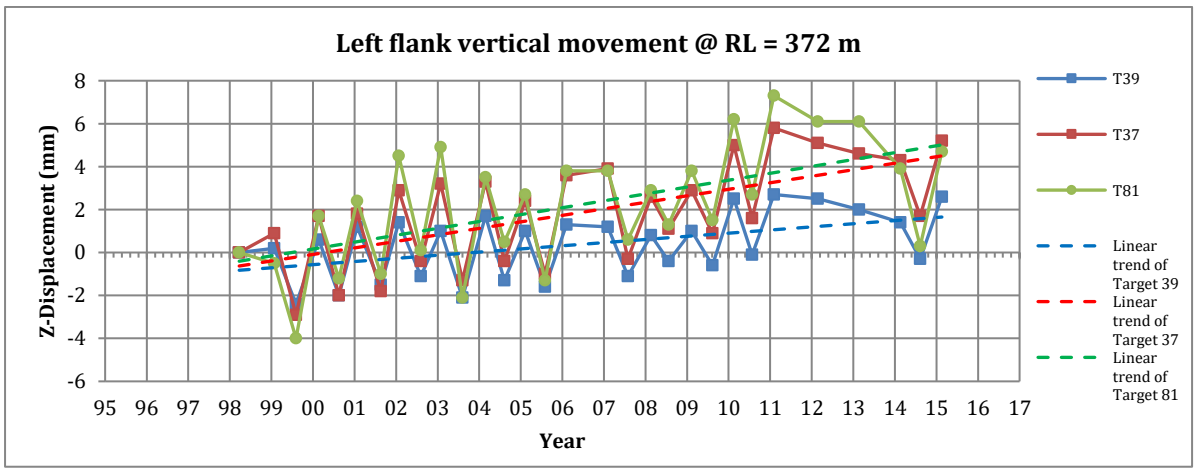

Figure 5-50: Vertical movements of T39, T37 and T81 at Poortjieskloof Dam

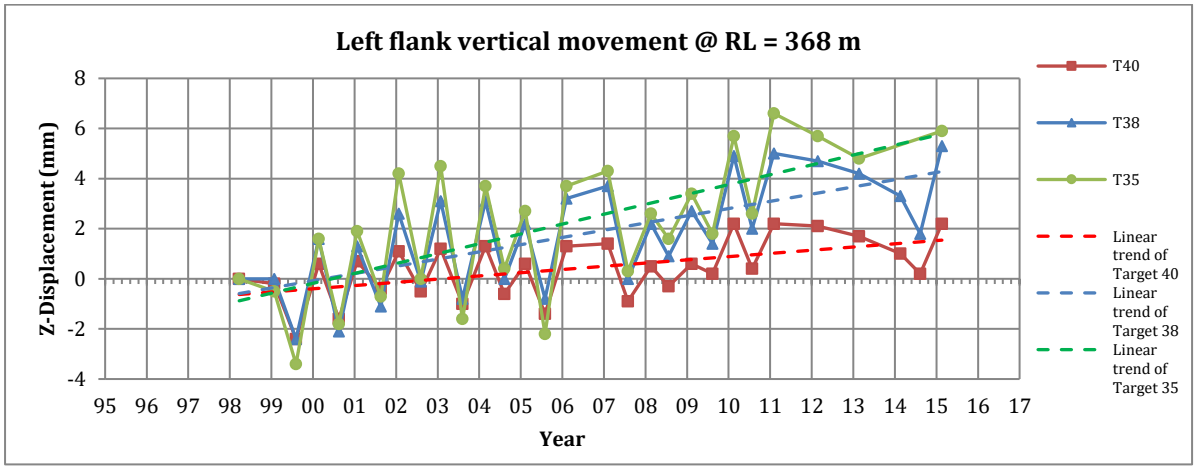

Figure 5-51: Vertical movements of T40, T38 and T35 at Poortjieskloof Dam

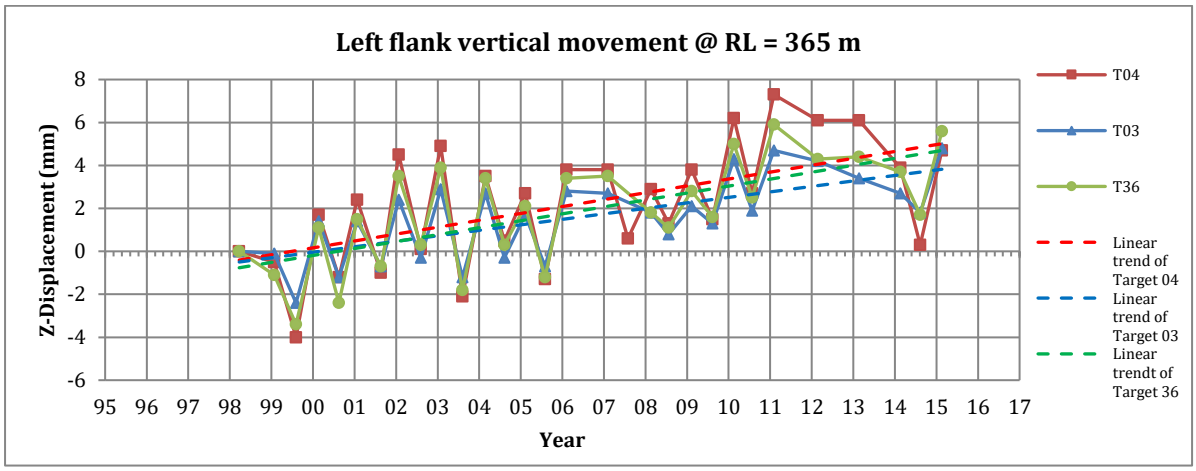

Figure 5-52: Vertical movements of T04, T03 and T36 at Poortjieskloof Dam

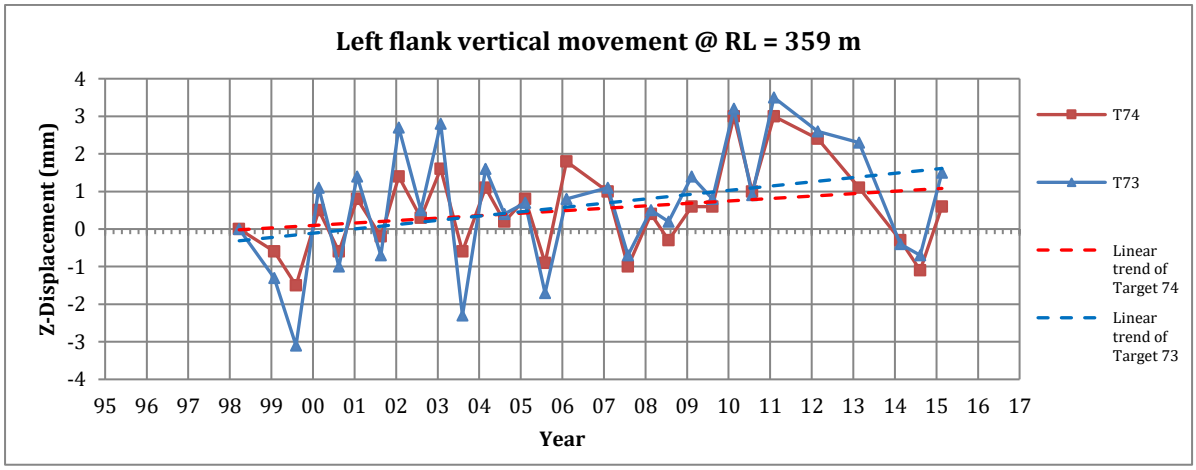

Figure 5-53: Vertical movements of T74 and T73 at Poortjieskloof Dam

The right flank targets generally show trends of permanent rising elevation levels. The targets located on the spillway splitter (T80) and Block 6 (T31, T32) display the largest permanent trends. Trends do not exceed 6 mm. The targets located closer to the right abutment on Block 7 (T02, T29, and T30) display smaller permanent trends. Trends do not exceed 4 mm. The targets on RL 359 m (T70, T71) display the smallest trends - all less than 2 mm. (Refer Figure 5-43 to Figure 5-46).

The targets located in the middle of the arch dam show trends of permanent rising elevation levels. The upper targets display the largest trends. T33 displays a permanent rise of about 6

mm and T34 a permanent rise of about 5 mm. T72 on RL 359 m displays the smallest trend (less than 3 mm). (Refer Figure 5-47 to Figure 5-49).

The right flank targets generally show trends of permanent rising elevation levels. The targets located on the spillway splitter (T81) and Block 4 (T35, T36) display the largest permanent trends. These trends do not exceed 7 mm. The targets located closer to the left abutment on Blocks 2 & 3 (T03, T04, T37, and T38) display similar permanent trends. These trends do not exceed 6 mm. The targets on RL 359 m (T70, T71) display the smallest trends - all less than 2 mm. (Refer Figure 5-50 to Figure 5-53).

5.4. Crack Width Gauges

Vinchon 3-D crack width gauges were installed at several locations on the dam wall during 1984. During March 1995, several more 3-D crack width gauges were installed (Hagen, 1996). The results that are considered in this study are readings taken from 20 *DWAF95* and 23 *DWAF94* crack width gauges. The record of readings starts in 1997.

5.4.1. Vertical Joints on Left Flank Crest

The vertical joints on the left flank crest are monitored by crack width gauges K1, K2, K6 and K7. K1 (upstream side of crest) and K2 (downstream side of crest) monitor the movements between Block 2 and 3 and K6 (downstream side of crest) and K7 (upstream side of crest) monitor the movements between Block 1 and 2. The radial movement results are shown in Figure 5-54, the tangential movement results in Figure 5-55 and the vertical movement results in Figure 5-56.

Legend for positive directions (left and right as viewed from the upstream side):

- Radial = the block on the right side moves downstream relative to the block on the left side
- Tangential = the joint opening increases
- Vertical = the block on the right side moves upward relative to the block on the left side

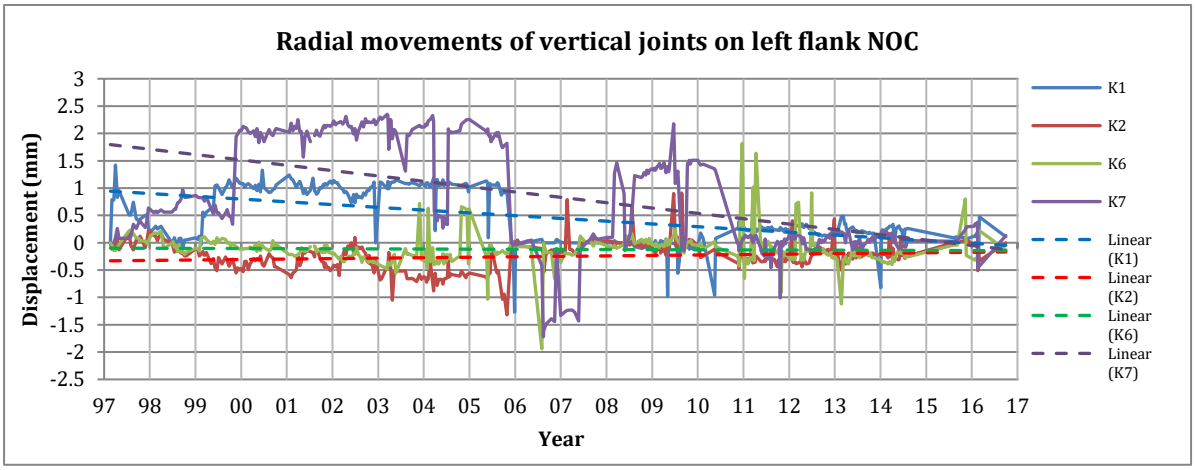

Figure 5-54: Radial movements of the vertical joints on the left flank NOC

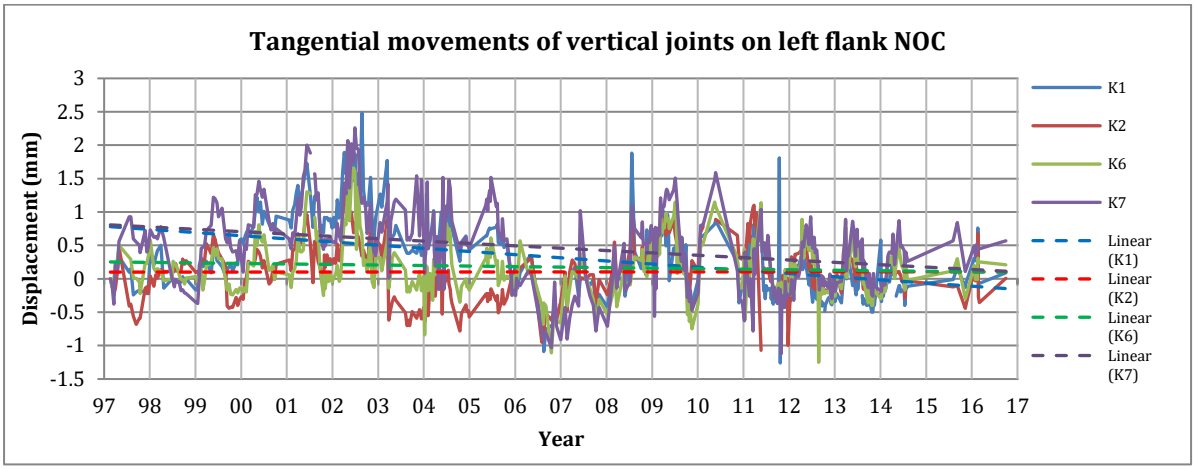

Figure 5-55: Tangential movements of the vertical joints on the left flank NOC

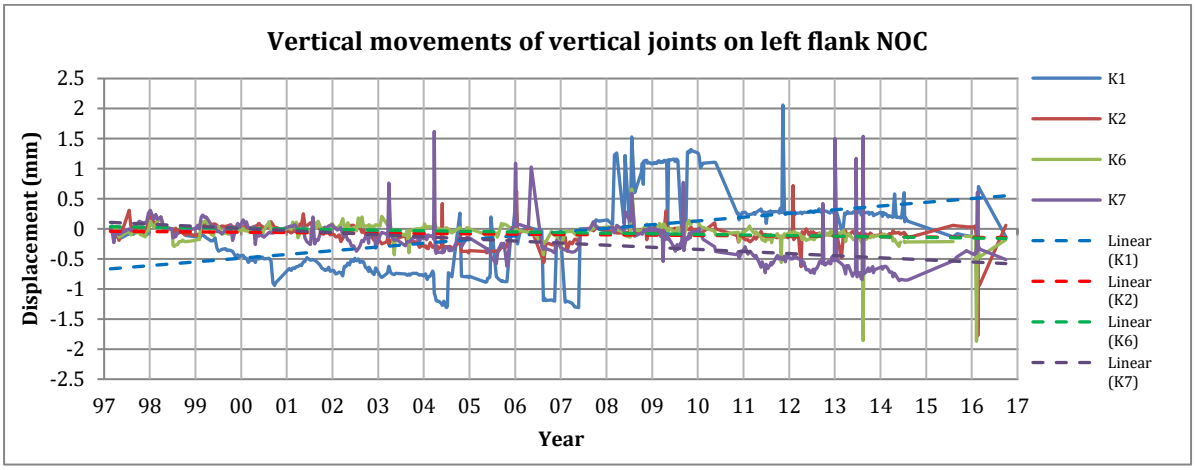

Figure 5-56: Vertical movements of the vertical joints on the left flank NOC

The radial measurements of K2 and K6 show little to no trends while the radial measurements of K1 and K7 show an upstream movement trend of the blocks (see Figure 5-54). The tangential measurements show that the joints seem to be closing generally with K1 and K7 displaying largest trends (see Figure 5-55). The vertical measurements show that Block 2 settled slightly relative to Block 1 and Block 3 shows a rising trend relative to Block 2 (see Figure 5-56). K1 and K7 display the largest trends.

5.4.2. Vertical Joints on Right Flank Crest

The vertical joints on the left flank crest are monitored by crack width gauges K33, K34, K36 and K42. K33 measures movements between Blocks 9 and 10, K34 measures movements between Blocks 8 and 9, K36 measures movements between Blocks 7 and 8, and K42 measures movements between Blocks 6 and 7. The radial movement results are shown in Figure 5-57, the tangential movement results in Figure 5-58 and the vertical movement results in Figure 5-59.

Legend for positive directions (left and right as viewed from the upstream side):

- Radial = the block on the right side moves downstream relative to the block on the left side
- Tangential = the joint opening increases
- Vertical = the block on the right side moves upward relative to the block on the left side

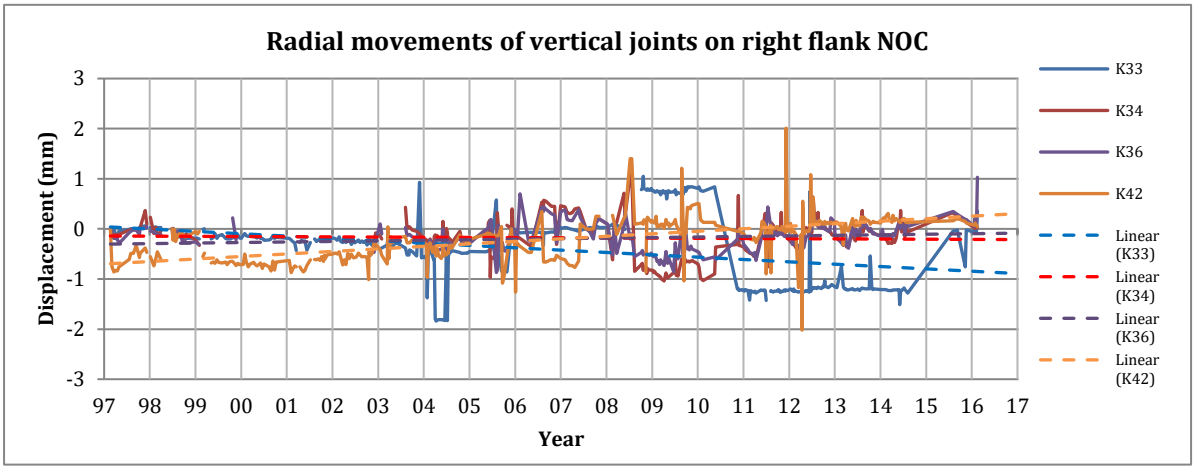

Figure 5-57: Radial movements of the vertical joints on the right flank NOC

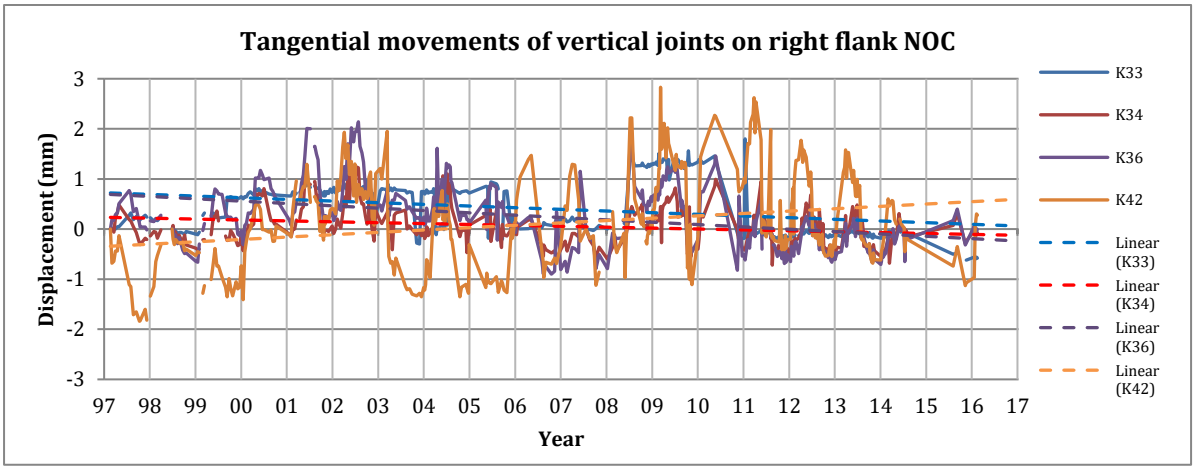

Figure 5-58: Tangential movements of the vertical joints on the right flank NOC

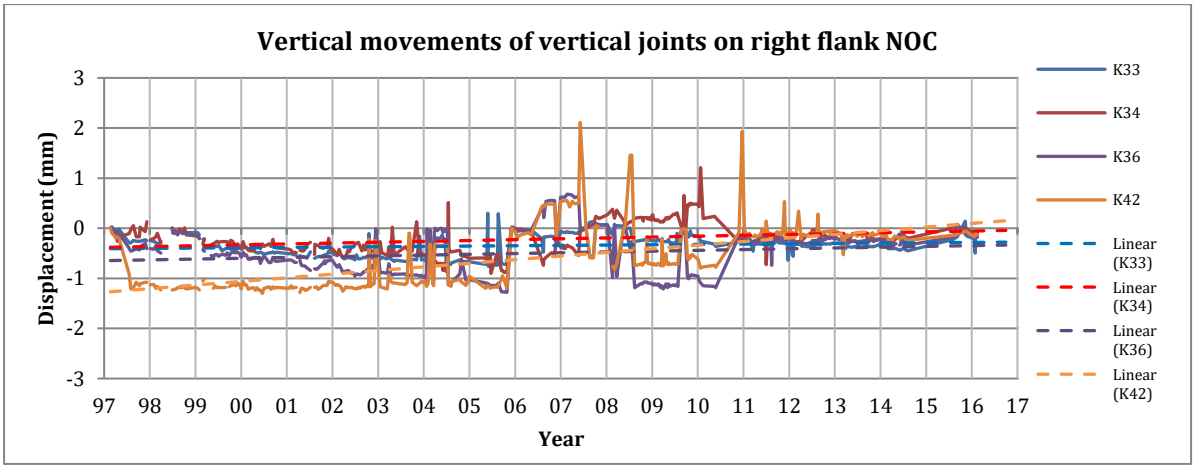

Figure 5-59: Vertical movements of the vertical joints on the right flank NOC

The radial measurements show little to no trends. If anything, the trend shows a slight upstream movement of the blocks (see Figure 5-57). The tangential measurements show that the joints seem to be closing generally toward the right flank with the exception of K42 (between Blocks 6 and 7) which shows an opening trend (see Figure 5-58). The vertical measurements show a trend of rising elevation (see Figure 5-59).

5.4.3. Vertical Joints Measured on Left Flank Downstream Face

The vertical joints on the left flank downstream face are monitored by several crack width gauges. Several of the crack width gauges have gaps in their record of readings. K8 measures movements between Blocks 1 and 2, K11 measures movements between Blocks 2 and 3, K16 measures movements between Blocks 3 and 4, and K24 measures movements between Blocks 4 and 5. The radial movement results are shown in Figure 5-60, the tangential movement results in Figure 5-61 and the vertical movement results in Figure 5-62.

Legend for positive directions (left and right as viewed from the upstream side):

- Radial = the block on the right side moves downstream relative to the block on the left side
- Tangential = the joint opening increases
- Vertical = the block on the right side moves upward relative to the block on the left side

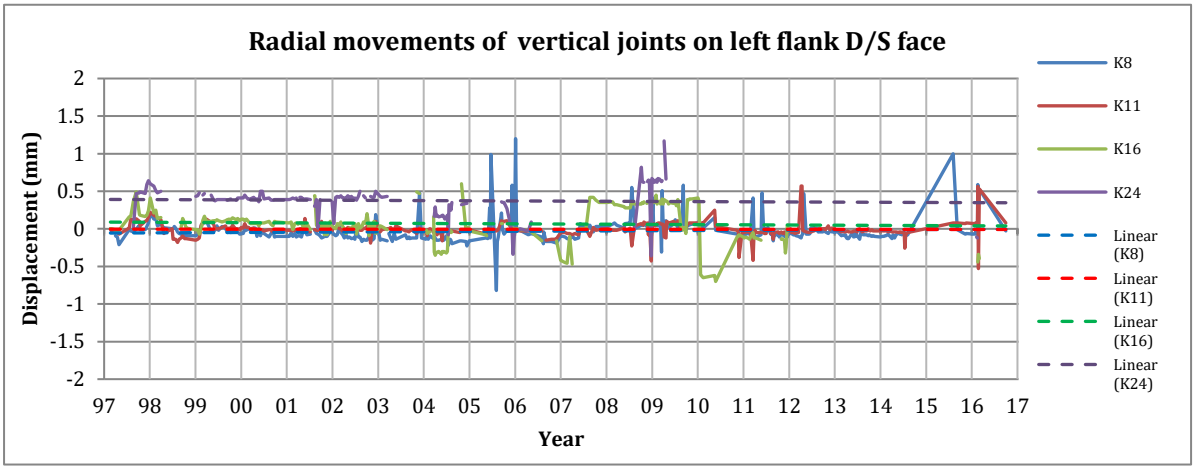

Figure 5-60: Radial movements of the vertical joints on the left flank downstream face

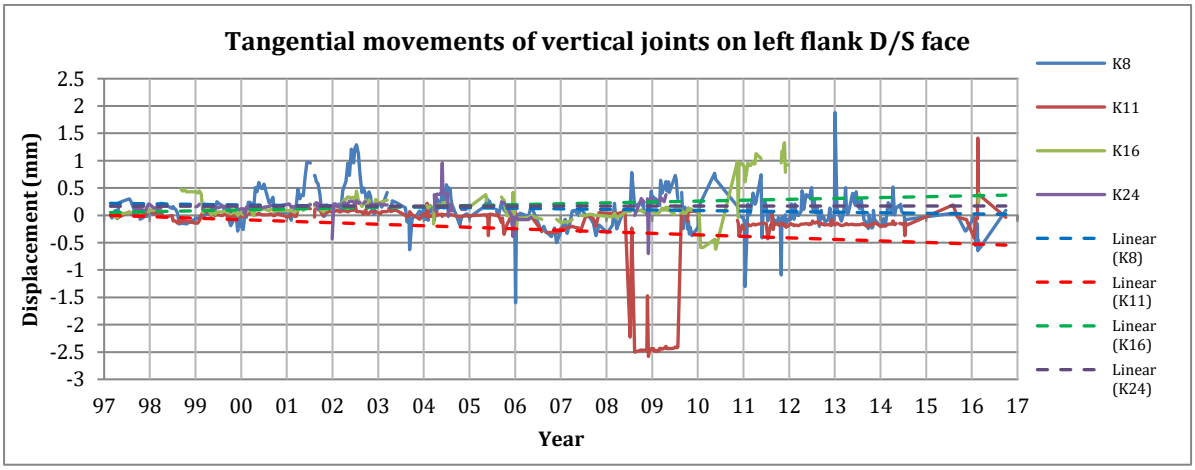

Figure 5-61: Tangential movements of the vertical joints on the left flank downstream face

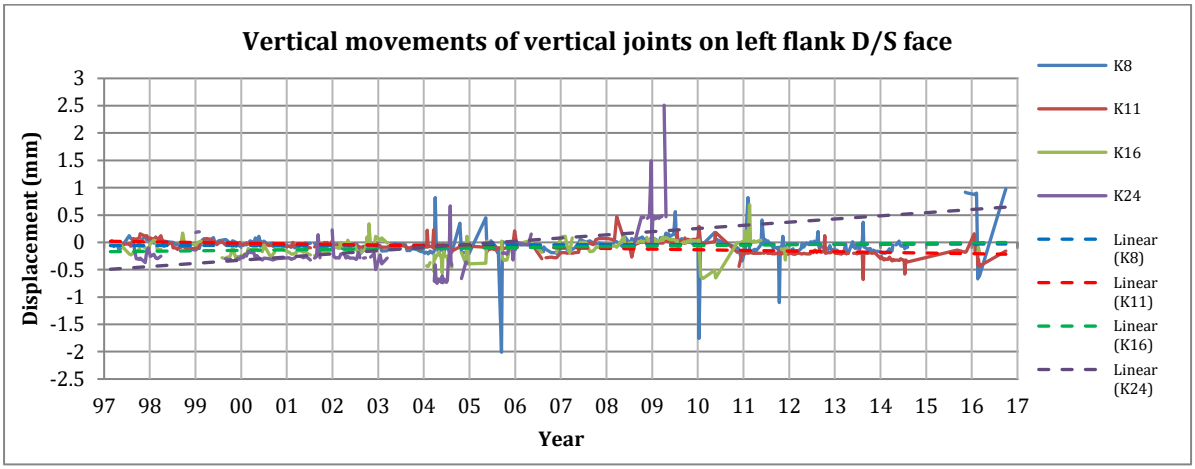

Figure 5-62: Vertical movements of the vertical joints on the left flank downstream face

The radial measurements show little to no trends (see Figure 5-60). The tangential measurements show little to no trends except for K11 which shows a slight closing of the joint (see Figure 5-61). The vertical measurements show little to no trends except for K24 which shows a slight rise in elevation of Block 5 relative to Block 4 (see Figure 5-62).

5.4.4. Vertical Joints Measured on Right Flank Downstream Face

The vertical joints on the right flank downstream face are monitored by several crack width gauges. Several of the crack width gauges have gaps in their record of readings. K26 measures movements between Blocks 5 and 6, K27 measures movements between Blocks 6 and 7, K29 measures movements between Blocks 7 and 8, K31 measures movements between Blocks 8 and 9, and K32 measures movements between Blocks 9 and 10. The radial movement results are shown in Figure 5-63, the tangential movement results in Figure 5-64 and the vertical movement results in Figure 5-65.

Legend for positive directions (left and right as viewed from the upstream side):

- Radial = the block on the right side moves downstream relative to the block on the left side
- Tangential = the joint opening increases
- Vertical = the block on the right side moves upward relative to the block on the left side

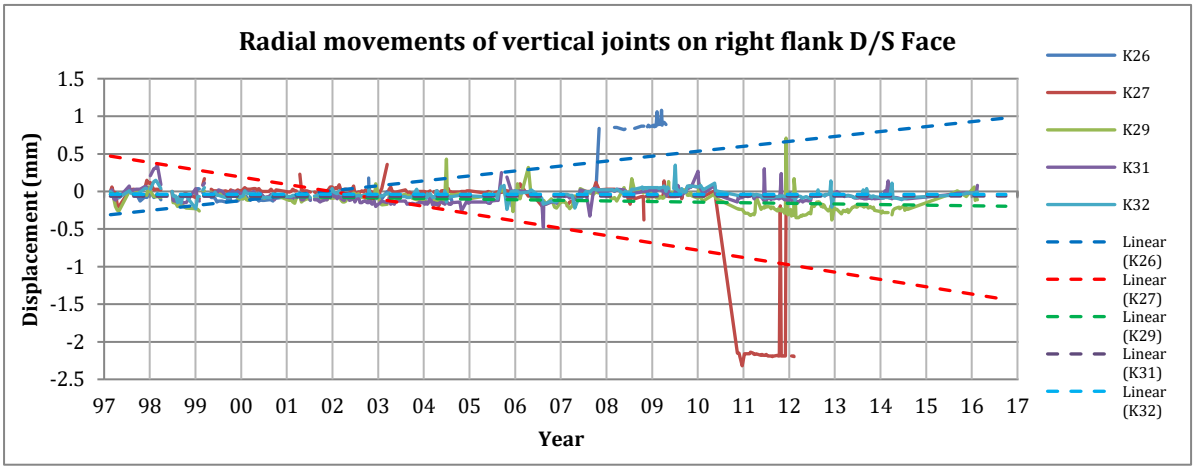

Figure 5-63: Radial movements of the vertical joints on the right flank downstream face

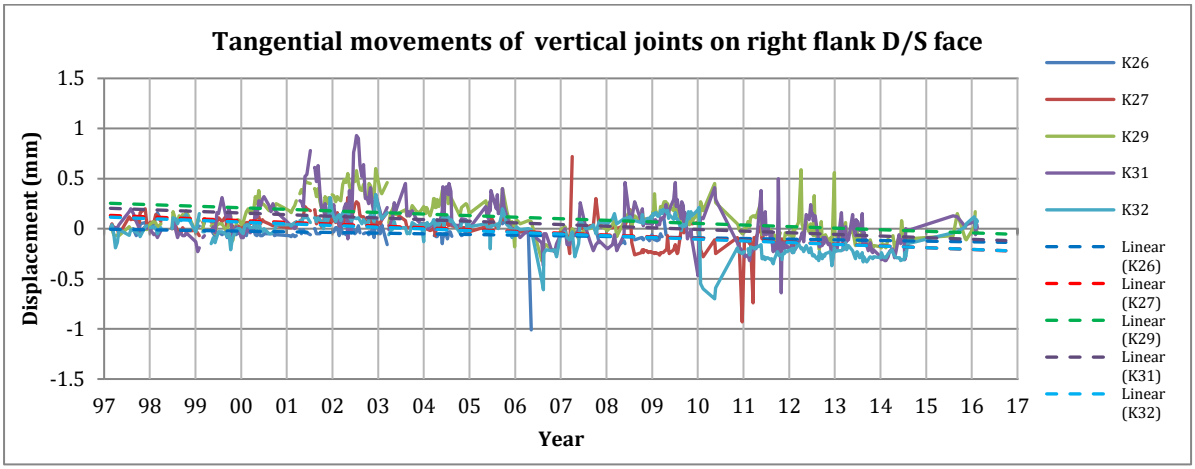

Figure 5-64: Tangential movements of the vertical joints on the right flank downstream face

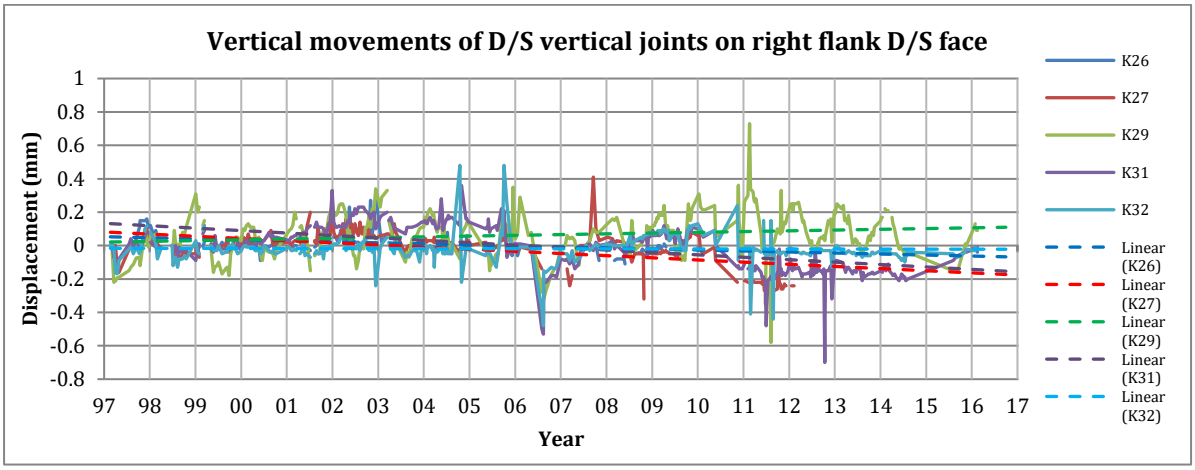

Figure 5-65: Vertical movements of the vertical joints on the right flank downstream face

The radial measurements show some erratic readings which make for unreliable trends in the readings of K26 and K27 (see Figure 5-63). Generally, there are no clear trends visible. The tangential measurements show that the joints have closed (see Figure 5-64). The vertical measurements show a slight drop in relative elevations with the exception of K29 (see Figure 5-65).

5.4.5. Horizontal Joints and Cracks Measured on the Downstream Face

Some horizontal joints and cracks joints on the downstream face are monitored by crack width gauges. Several of the crack width gauges have gaps in their record of readings. K14 and K15 measure horizontal joints on the downstream face of Block 3. K28 and K30 measure horizontal cracks on the downstream face of Blocks 7 and 8 respectively. The radial movement results are shown in Figure 5-66 and Figure 5-69, the tangential movement results in Figure 5-67 and Figure 5-70 and the vertical movement results in Figure 5-68 and Figure 5-71.

Legend for positive directions (left and right as viewed from the upstream side):

- Radial = the top lift moves downstream relative to the bottom lift
- Tangential = the top lift moves to the right relative to the bottom lift
- Vertical = the joint opening increases

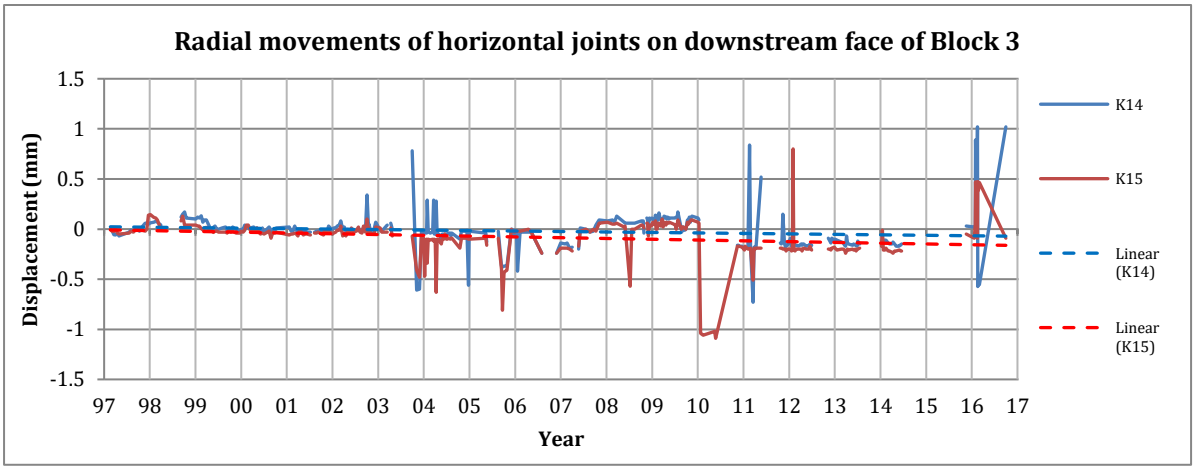

Figure 5-66: Radial movements of the horizontal joints on the downstream face of Block 3

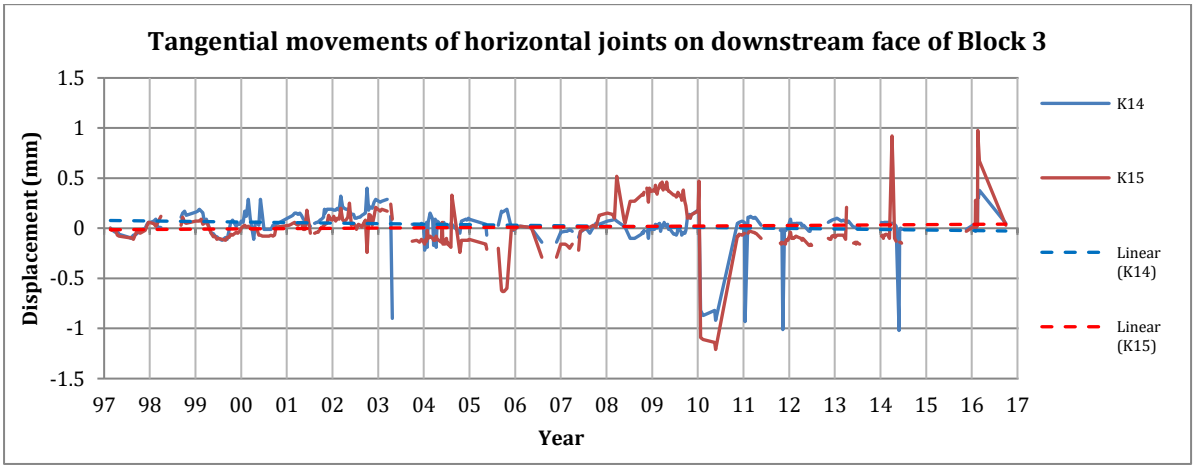

Figure 5-67: Tangential movements of the horizontal joints on the downstream face of Block 3

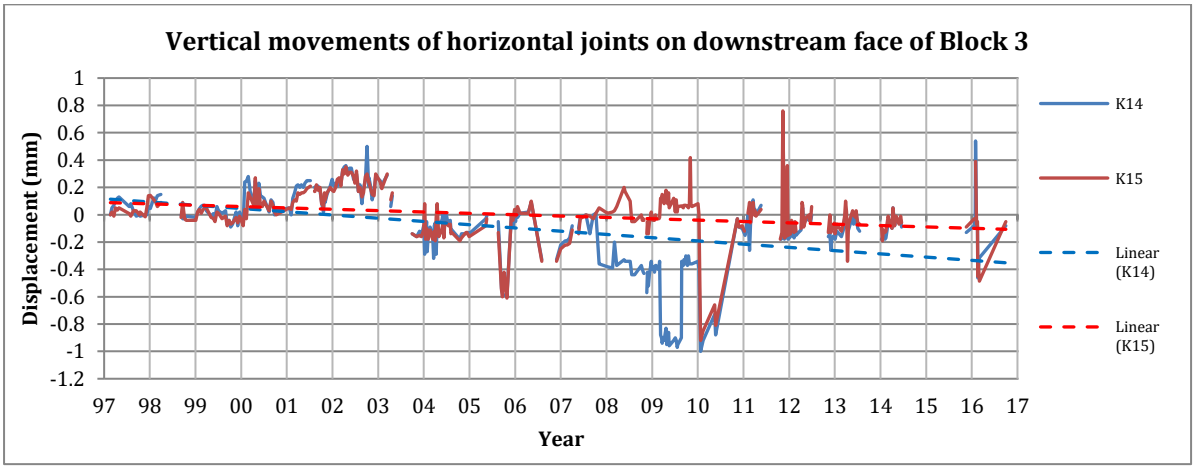

Figure 5-68: Vertical movements of the horizontal joints on the downstream face of Block 3

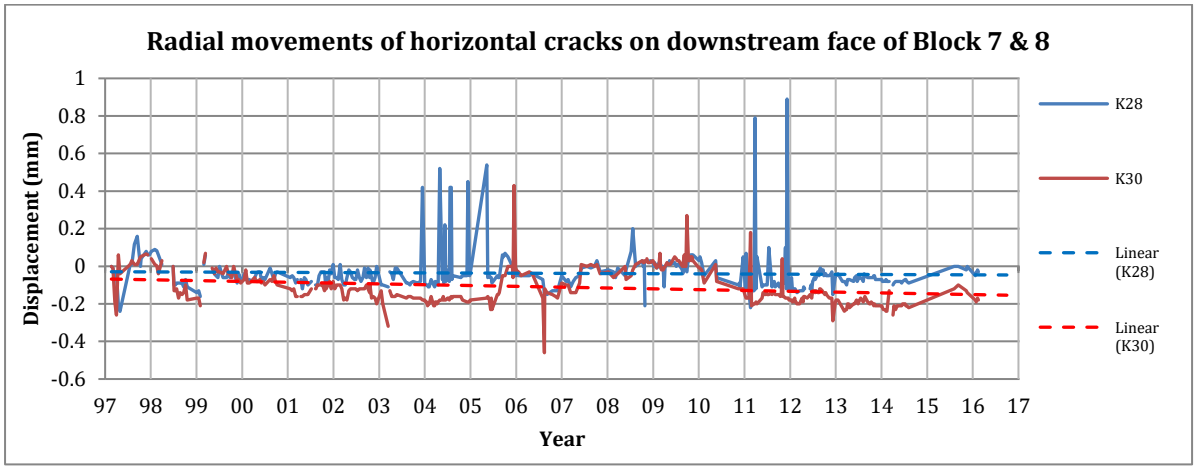

Figure 5-69: Radial movements of the horizontal cracks on the downstream face of Block 7 and 8

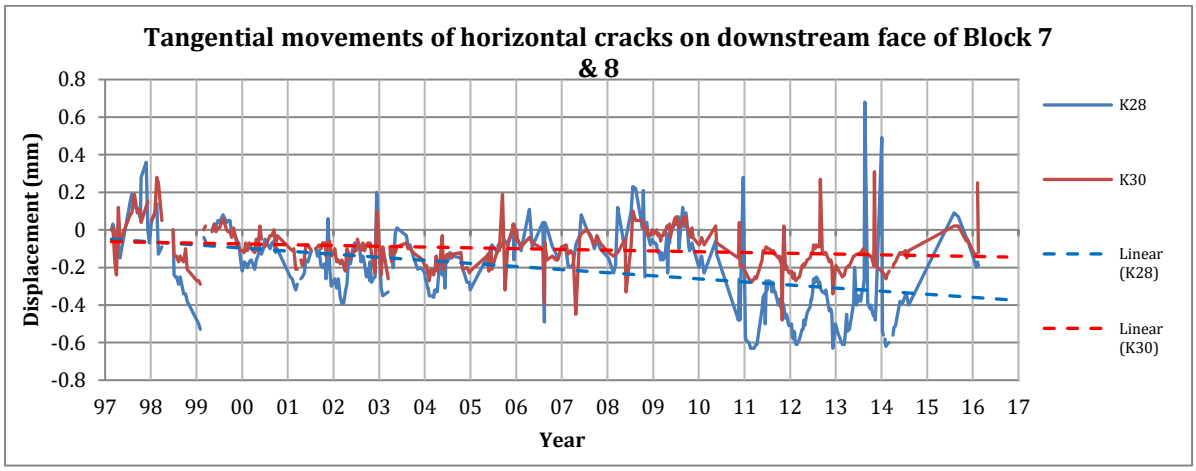

Figure 5-70: Tangential movements of the horizontal cracks on the downstream face of Block 7 and 8

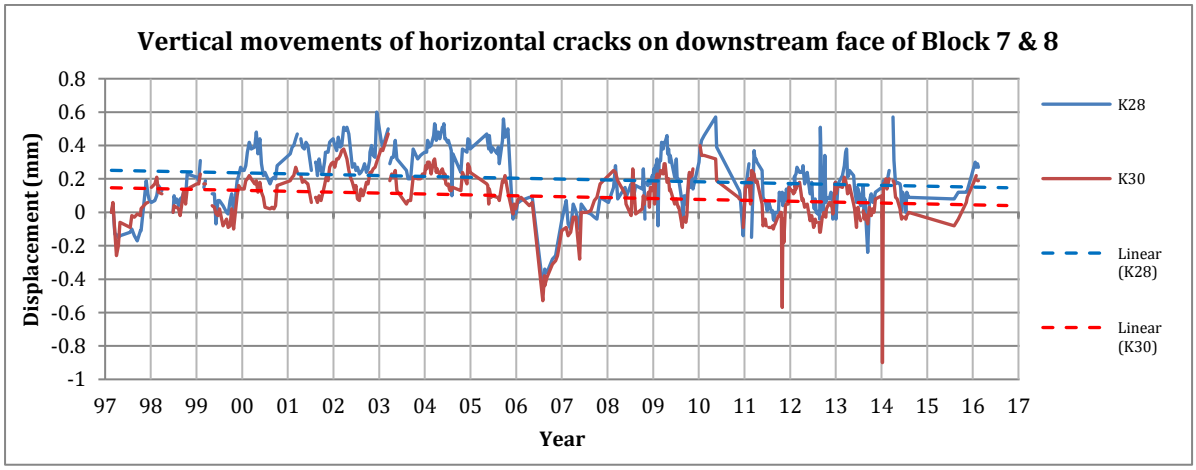

Figure 5-71: Vertical movements of the horizontal cracks on the downstream face of Block 7 and 8

Radial movements:

The radial measurements show little to no trends. If anything, the trend hints at an upstream movement (see Figure 5-66 and Figure 5-69). The tangential measurements show little to no trends except the horizontal cracks which show a slight trend where the top lifts move toward the left flank (see Figure 5-67 and Figure 5-70). The vertical measurements show that the joints and cracks both display a slight closing trend (see Figure 5-68 and Figure 5-71).

5.5. Trivec Results

There are four Trivec installations at Poortjieskloof Dam. The readings are taken twice a year by the DWS, once in the summer and once in the winter. The holes are titled Pokr1 - Pokr4 (see Figure 5-72).

Figure 5-72: The positions of the Trivec boreholes at Poortjieskloof Dam

5.5.1. Trivec Installation 1

Pokr1 is the far left Trivec borehole. Figure 5-73 to Figure 5-78 present the results for this Trivec installation since 2000. The base date is 27/02/1992. Positive directions are defined as downstream when considering radial movements, left flank when considering tangential movements and downwards when considering vertical movements.

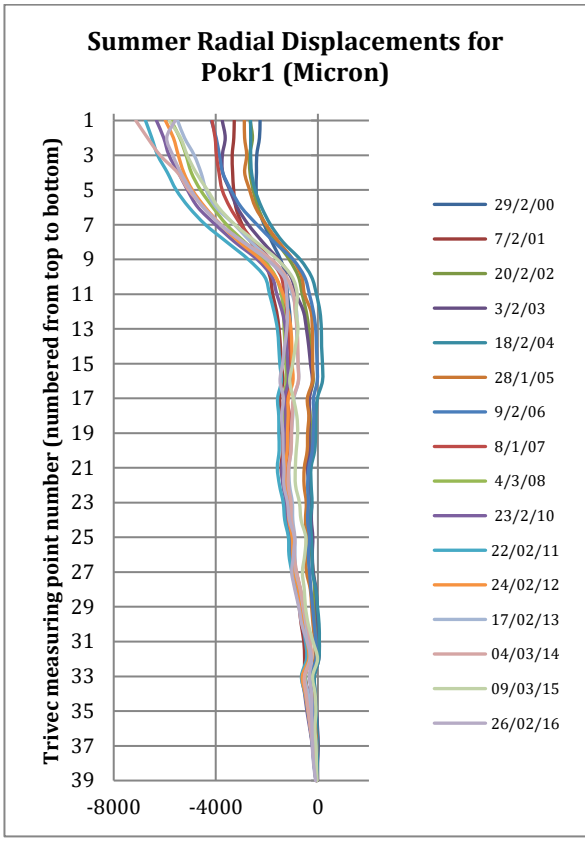

Figure 5-73: Summer radial displacements of Trivec borehole Pokr1

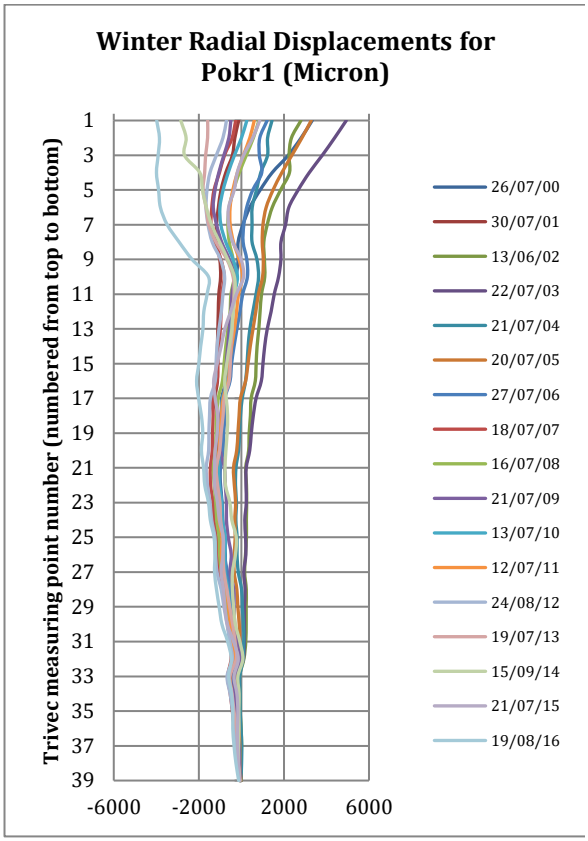

Figure 5-74: Winter radial displacements of Trivec borehole Pokr1

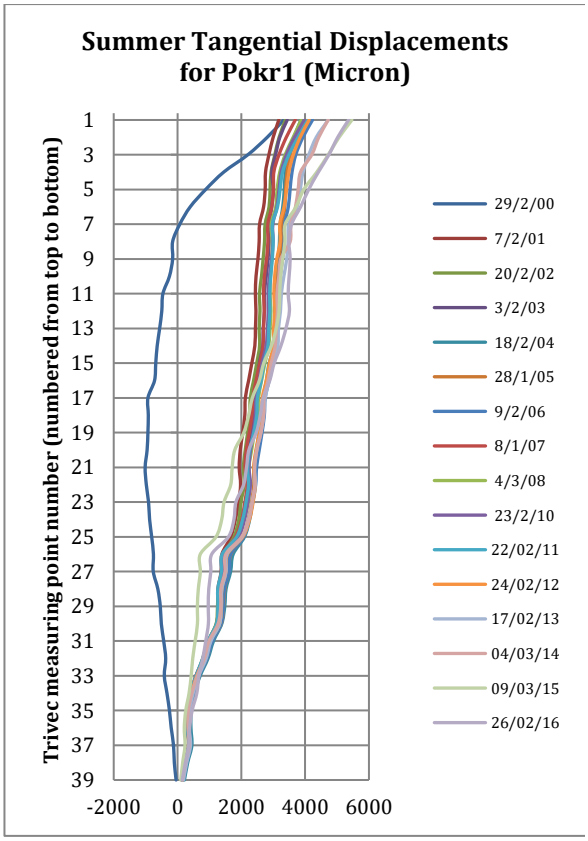

Figure 5-75: Summer tangential displacements of Trivec borehole Pokr1

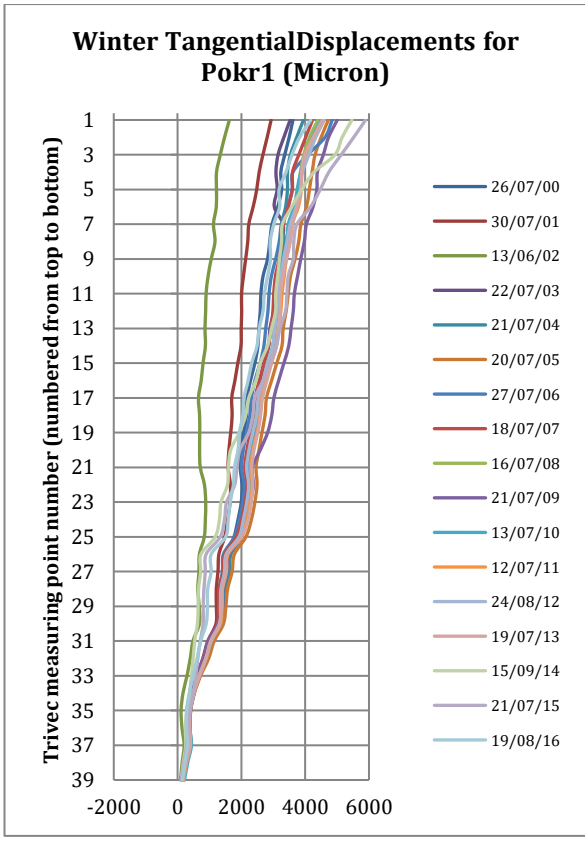

Figure 5-76: Winter tangential displacements of Trivec borehole Pokr1

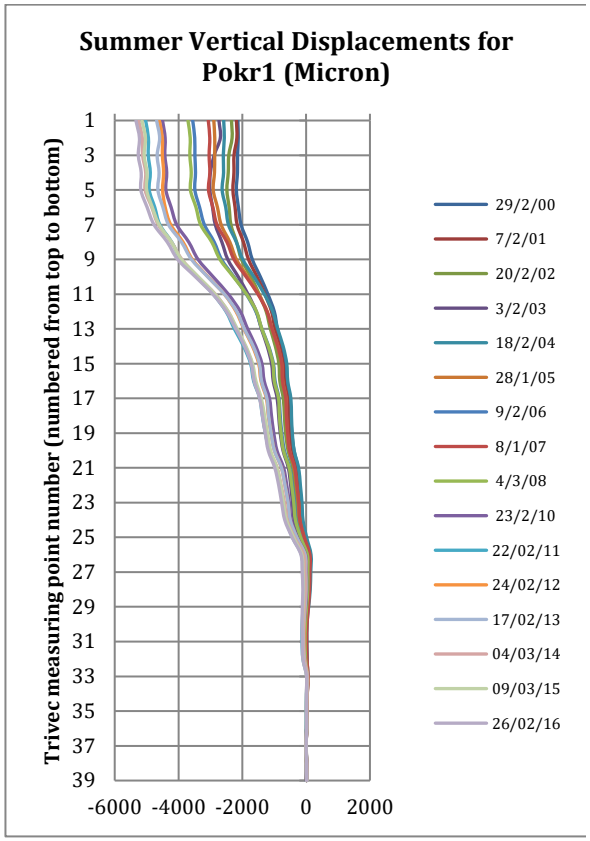

Figure 5-77: Summer vertical displacements of Trivec borehole Pokr1

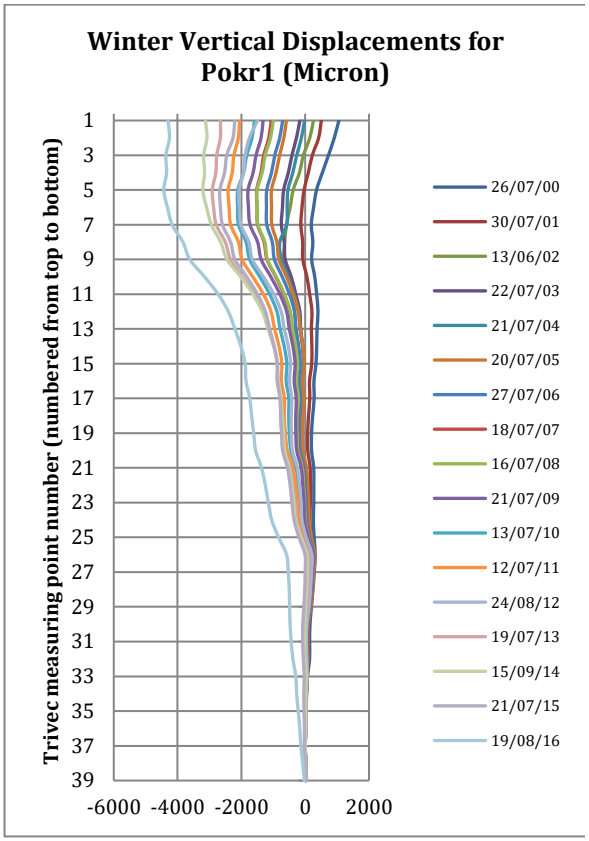

Figure 5-78: Winter vertical displacements of Trivec borehole Pokr1

The radial movements show a clear upstream displacement trend relative to the base date, especially in the upper parts of the dam wall. A permanent upstream displacement of approximately 5 mm can be observed at the crest since the base date (see Figure 5-73 and Figure 5-74).

The tangential movements show a definite trend of displacement toward the left flank since the base date, which become more exaggerated in the upper parts of the dam wall. A permanent displacement towards the left flank of approximately 2.5 mm can be observed at the crest since the base date (see Figure 5-75 and Figure 5-76).

The vertical movements show a definite trend of rising elevations throughout the height of the dam wall relative to the base date, with the upper parts displaying the biggest displacements. A permanent rise in elevation of approximately 5 mm can be observed at the crest since the base date (see Figure 5-77 and Figure 5-78).

5.5.2. Trivec Installation 2

Pokr2 is the second Trivec borehole just to the left of the spillway. Figure 5-79 to Figure 5-84 present the results for this Trivec installation relative to 2000. The base date is 27/02/1992. Positive directions are defined as downstream when considering radial movements, left flank when considering tangential movements and downwards when considering vertical movements.

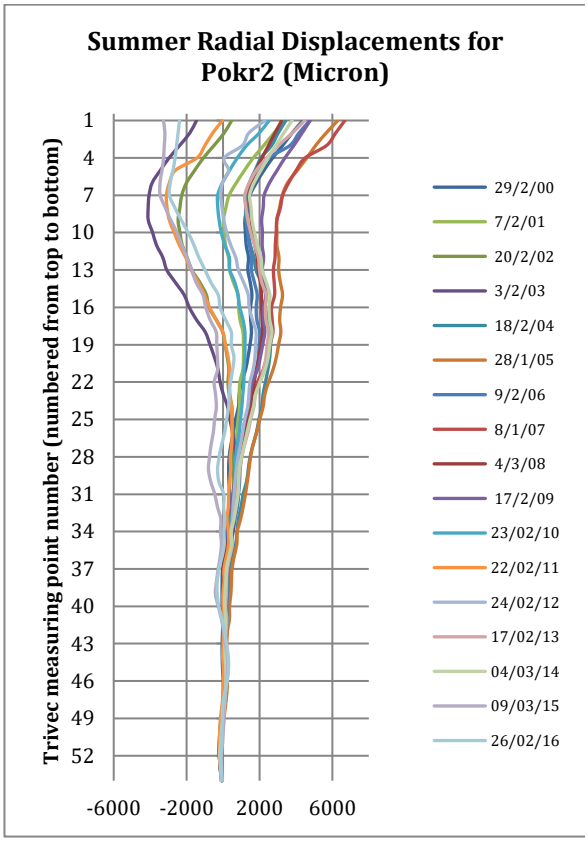

Figure 5-79: Summer radial displacements of Trivec borehole Pokr2

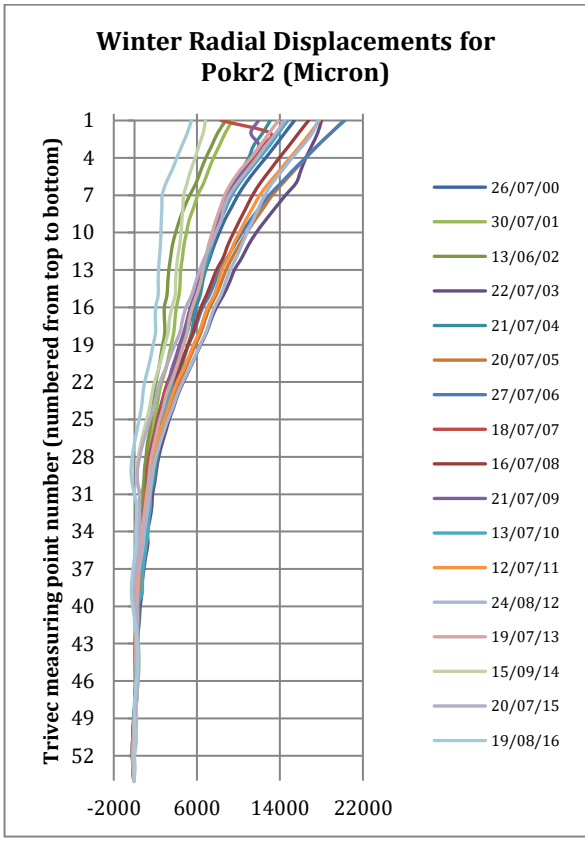

Figure 5-80: Winter radial displacements of Trivec borehole Pokr2

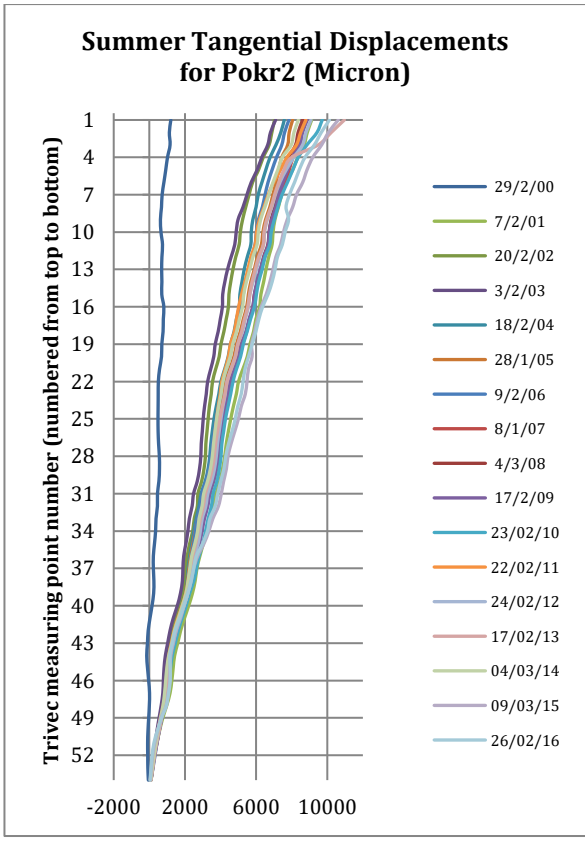

Figure 5-81: Summer tangential displacements of Trivec borehole Pokr2

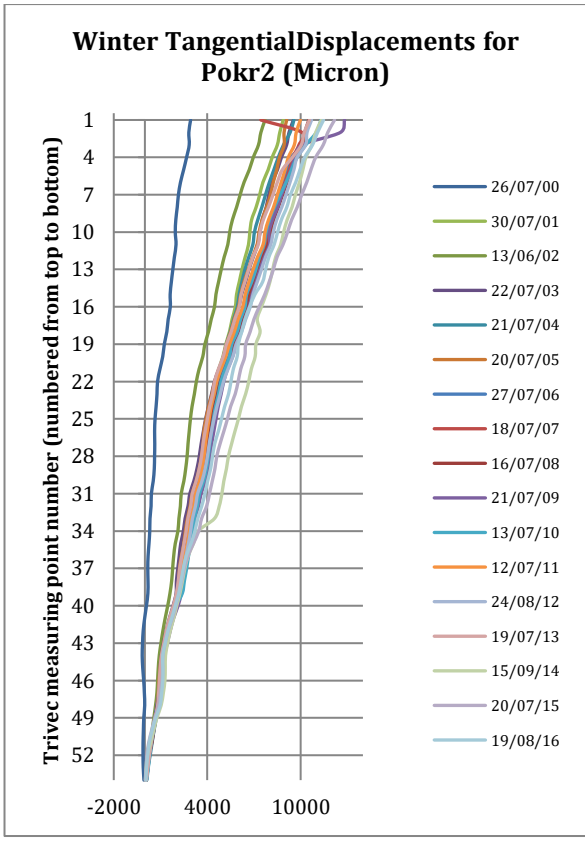

Figure 5-82: Winter tangential displacements of Trivec borehole Pokr2

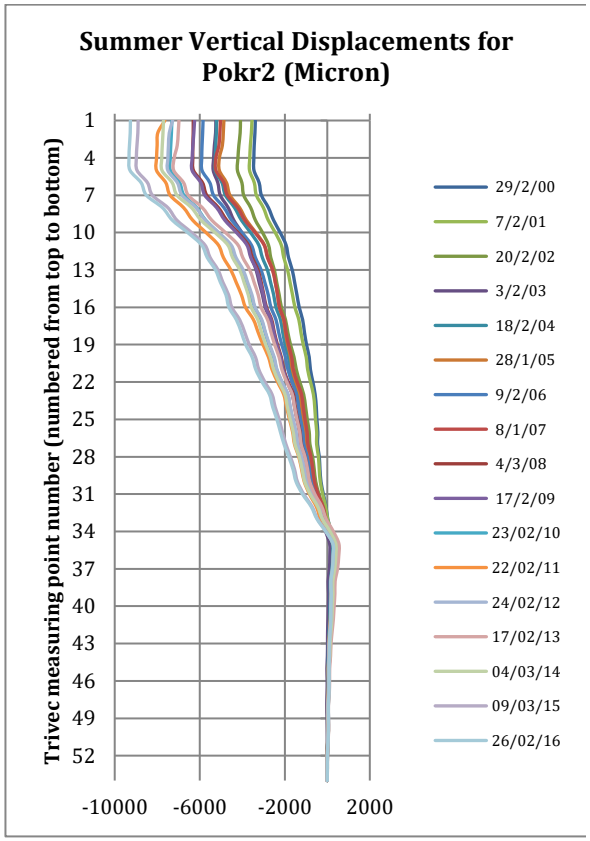

Figure 5-83: Summer vertical displacements of Trivec borehole Pokr2

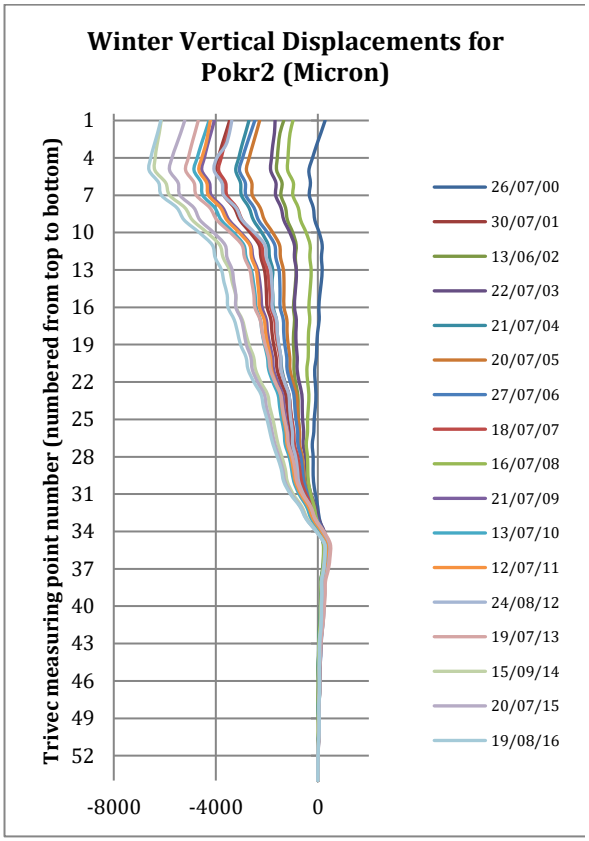

Figure 5-84: Winter vertical displacements of Trivec borehole Pokr2

The radial movements show a clear upstream displacement trend relative to the base date, especially in the upper parts of the dam wall, but the trend is much smaller than Pokr 1. A permanent upstream displacement of approximately 2.5 mm can be observed at the crest since the base date (see Figure 5-79 and Figure 5-80).

The tangential movements show a definite trend of displacement toward the left flank relative to the base date which become more exaggerated in the upper parts of the dam wall. A permanent displacement towards the left flank of approximately 5.5 mm can be observed at the crest since the base date (see Figure 5-81 and Figure 5-82).

The vertical movements show a definite trend of rising elevations throughout the height of the dam wall relative to the base date, with the upper parts displaying the biggest displacements. A permanent rise in elevation of approximately 5 mm can be observed at the crest since the base date (see Figure 5-83 and Figure 5-84).

5.5.3. Trivec Installation 3

Pokr3 is the third Trivec borehole just to the right of the spillway. Figure 5-85 to Figure 5-90 present the results for this Trivec installation relative to 2000. The base date is 27/02/1992. Positive directions are defined as downstream when considering radial movements, left flank when considering tangential movements and downwards when considering vertical movements.

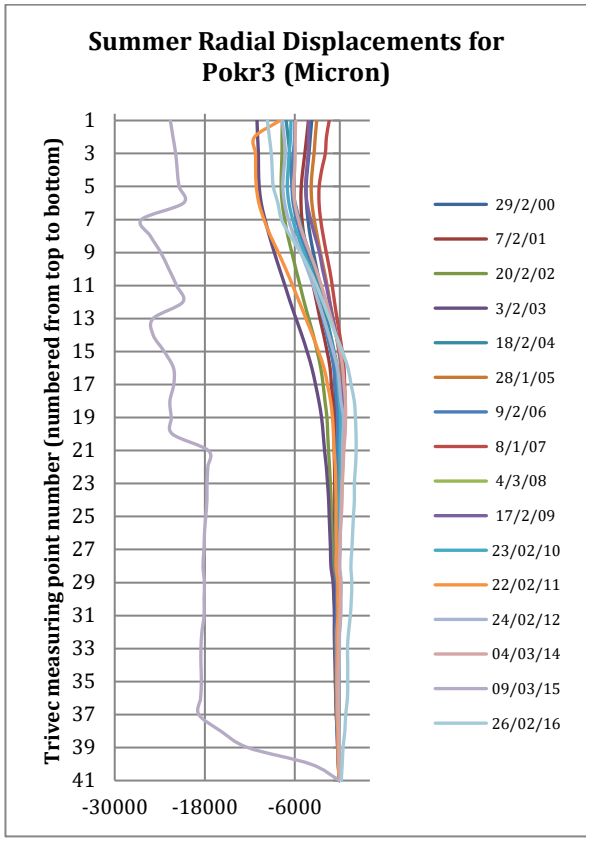

Figure 5-85: Summer radial displacements of Trivec borehole Pokr3

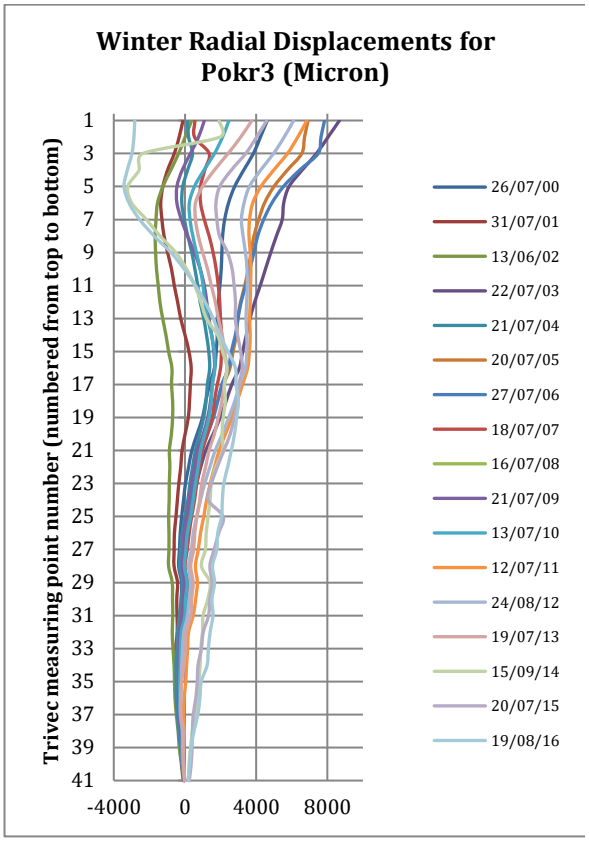

Figure 5-86: Winter radial displacements of Trivec borehole Pokr3

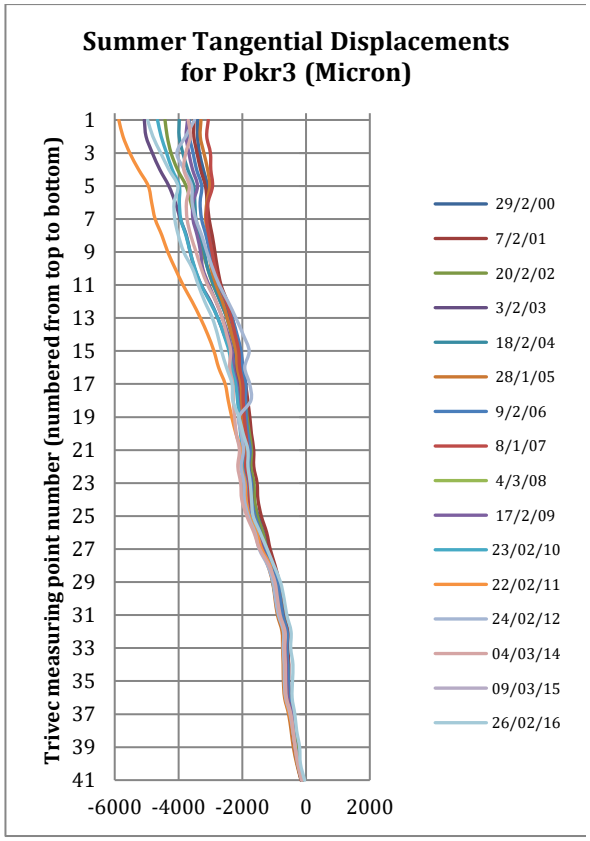

Figure 5-87: Summer tangential displacements of Trivec borehole Pokr3

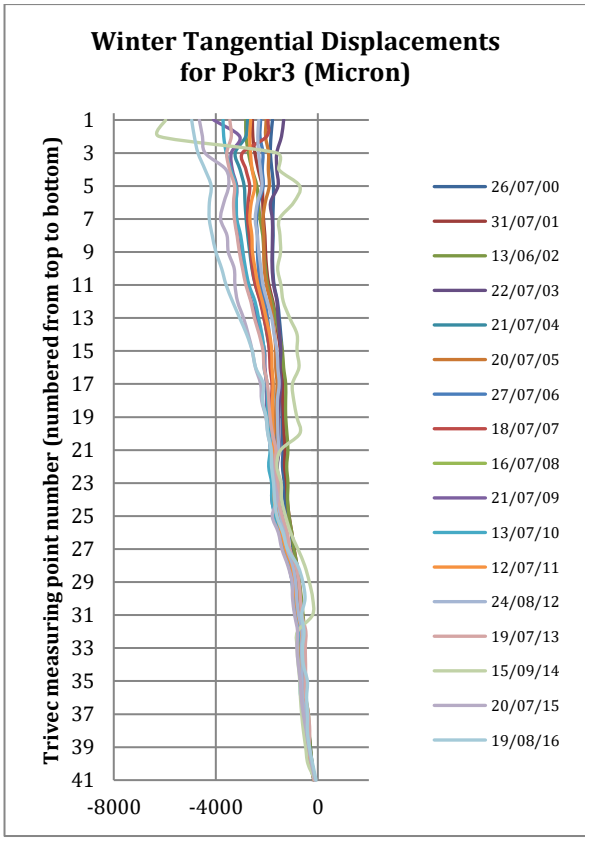

Figure 5-88: Winter tangential displacements of Trivec borehole Pokr3

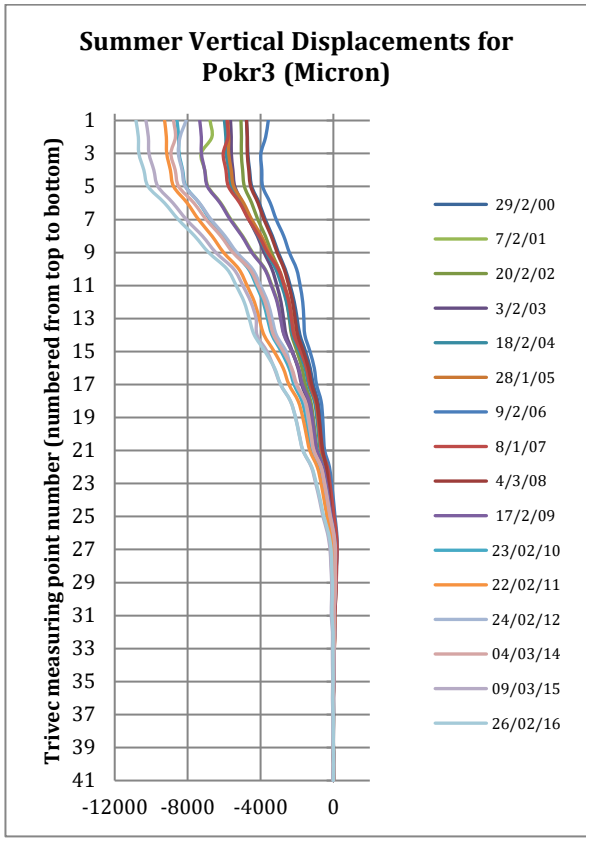

Figure 5-89: Summer vertical displacements of Trivec borehole Pokr3

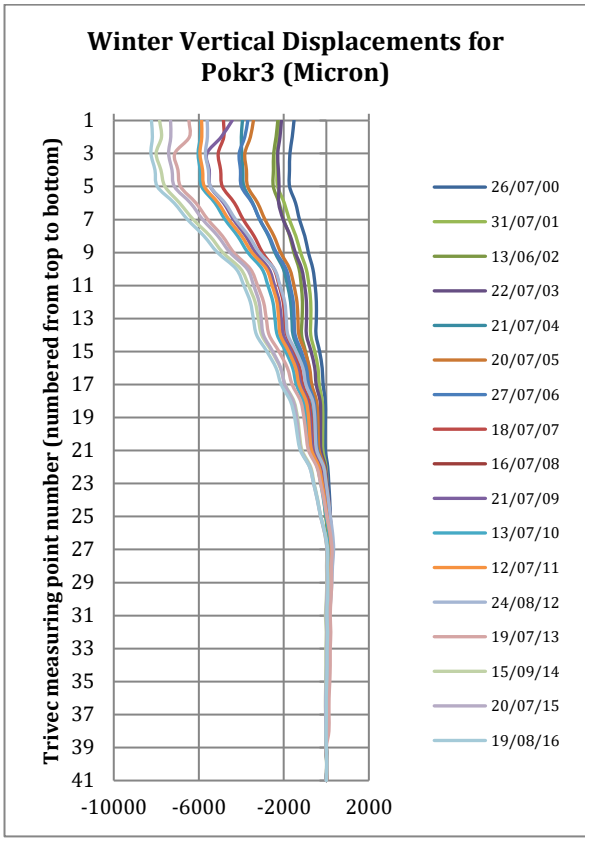

Figure 5-90: Winter vertical displacements of Trivec borehole Pokr3

The radial movements show a clear upstream displacement trend relative to the base date, especially in the upper parts of the dam wall. A permanent upstream displacement of approximately 3 mm can be observed at the crest since the base date (see Figure 5-85 and Figure 5-86).

The tangential movements show a definite trend of displacement toward the right flank relative to the base date which become more exaggerated in the upper parts of the dam wall. A permanent displacement towards the right flank of approximately 2 mm can be observed at the crest since the base date (see Figure 5-87 and Figure 5-88).

The vertical movements show a definite trend of rising elevations throughout the height of the dam wall relative to the base date, with the upper parts displaying the biggest displacements. A permanent rise in elevation of approximately 6 mm can be observed at the crest since the base date (see Figure 5-89 and Figure 5-90).

5.5.4. Trivec installation 4

Pokr4 is the fourth Trivec borehole located on the far-right flank. Figure 5-91 to Figure 5-96 present the results for this Trivec installation relative to 2000. The base date is 27/02/1992. Positive directions are defined as downstream when considering radial movements, left flank when considering tangential movements and downwards when considering vertical movements.

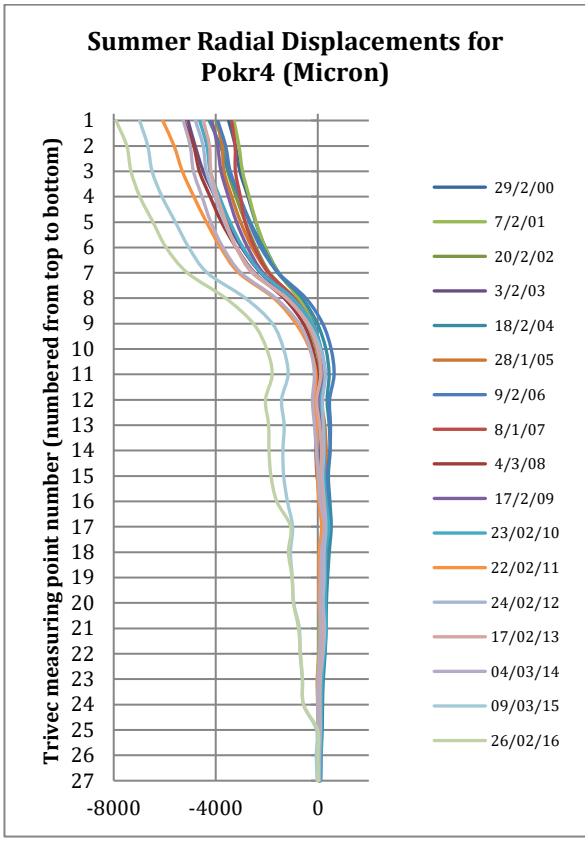

Figure 5-91: Summer radial displacements of Trivec borehole Pokr4

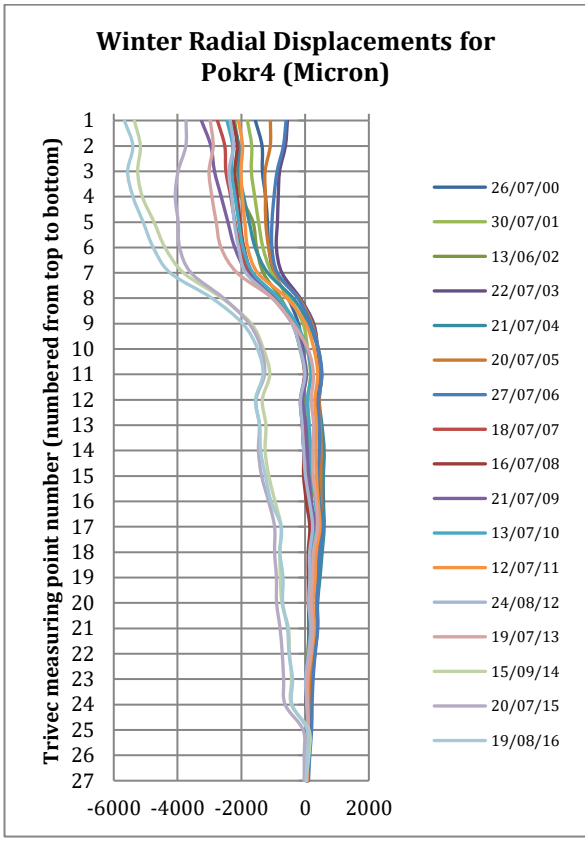

Figure 5-92: Winter radial displacements of Trivec borehole Pokr4

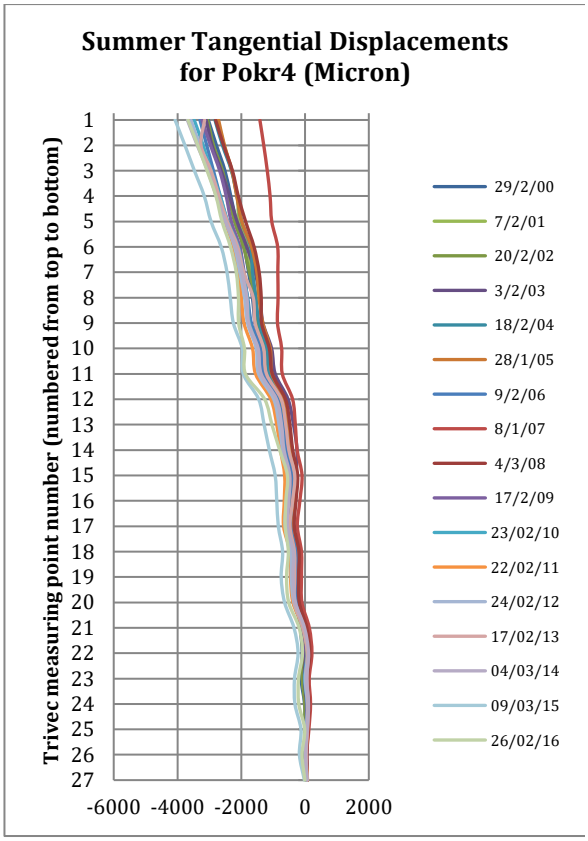

Figure 5-93: Summer tangential displacements of Trivec borehole Pokr4

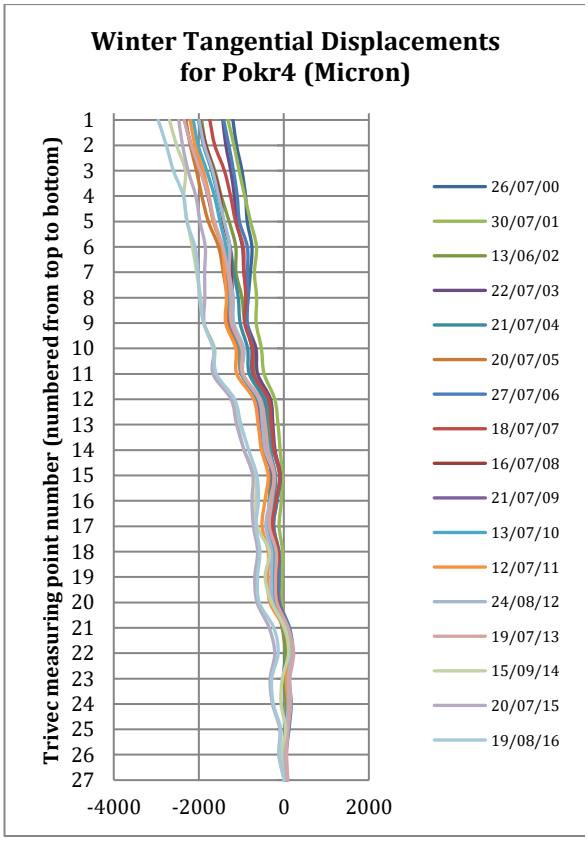

Figure 5-94: Winter tangential displacements of Trivec borehole Pokr4

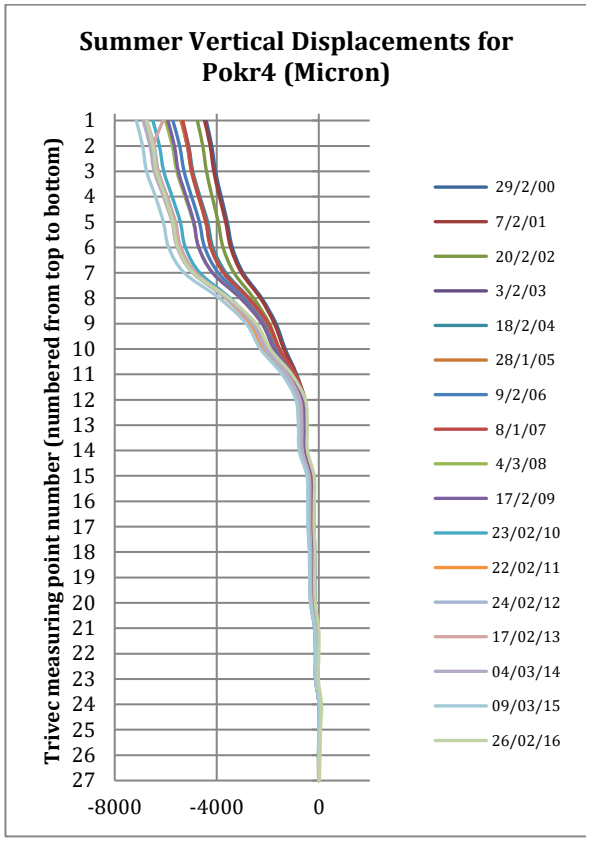

Figure 5-95: Summer vertical displacements of Trivec borehole Pokr4

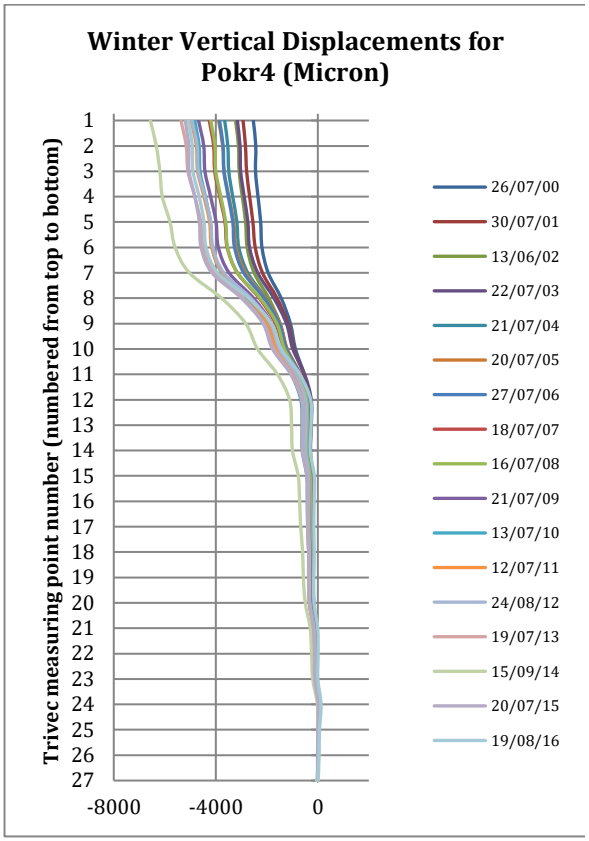

Figure 5-96: Winter vertical displacements of Trivec borehole Pokr4

The radial movements show a clear upstream displacement trend relative to the base date, especially in the upper parts of the dam wall. A permanent upstream displacement of approximately 3.5 mm can be observed at the crest since the base date (see Figure 5-91 and Figure 5-92).

The tangential movements show a definite trend of displacement toward the right flank relative to the base date which become more exaggerated in the upper parts of the dam wall. A permanent displacement towards the right flank of approximately 1.5 mm can be observed at the crest since the base date (Figure 5-93 and Figure 5-94).

The vertical movements show a definite trend of rising elevations throughout the height of the dam wall relative to the base date, with the upper parts displaying the biggest displacements. A permanent rise in elevation of approximately 3 mm can be observed at the crest since the base date (see Figure 5-95 and Figure 5-96).

5.6. Chapter Summary

This chapter looked at the behaviour of Poortjieskloof Dam in order to gain evidence of the effects of AAR-related expansion. The behaviour of Poortjieskloof Dam is monitored by geodetic surveys, crack width gauges, trivec installations and 5-yearly visual inspections.

Visual inspection:

The downstream face displayed many significant cracks including peripheral cracks which run approximately parallel to the abutment interfaces and map pattern cracks in areas where the concrete is confined. The staining around the cracks and the orientation of the cracks suggest

evidence of AAR-related swelling and a principal stress distribution that is not ideal for an arch dam.

Geodetic surveys:

The geodetic surveys revealed that the upper parts of the right and left flanks moved permanently in an upstream direction since 1998. The upper parts of the spillway section of the dam moved slightly downstream. The geodetic surveys revealed that, generally, the right and left flanks have moved permanently towards the abutments since 1998. All the targets displayed trends of permanent rising elevation levels, with displacements more exaggerated in the upper parts of the dam wall.

Crack width gauges:

The crack width gauges did not reveal any major permanent trends and most of the trends did not exceed 2.5 mm. In general, the results hint at upstream movements and rising crest elevations.

Trivec results:

The trivec results correlate well with the geodetic survey results and, to some degree, with the crack width results. The results show that the right and left flanks moved permanently upstream while downstream trends were evident toward the spillway section of the arch dam wall. Generally, the right and left flanks have moved permanently towards the abutments. A permanent rise in elevations were evident throughout all the results.

6. Thabina Dam

6.1. Introduction

The Thabina Dam is situated on the Thabina River, a tributary of the Letsitele River, approximately 20 km south of Tzaneen in the Limpopo Province. The dam was constructed between 1980 and 1984. The dam wall consists of a single curvature mass concrete arch with a mass concrete gravity spillway section on the left flank. The dam wall is 59 m high and has a total crest length of 125 m.

Thabina Dam

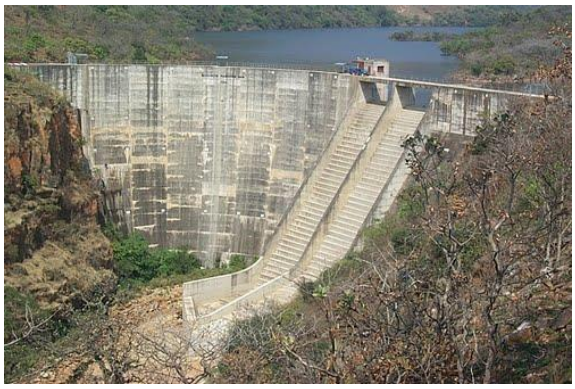

Figure 6-1: Thabina Dam

Structure type:	Single curvature arch dam with gravity spillway section on the left flank
Age of dam:	33 years
Wall height:	59 m
Climate region:	Humid, sub-tropical climate; average maximum temperature of 27°C (based on temperature data gained from three online resources*); average minimum temperature of 16 °C (based on temperature data gained from three online resources*); average annual precipitation of 720 mm (based on temperature data gained from three online resources*)
Structure orientation:	The downstream face of the dam wall faces east (this implies that the downstream face is generally exposed to direct sunlight in the morning whilst the upstream face is generally exposed to direct sunlight in the afternoon).
Construction materials:	Concrete arch section: 30MPa concrete Concrete gravity section: 25MPa concrete 50/50 Mixture of Portland Cement and Blast Furnace Slag as binders. Fine and coarse aggregate sourced by crushing granite rock (SKC and Keller Consulting Engineers, 1997).

*en.climate-data.org; meteoblue.com; worldweatheronline.com

Thabina Dam is situated in an area which has a sub-tropical climate. A sub-tropical climate is distinguished by hot, humid summers and mild winters. The average annual rainfall typically ranges from 700 mm to 1500 mm.

SKC and Keller Consulting Engineers (1997) mentioned that the dam wall could develop AAR considering its construction materials. The use of 50% Blast Furnace Slag as binder would however greatly reduce the probability of occurrence of AAR. SKC and Keller Consulting Engineers (1997) reported that no signs of AAR were yet detected at the time of their inspection. They do, however, stress the fact that AAR may still occur in the concrete in the future and that cognisance of this should be taken during future dam safety evaluations.

Beukes (2005) mentioned that boreholes were drilled from the NOC into the arch section of the wall in 1997 and from the gallery into the gravity section of the wall in 2000. The core logs revealed that the aggregate mainly consisted of quartzite with some dolerite also present. It was stated that the cores revealed no obvious signs of AAR. No mention was made of any specific diagnostic tests that were performed on the concrete cores to confirm this.

From the above it is clear that no formal confirmation has been made with regards to the presence of AAR concrete. The instrumentation results have started showing signs of possible swelling effects that could possibly be related to AAR. Further tests to confirm the presence of AAR will have to be conducted to confirm this beyond all doubt.

6.2. Visual Inspection

A visual inspection was carried out on the 12th of October 2015. This inspection was carried out as part of a 5-yearly dam safety evaluation exercise undertaken by the Sub-Directorate: Dam Safety Surveillance within the DWS.

6.2.1. Left Flank (Gravity Section)

The left flank comprises the gravity section of the dam that also includes the spillway. The spillway was raised by 2.4 m in 2000 and subsequently, the concrete is much younger than that comprising the rest of the dam wall. The upstream face could not be thoroughly inspected due to the water level and access restrictions. The visible sections were in a good condition.

The NOC was in a very good condition with minor cracking visible.

Apart from occasional cracking and some seepage characterised by calcite staining on the horizontal lift joints, there were no signs of distress in the concrete on the downstream face (see Figure 6-2 and Figure 6-3). Seepage could indicate separation of the horizontal lift joints due to swelling in the concrete.

Figure 6-2: The right flank downstream face as viewed from the right flank NOC

Figure 6-3: The stepped downstream profile of the spillway as viewed from the left flank NOC

6.2.2. Right Flank (Arch Section)

The visible section of the upstream face revealed no evidence of distress in the concrete.

The NOC was generally in a good condition with very small cracking evident which could be the result of shrinkage due to the size and orientation of the cracks.

The downstream face displayed frequent areas of calcite staining along the horizontal lift joints (see Figure 6-6). The frequency seemed to increase towards the right flank abutment area. Near the base of the right flank there was a fairly major crack which orientation hints at a slightly unfavourable stress distribution (see Figure 6-4). The crack is orientated about 20° upwards from the horizontal plane. There were no major peripheral cracks that run parallel to the abutment contact. There was one lift joint which displayed active seepage (see Figure 6-5).

Figure 6-4: The prominent crack near the base of the right flank abutment area

Figure 6-5: View of the horizontal lift joint that displays active seepage

Figure 6-6: General view of the downstream face of the arch

6.3. Crack Width Gauges

A total of thirteen 3-D crack width gauges were installed at the Thabina Dam in 2000. There are ten gauges on the crest of the dam wall and three gauges on the downstream face of the arch near the right abutment. The crest gauges are installed at the vertical construction joints. The gauges on the downstream face are not read regularly due to difficult access. Only the results from the crest gauges are discussed in this study. The layout of the vertical blocks (monoliths) are shown in Figure 6-7 below.

Figure 6-7: The positions of the blocks comprising the arch section at Thabina Dam

6.3.1. Vertical Joints on the Crest of the Gravity Section

The vertical joints on the crest of the gravity section of the dam wall are monitored by crack width gauges K1 and K2. K1 and K2 monitor the movements between Block 1 and 2 and Block 2 and 3 respectively. The radial movement results are shown in Figure 6-8, the tangential movement results in Figure 6-9 and the vertical movement results in Figure 6-10.

Legend for positive directions (left and right as viewed from the upstream side):

- Radial = the block on the right side moves downstream relative to the block on the left side
- Tangential = the joint opening increases
- Vertical = the block on the right side moves upward relative to the block on the left side

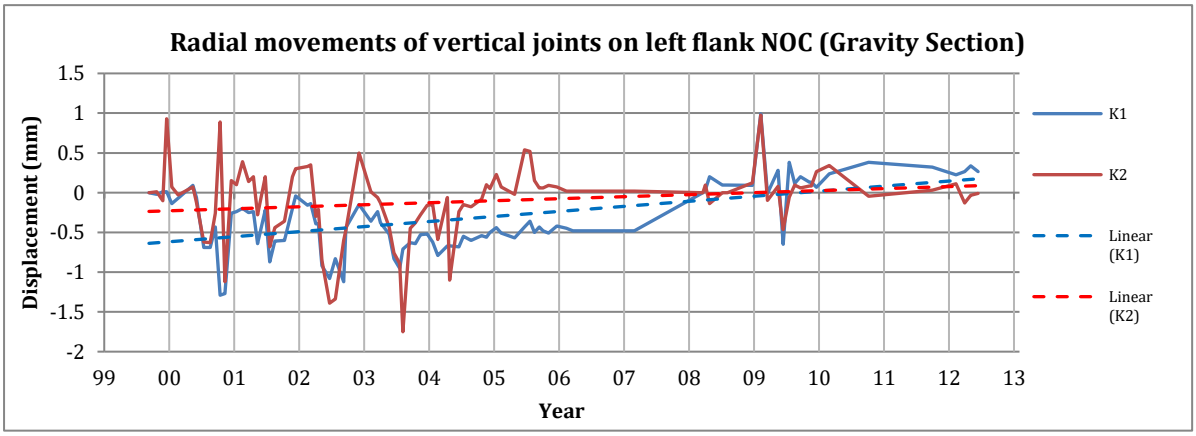

Figure 6-8: Radial movements of the vertical joints on the left flank NOC

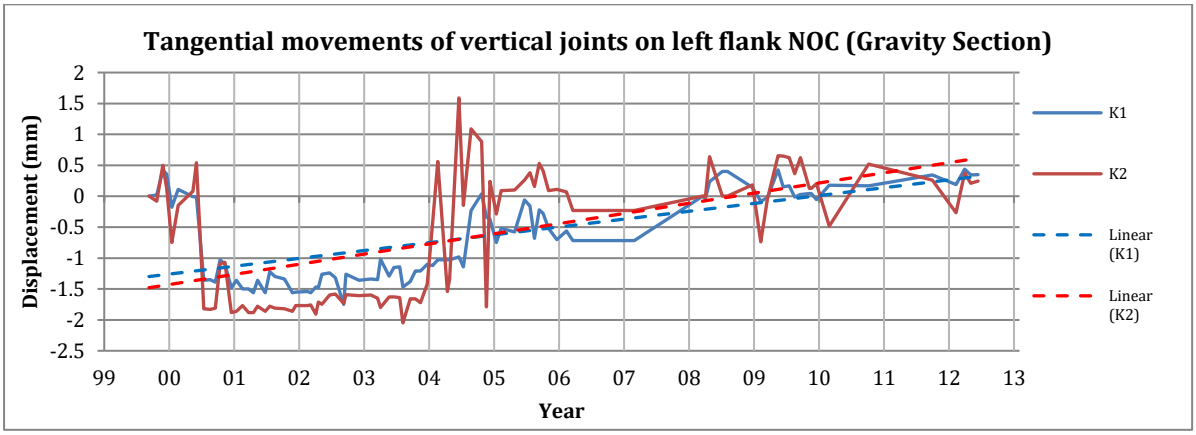

Figure 6-9: Tangential movements of the vertical joints on the left flank NOC

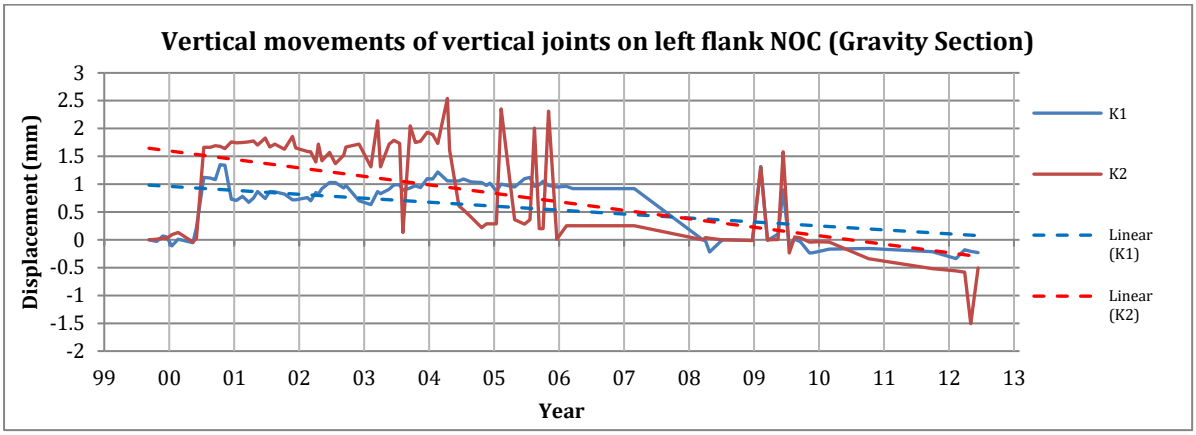

Figure 6-10: Vertical movements of the vertical joints on the left flank NOC

The radial measurements from both K1 and K2 show that the blocks to the right have moved downstream slightly relative to the blocks on the left (see Figure 6-8). Permanent trends are approximately 0.5 - 1 mm. The tangential measurements from both K1 and K2 show trends of the joints opening (see Figure 6-9). Permanent trends are approximately 1.5 - 2 mm. The vertical measurements from both K1 and K2 show that the blocks to the right have decreased in elevation relative to the blocks on the left (see Figure 6-10). Permanent trends are approximately 1.5 - 2 mm.

6.3.2. Vertical Joints on the Central Crest of the Arch Section

The vertical joints on the central crest of the arch section of the dam wall are monitored by crack width gauges K3 to K6 and they monitor the relative movements of Blocks 4 to 8. The radial movement results are shown in Figure 6-11, the tangential movement results in Figure 6-12 and the vertical movement results in Figure 6-13.

Legend for positive directions (left and right as viewed from the upstream side):

- Radial = the block on the right side moves downstream relative to the block on the left side
- Tangential = the joint opening increases
- Vertical = the block on the right side moves upward relative to the block on the left side

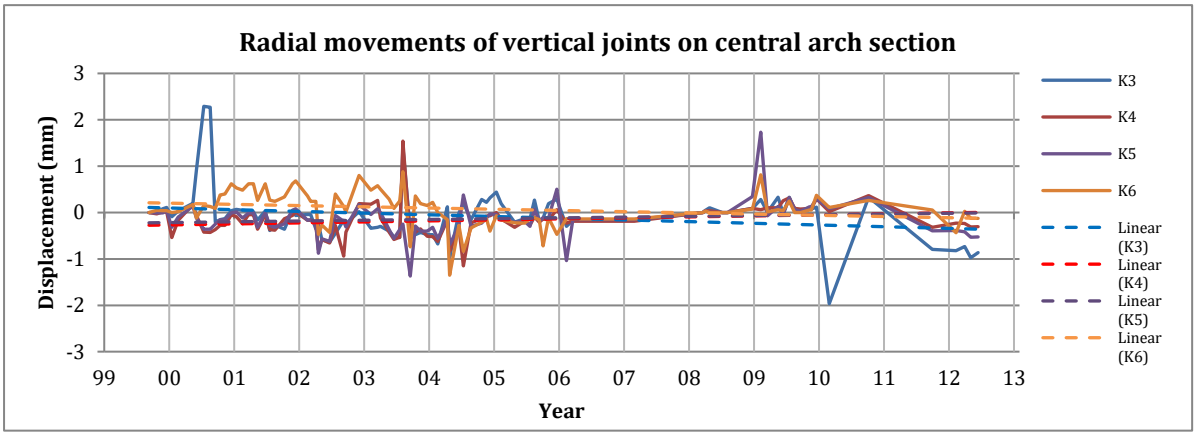

Figure 6-11: Radial movements of the vertical joints on the NOC of the central arch section

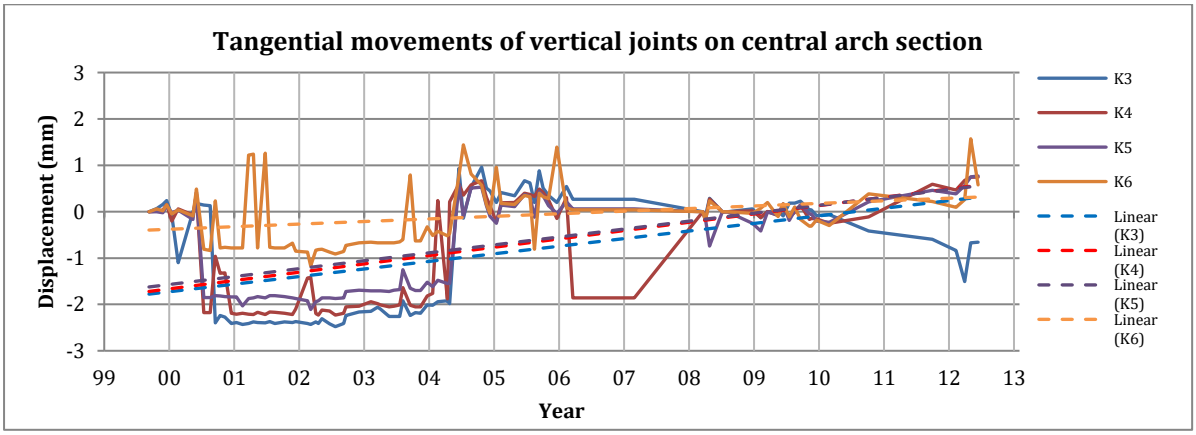

Figure 6-12: Tangential movements of the vertical joints on the NOC of the central arch section

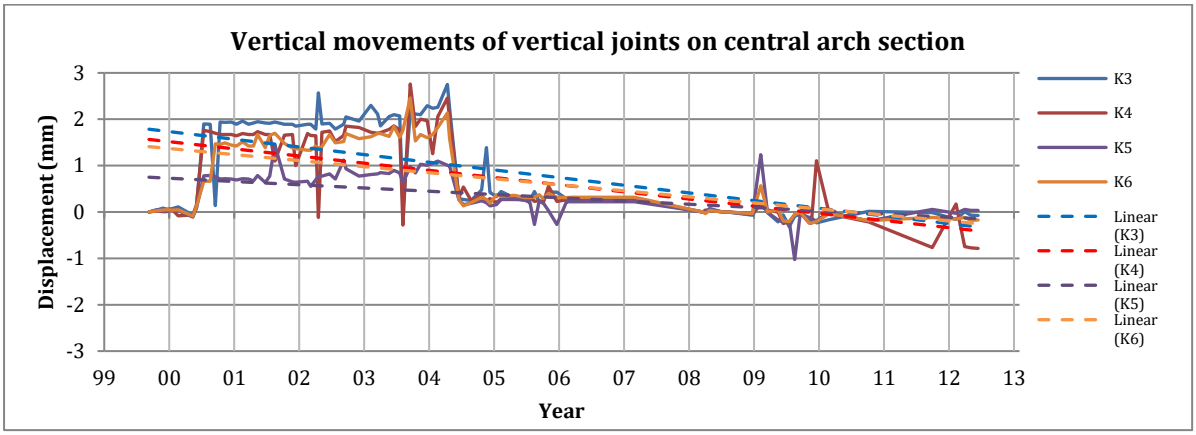

Figure 6-13: Vertical movements of the vertical joints on the NOC of the central arch section

The radial measurements of K3 to K6 show little to no trends (see Figure 6-11). The tangential measurements of K3 to K6 all show trends of joints opening (see Figure 6-12). Permanent trends are approximately 1 - 2.5 mm. The vertical measurements of K3 to K6 show that the blocks to the right have decreased in elevation relative to the blocks on the left (see Figure 6-13). Permanent trends are approximately 1 - 2.5 mm.

6.3.3. Vertical Joints on the Right Flank Arch Section

The vertical joints on the central crest of the arch section of the dam wall are monitored by crack width gauges K7 to K10 and they monitor the relative movements of Blocks 7 to 11. The radial movement results are shown in Figure 6-14, the tangential movement results in Figure 6-15 and the vertical movement results in Figure 6-16.

Legend for positive directions (left and right as viewed from the upstream side):

- Radial = the block on the right side moves downstream relative to the block on the left side
- Tangential = the joint opening increases
- Vertical = the block on the right side moves upward relative to the block on the left side

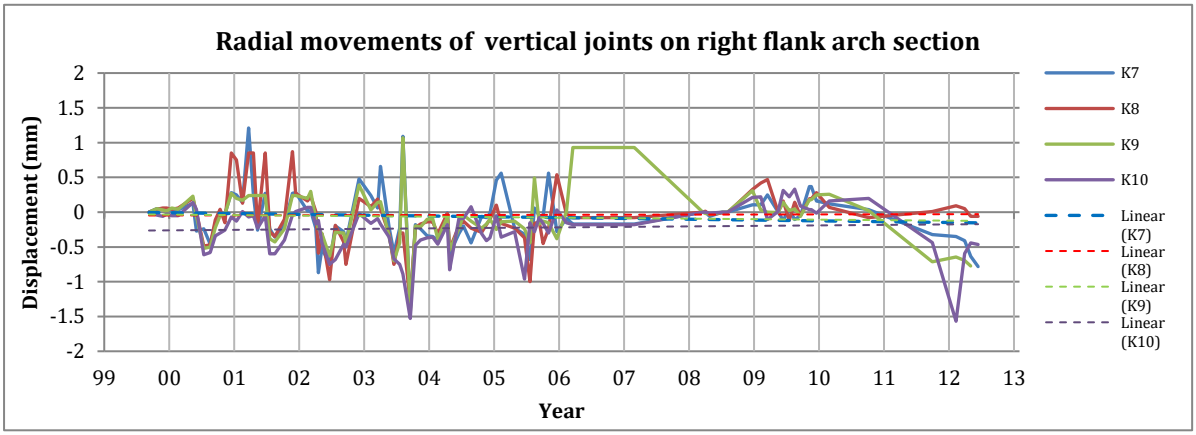

Figure 6-14: Radial movements of the vertical joints on the NOC of the right flank arch section

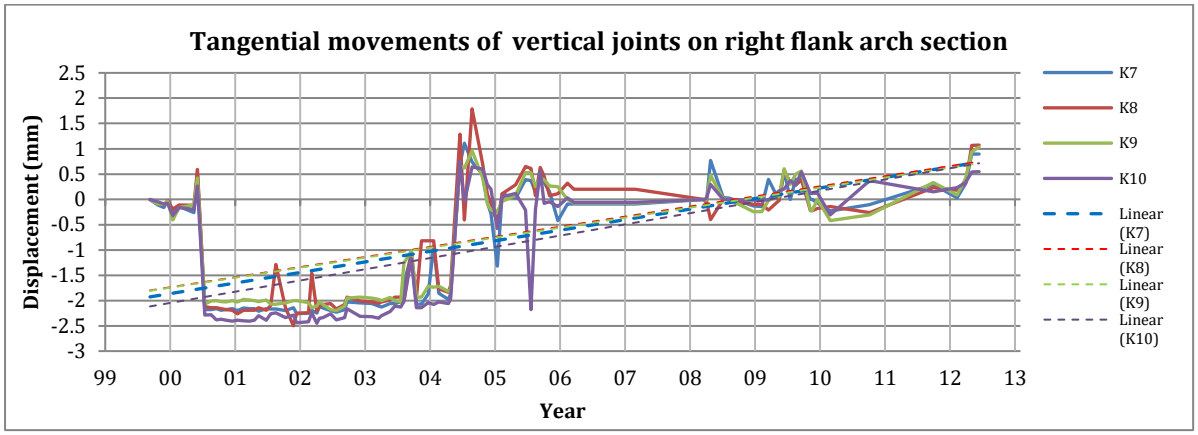

Figure 6-15: Tangential movements of the vertical joints on the NOC of the right flank arch section

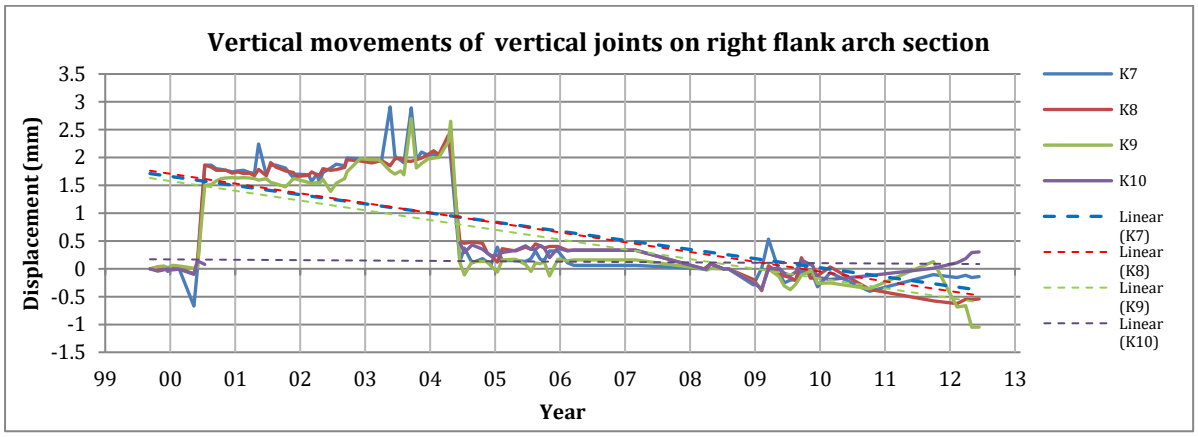

Figure 6-16: Vertical movements of the vertical joints on the NOC of the central arch section

The radial measurements of K7 to K10 show little to no trends (see Figure 6-14). The tangential measurements of K7 to K10 all show trends of the joints opening (see Figure 6-15). Permanent trends are approximately 2.2 - 2.75 mm. The vertical measurements of K7 to K10 show that the blocks to the right have decreased in elevation relative to the blocks on the left (see Figure 6-16). Permanent trends are approximately 2.4 - 2.6 mm.

6.4. Trivec Results

There are three Trivec installations at Thabina Dam. The readings are taken twice a year by the Department of Water and Sanitation, once in the summer and once in the winter. The holes are titled Thar1 - Thar4 (see Figure 6-17).

Figure 6-17: The positions of the Trivec boreholes at Thabina Dam

6.4.1. Trivec Installation 1

Thar1 is the far left Trivec borehole located in the arch section adjacent to the gravity spillway section. Figure 6-18 to Figure 6-23 present the results for this Trivec installation since 2000. Positive directions are defined as downstream when considering radial movements, left flank when considering tangential movements and downwards when considering vertical movements.

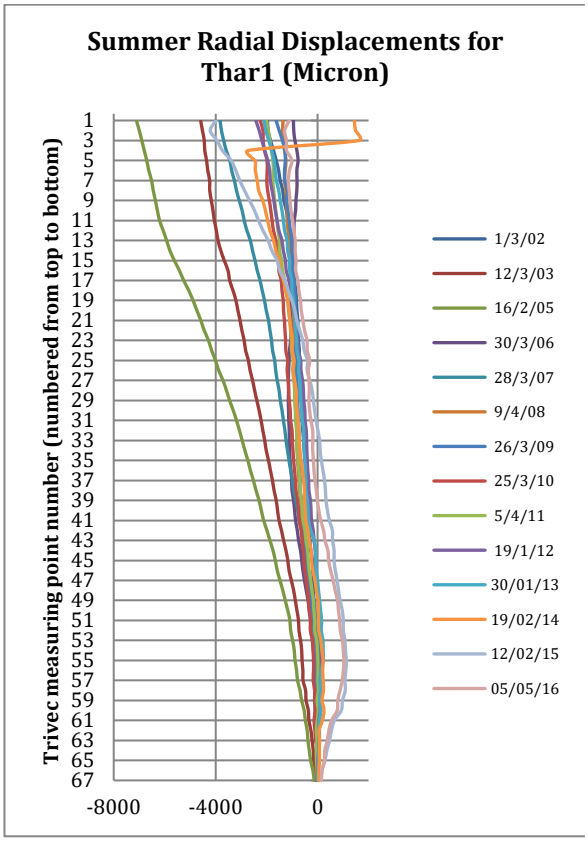

Figure 6-18: Summer radial displacements of Trivec borehole Thar1

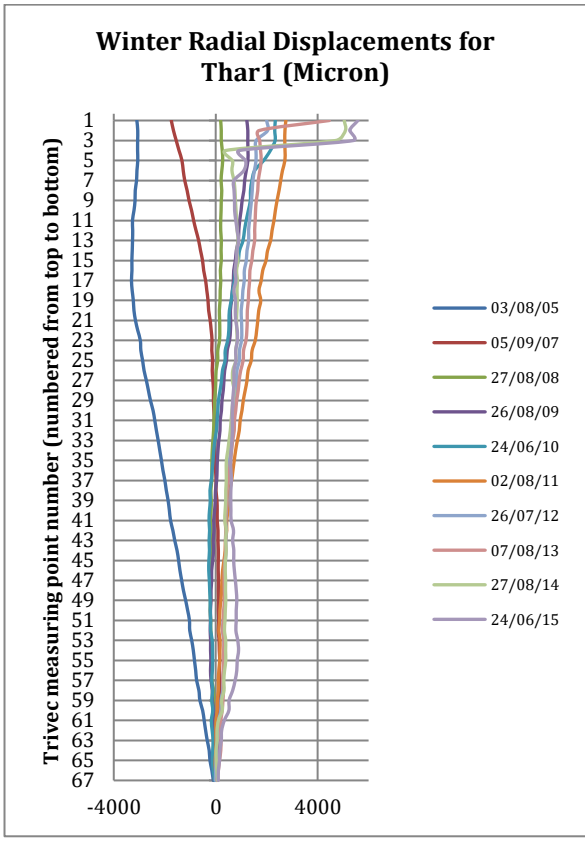

Figure 6-19: Winter radial displacements of Trivec borehole Thar1

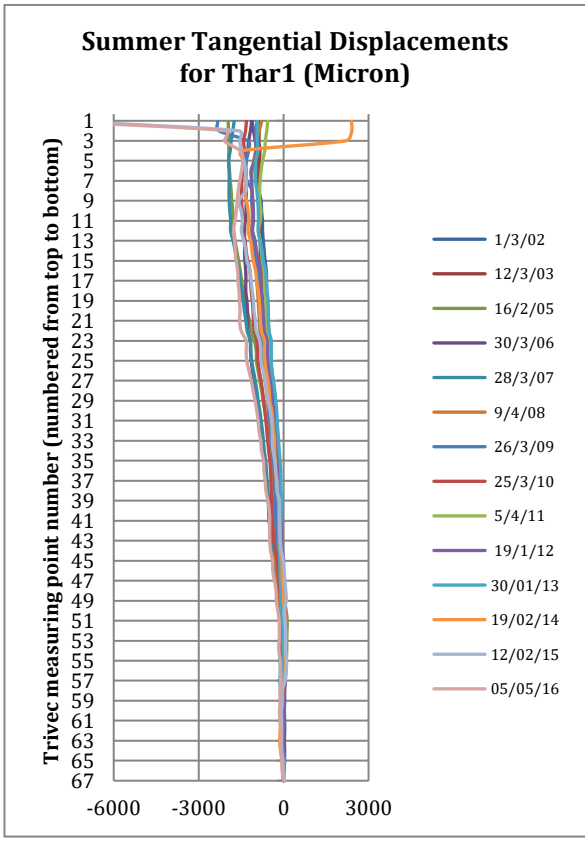

Figure 6-20: Summer tangential displacements of Trivec borehole Thar1

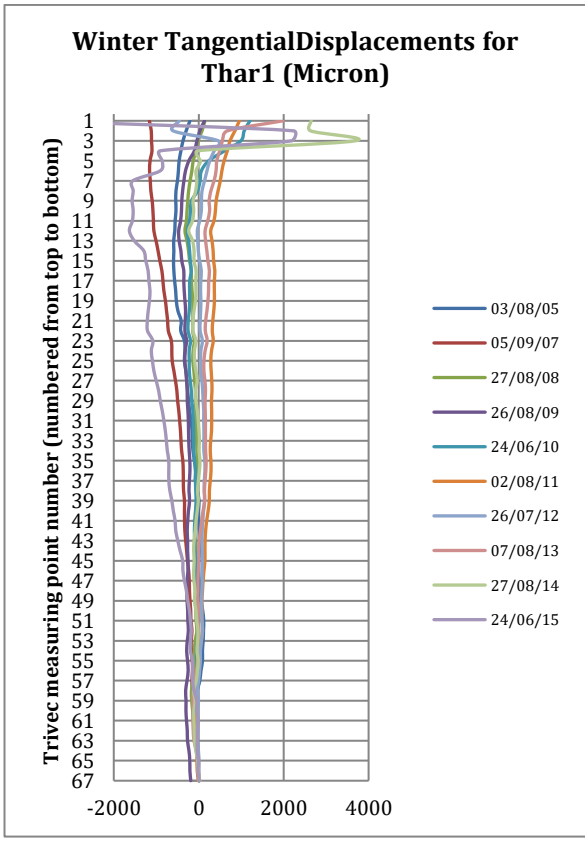

Figure 6-21: Winter tangential displacements of Trivec borehole Thar1

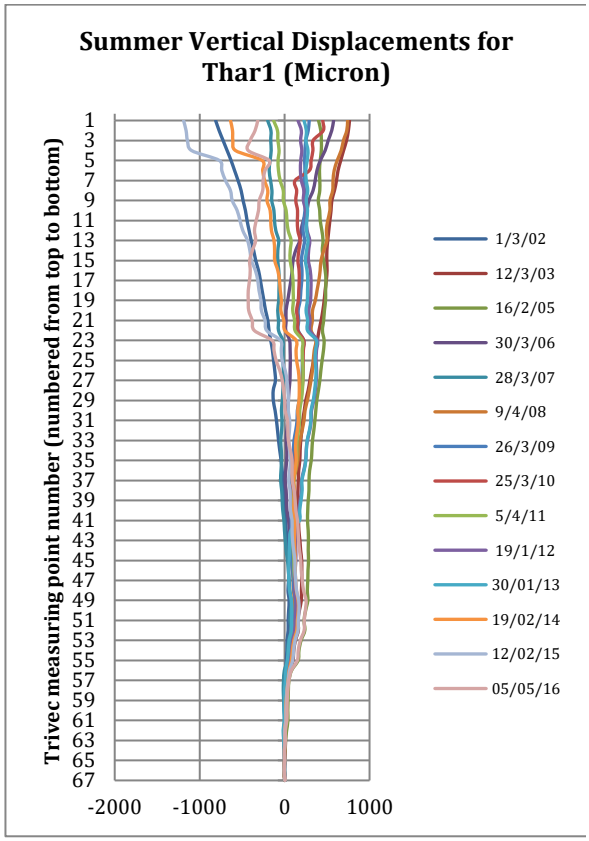

Figure 6-22: Summer vertical displacements of Trivec borehole Thar1

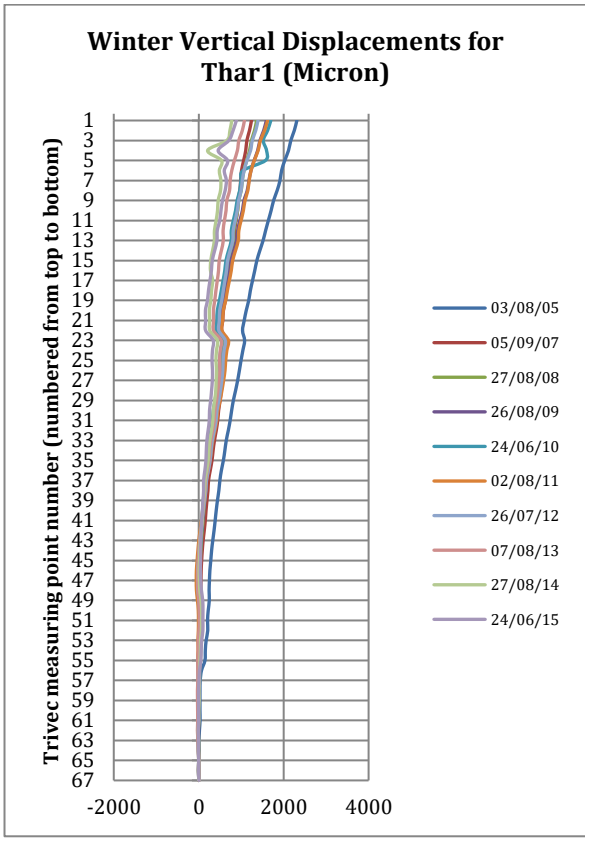

Figure 6-23: Winter vertical displacements of Trivec borehole Thar1

The radial movements show a downstream displacement trend since 2002 especially in the upper parts of the dam wall. A permanent downstream displacement of approximately 6 mm can be observed at the crest since 2002 (see Figure 6-18 and Figure 6-19).

The tangential movements show a slight but definite trend of displacement toward the right flank relative to the base date, which become more exaggerated in the upper parts of the dam wall. A permanent displacement towards the right flank of approximately 2 mm can be observed at the crest since the base date (see Figure 6-20 and Figure 6-21).

The vertical movements show a slight trend of rising elevations relative to the base date, and movements are more exaggerated in the upper parts of the dam wall. A permanent rise in elevation of approximately 0.5 mm can be observed at the crest since the base date (see Figure 6-22 and Figure 6-23).

6.4.2. Trivec Installation 2

Thar2 is the middle Trivec borehole located in the middle of the arch section. Figure 6-24 to Figure 6-29 present the results for this Trivec installation relative to 2000. Positive directions are defined as downstream when considering radial movements, left flank when considering tangential movements and downwards when considering vertical movements.

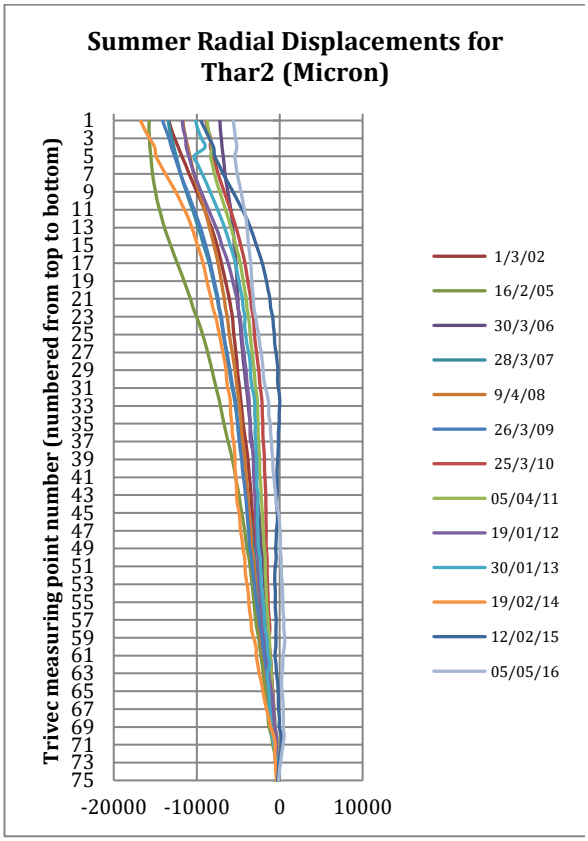

Figure 6-24: Summer radial displacements of Trivec borehole Thar2

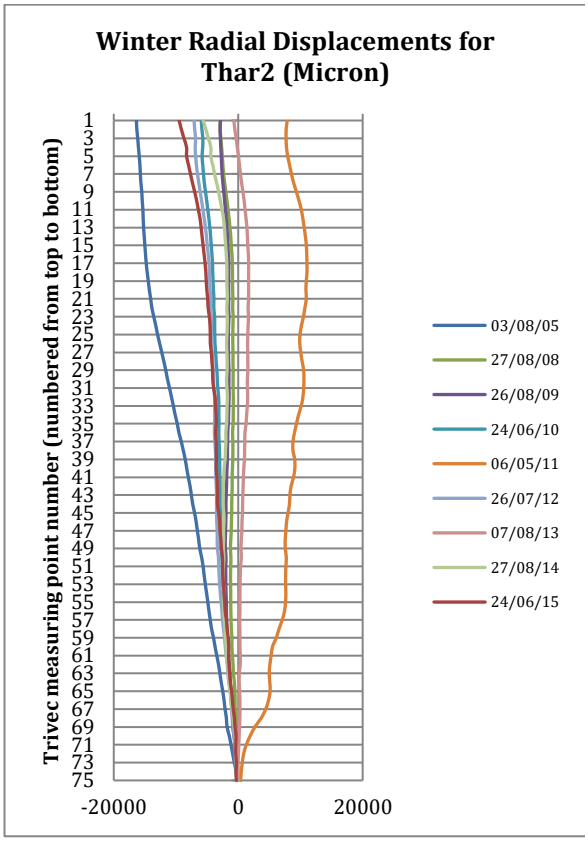

Figure 6-25: Winter radial displacements of Trivec borehole Thar2

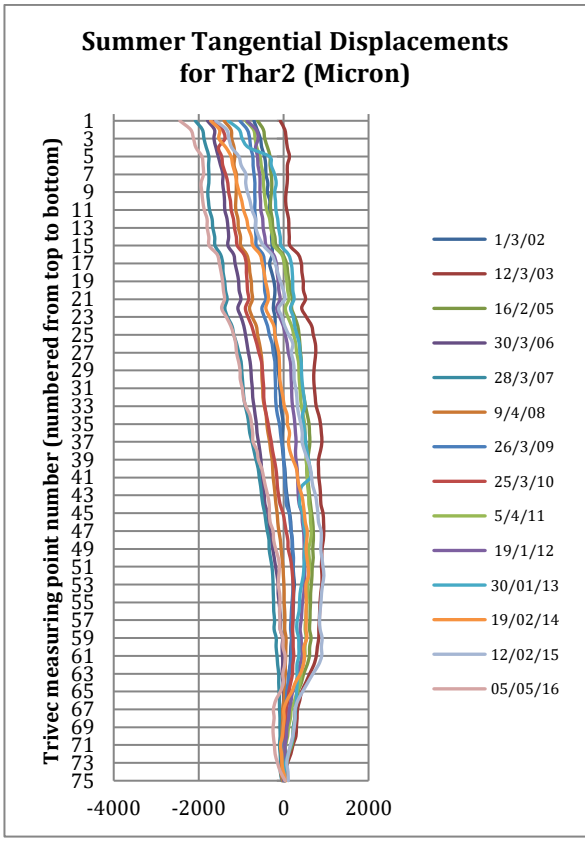

Figure 6-26: Summer tangential displacements of Trivec borehole Thar2

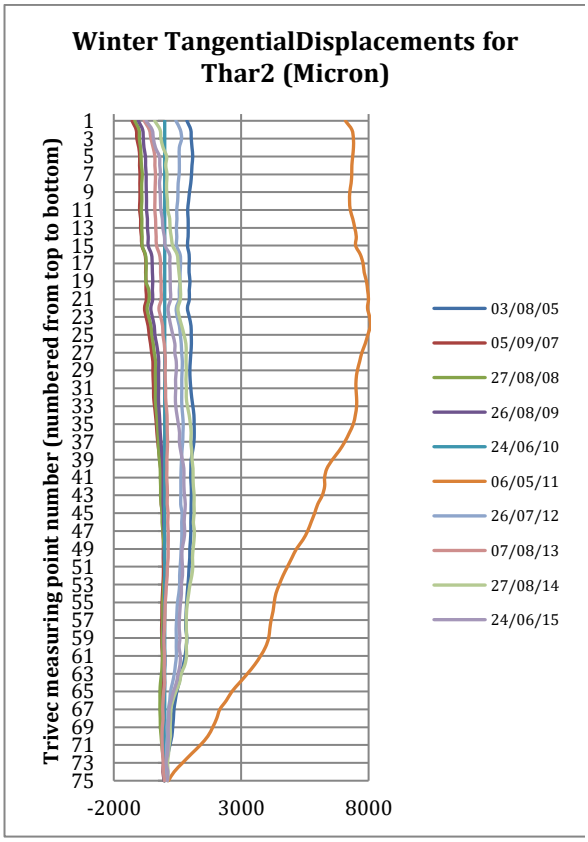

Figure 6-27: Winter tangential displacements of Trivec borehole Thar2

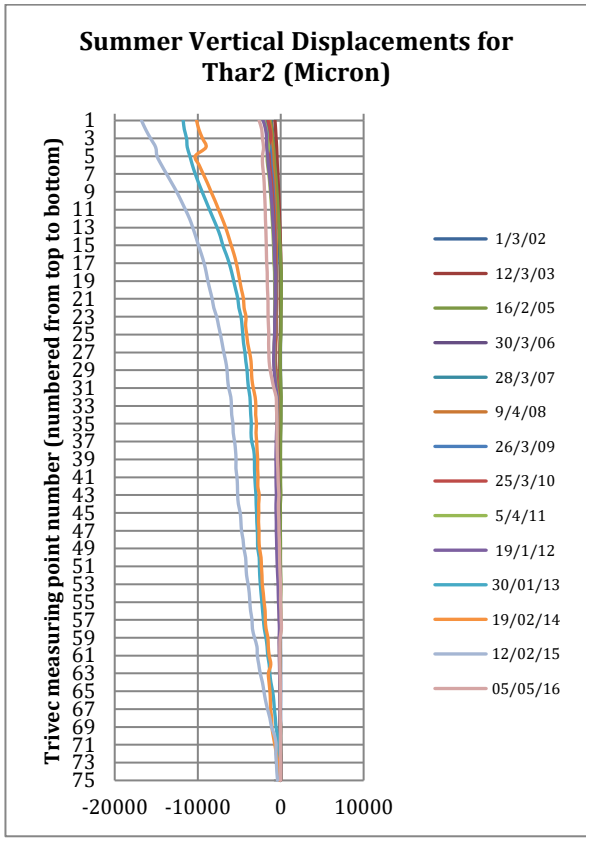

Figure 6-28: Summer vertical displacements of Trivec borehole Thar2

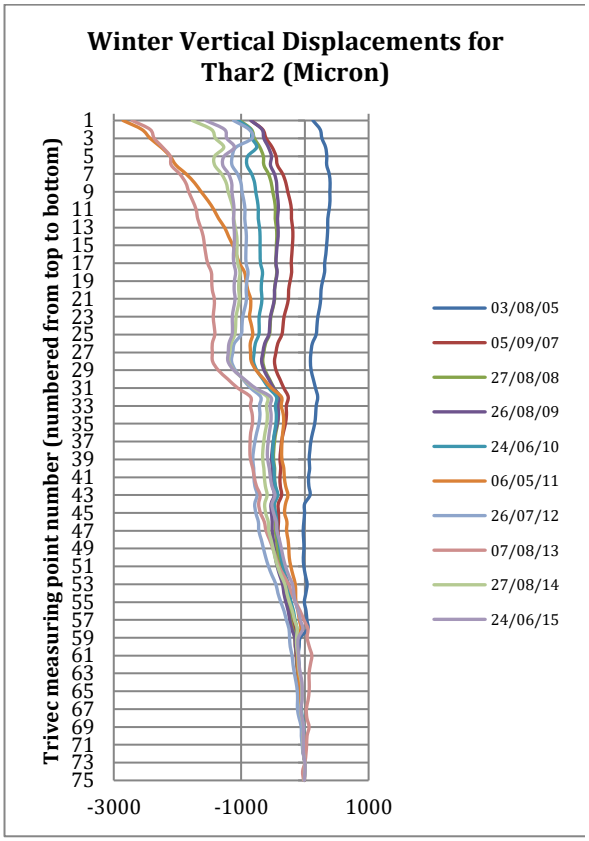

Figure 6-29: Winter vertical displacements of Trivec borehole Thar2

The radial movements show a very slight downstream trend since 2002 especially in the upper parts of the dam wall. A permanent downstream displacement of approximately 2.5 mm can be observed at the crest since 2002 (see Figure 6-24 and Figure 6-25).

The tangential movements show a very slight trend of displacement towards the right flank relative to the base date, which become more exaggerated in the upper parts of the dam wall. A permanent displacement towards the right flank of approximately 1 mm can be observed at the crest since the base date (see Figure 6-26 and Figure 6-27).

The vertical movements show a definite trend of rising elevations relative to the base date, and movements are more exaggerated in the upper parts of the dam wall. A permanent rise in elevation of approximately 2 mm can be observed at the crest since the base date (see Figure 6-28 and Figure 6-29).

6.4.3. Trivec Installation 3

Thar3 is the far-right Trivec borehole located in the arch section next to the right abutment. Figure 6-30 to Figure 6-35 present the results for this Trivec installation relative to 2000. Positive directions are defined as downstream when considering radial movements, left flank when considering tangential movements and downwards when considering vertical movements.

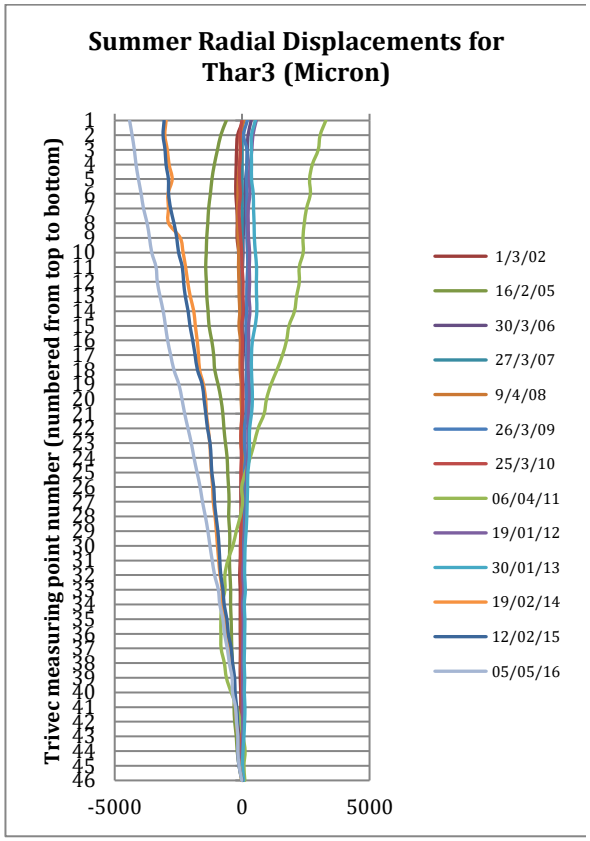

Figure 6-30: Summer radial displacements of Trivec borehole Thar3

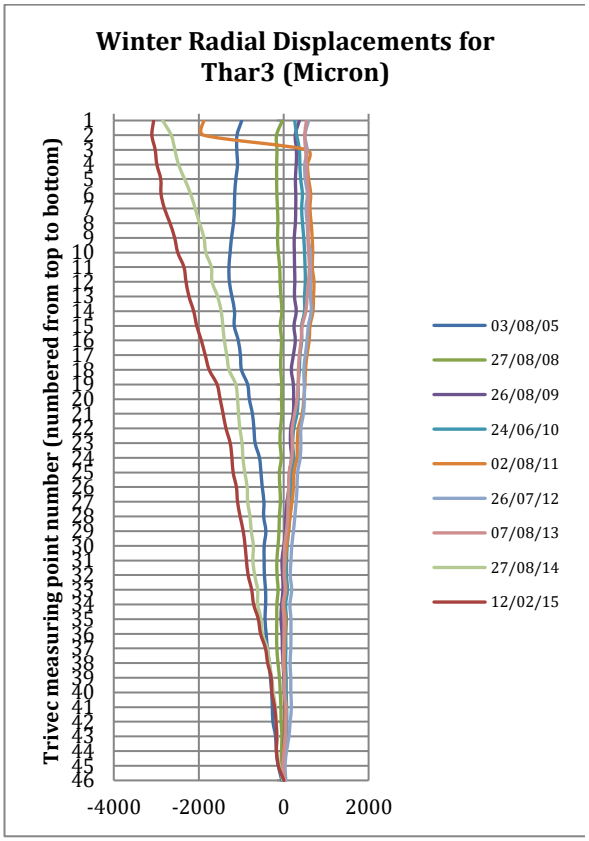

Figure 6-31: Winter radial displacements of Trivec borehole Thar3

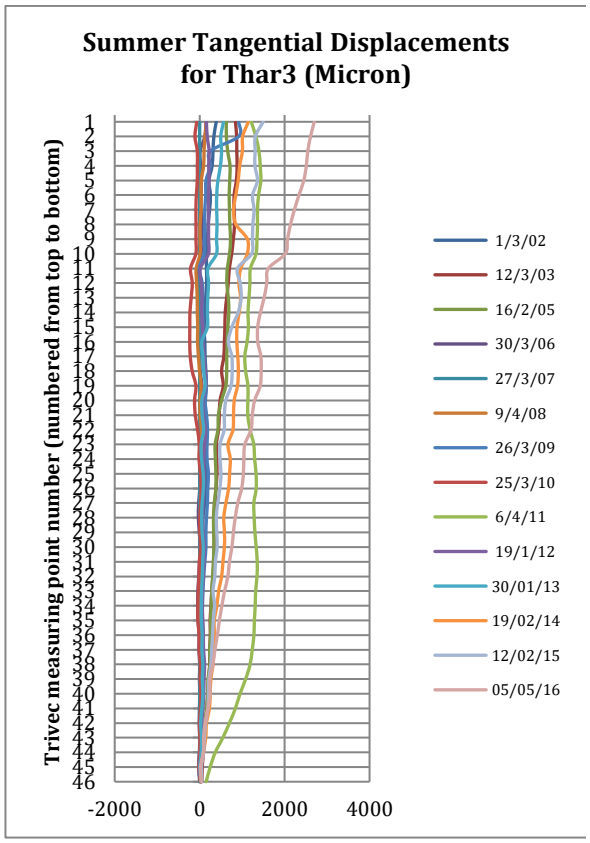

Figure 6-32: Summer tangential displacements of Trivec borehole Thar3

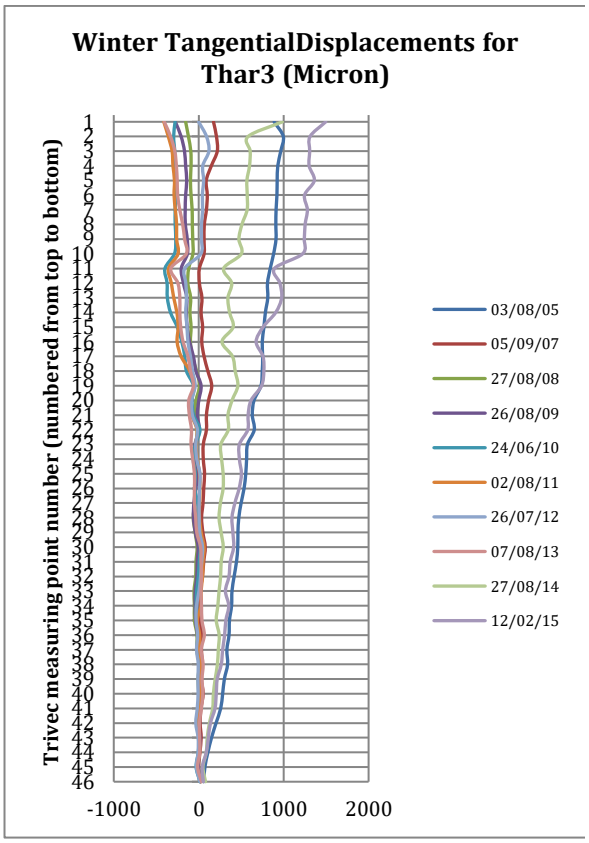

Figure 6-33: Winter tangential displacements of Trivec borehole Thar3

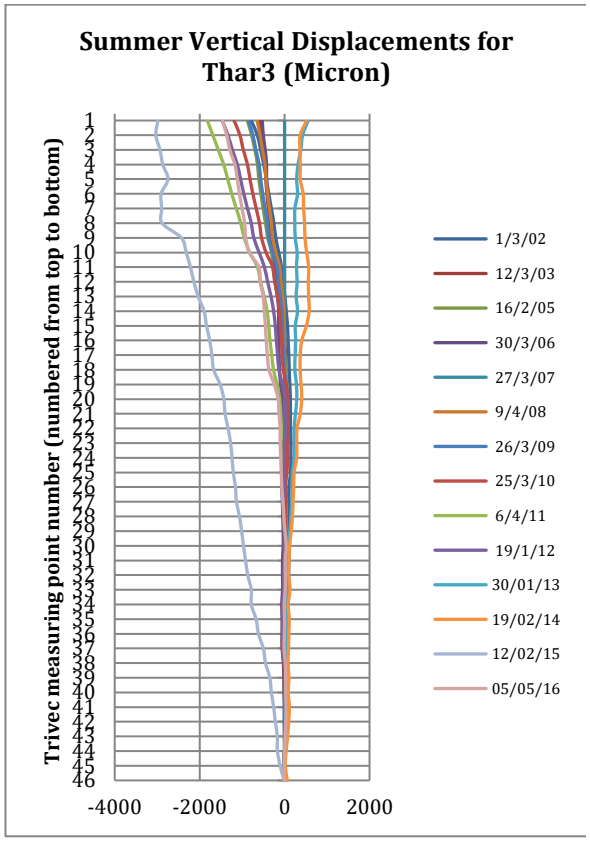

Figure 6-34: Summer vertical displacements of Trivec borehole Thar3

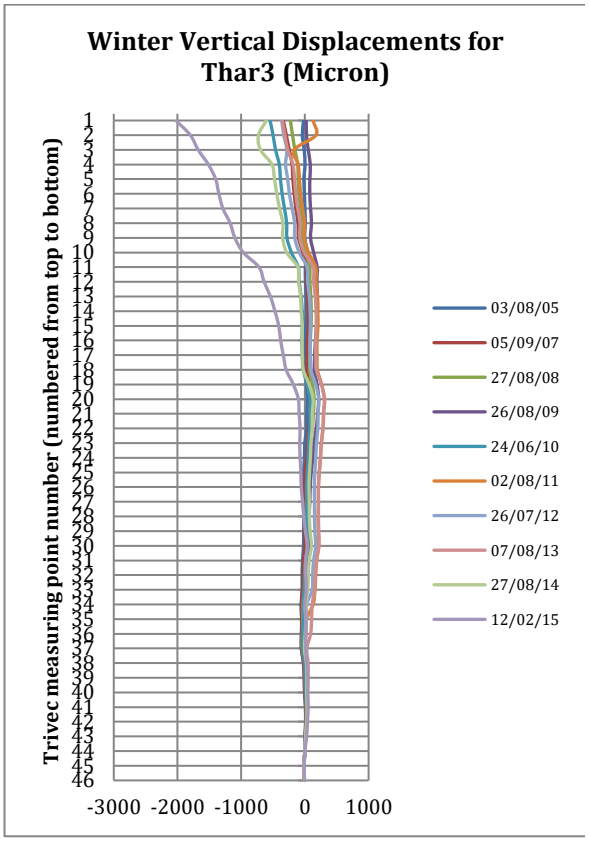

Figure 6-35: Winter vertical displacements of Trivec borehole Thar3

The radial movements show an upstream displacement trend relative to 2002, especially in the upper parts of the dam wall. A permanent upstream displacement of approximately 3 mm can be observed at the crest since 2002 (see Figure 6-30 and Figure 6-31).

The tangential movements show a very slight trend of displacement towards the left flank relative to the base date, which become more exaggerated in the upper parts of the dam wall. A permanent displacement towards the left flank of approximately 1 mm can be observed at the crest since the base date (see Figure 6-32 and Figure 6-33).

The vertical movements show a definite trend of rising elevations relative to the base date, and movements are more exaggerated in the upper parts of the dam wall. A permanent rise in elevation of approximately 1.5 mm can be observed at the crest since the base date (see Figure 6-34 and Figure 6-35).

6.5. Chapter Summary

This chapter looked at the structural behaviour of Thabina Dam in order to gain any possible evidence of the effects of AAR-related expansion. The structural behaviour of Thabina Dam is monitored by crack width gauges, trivec installations and 5-yearly visual inspections.

Visual inspection:

The downstream face displays frequent areas of calcite staining along the horizontal lift joints and the frequency seems to increase towards the right flank abutment area. There was one major peripheral crack close to the abutment contact visible on the right flank. One lift joint displayed active seepage.

Crack width gauges:

The crack width gauge results hint at the opening of the vertical joints. The trends are very small.

Trivec results:

The results show that the right flank of the arch generally moved permanently upstream especially when looking at the most recent results (since 2011). The middle and left flank of the arch shows a very slight downstream trend. The results show that the left flank and right flanks have moved slightly towards each other. Generally, a permanent rise in elevations of the arch structure is also evident from the readings.

7. Discussion of Results

7.1. Introduction

Swelling concrete in arch dams adds to the stress patterns already present within the structure. The additional internal stress manifests in different macroscopic ways such as rising crest elevations and upstream drift, cracking and opening of horizontal construction joints (these have been described in detail in Section 2). Swelling in the concrete would typically not occur uniformly through the structure, thus creating complex stress concentrations. Although some of these phenomena can be linked to AAR, the role of creep, elastic deformation, and shrinkage should be considered when drawing conclusions on measured behaviour of arch dams.

7.2. Comparative Results

The behaviour in terms of deformations and movements as well as observed deterioration of three concrete arch dams in South Africa, namely Hartebeeskuil Dam, Poortjieskloof Dam and Thabina Dam, were investigated by the use of visual inspections and the interpretation of instrumentation results. The specific aim was to pick up on possible swelling phenomena in these dams and to compare them. The instrumentation installed at the dams were described in Chapter 3. The average annual permanent displacement and strain rates for the entire period of measurements for each dam are shown in Table 7-1.

Table 7-1: Summary of comparative displacement and strain rates

Dam		**Hartebeeskuil Dam[1]**	**Poortjieskloof Dam[1]**	**Thabina Dam[2]**
Age (years)		48	62	33
Structure orientation (upstream to downstream)		West to East	South to North	West to East
Radial Displacement Rate[4] (mm/annum)	**Right flank quarter point[3]**	-0.3	-0.4	-0.2
	Middle point[3]	-0.25	0.6	0.2
	Left flank quarter point[3]	-0.3	-0.25	0.4
Tangential Strain Rate[5] (με/annum)	**Right flank quarter point[3]**	1.8	3.1	-0.5
	Left flank quarter point[3]	-1.8	-1.6	1
Vertical Strain Rate[6] (με/annum)	**Right flank quarter point[3]**	-1	7.4	1.6
	Middle point[3]	1.4	9	2.2
	Left flank quarter point[3]	-1.2	8.2	0.5

[1]Geodetic results were used to determine permanent displacement and strain trends
[2]Trivec results were used to determine permanent displacement and strain trends
[3]The target/measuring point closest to or on the crest of the dam wall was selected
[4]Positive values indicate downstream displacement
[5]Positive values indicate strain towards right flank
[6]Positive values indicate strain vertically upwards

7.3. Comparative Discussion

Hartebeeskuil Dam is the second oldest of the three dams. The history of AAR at the dam has been described in successive dam safety inspection reports over the years.

Generally, the upstream face of the dam wall has experienced a constant pattern of wetting and drying over the years. The water level mostly fluctuates between the FSL (when the dam spills in the winter) and approximately 5 m below the FSL (mostly during the dryer summer months).

The dam wall faces in an easterly direction and this implies that the downstream face of the dam wall will receive the most direct sunlight in the mornings while the upstream face will receive the most direct sunlight in the afternoons. This results in varying temperatures throughout the structure during a normal day.

The permanently displaced dam wall (in plan) based on the instrumentation results is shown in Figure 7-2 (exaggerated scale).

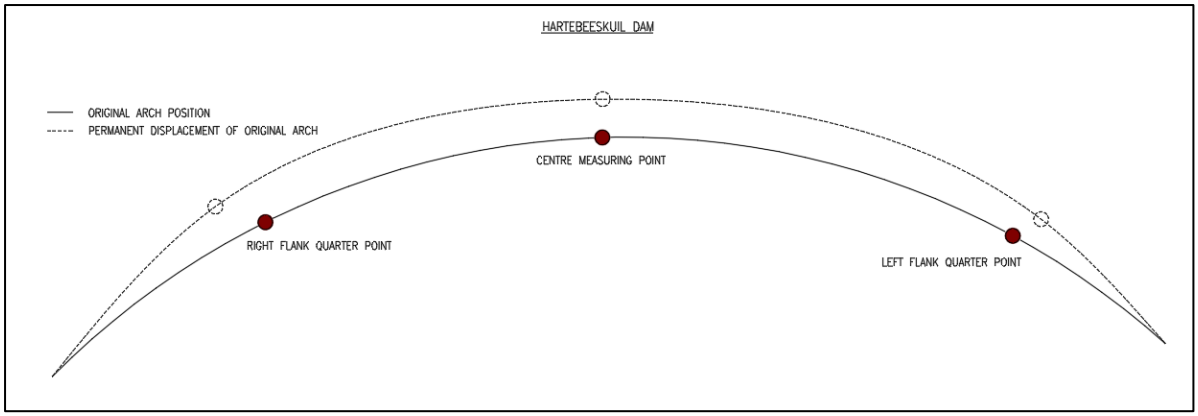

Figure 7-1: Schematic of permanent x-y displacement of Hartebeeskuil Dam

The permanent displacement and strain rates are all low, which may suggest that the AAR in the concrete has been happening at a slow rate. The vertical strain rates suggest that expansion only occurs in the centre of the dam. The entire arch has drifted upstream at a slow rate and the tangential strain rates suggest expansion in the direction of the abutments.

More recently there seems to be a slight decrease in the radial displacement and tangential strain rates and a slight increase in the vertical strain rate (refer to

Table 7-2 which shows strain rates since 2010).

Table 7-2: Average strain and displacement rates at Hartebeeskuil Dam since 2010

Hartebeeskuil Dam Dam crest swelling rates since 2010		
Radial Displacement Rate (mm/annum)	**Right flank quarter point**	0
	Middle point	-0.2
	Left flank quarter point	-0.24
Tangential Strain Rate (με/annum)	**Right flank quarter point**	1.2
	Left flank quarter point	-0.7
Vertical Strain Rate (με/annum)	**Right flank quarter point**	-0.7
	Middle point	5.5
	Left flank quarter point	-1.5

Poortjieskloof Dam is the oldest dam of the three and shows the most severe visible signs of deterioration due to AAR-related swelling of the concrete (severe, stained cracking on the downstream face and separation of the horizontal construction joints). The history of AAR at the dam has been described in successive dam safety inspection reports over the years.

The upstream face of the dam wall has experienced a fairly constant pattern of wetting and drying over the years. The water level mostly fluctuates between the full supply level (FSL) (when the dam spills in the winter) and approximately 3 m below the FSL (mostly during the dryer summer months).

The dam wall faces in a northerly direction and this implies that the downstream face of the dam wall will receive the most direct sunlight. This results in varying temperatures throughout the structure during a normal day.

The permanently displaced dam wall (in plan) based on the instrumentation results is shown in Figure 7-2 (exaggerated scale).

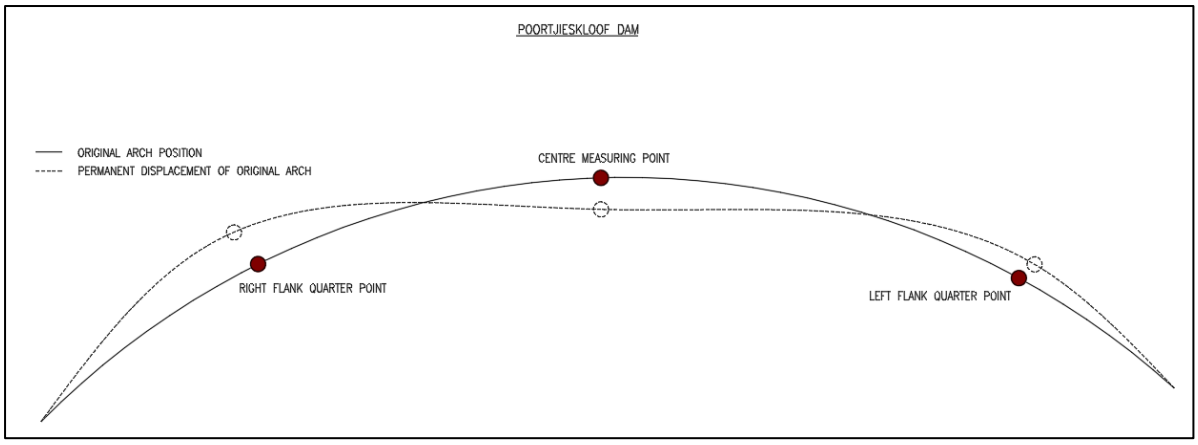

Figure 7-2: Schematic of permanent x-y displacement of Poortjieskloof Dam

The largest average annual strain rates are in the vertical direction. Generally, this is due to the fact that the concrete is mostly unrestrained in this direction, except at the interface with the abutments. As can be expected, the vertical strain rates increase towards the centre of the dam. Upstream drift is only evident at the flanks, but the centre of the dam has moved in a downstream direction. The tangential strain rates suggest expansion in the direction of the abutments.

More recently, there seems to be a decrease in the average strain rates at Poortjieskloof Dam (refer to Table 7-3 which shows strain rates since 2010). This decrease is especially evident in the vertical strain rates. This could be an indication that the rate of expansion due to AAR is slowing down.

Table 7-3: Average strain and displacement rates at Poortjieskloof Dam since 2010

Poortjieskloof Dam crest swelling rates since 2010		
Radial Displacement Rate (mm/annum)	**Right flank quarter point**	0
	Middle point	0.5
	Left flank quarter point	-0.2
Tangential Strain Rate (με/annum)	**Right flank quarter point**	2.9
	Left flank quarter point	-0.7
Vertical Strain Rate (με/annum)	**Right flank quarter point**	2.6
	Middle point	2.6
	Left flank quarter point	1.6

Thabina Dam is the youngest of the three dams. No clear evidence of the presence of AAR has yet been documented.

The water level data was not as reliable and comprehensive as that of Hartebeeskuil and Poortjieskloof Dams and a clear wetting and drying pattern could not be determined. From the available data, the following was observed:

- The water level dropped significantly between the latter stages of 2002 and the beginning of 2003 after which the level increased again significantly.
- The dam seemed to have remained relatively full since 2006 with maximum fluctuations of about 5 m in the water level up to 2016.

The dam wall faces in an easterly direction and this implies that the downstream face of the dam wall will receive the most direct sunlight in the mornings while the upstream face will receive the most direct sunlight in the afternoons. This results in varying temperatures throughout the structure during a normal day.

The permanently displaced dam wall (in plan) based on the instrumentation results is shown in Figure 7-3 (exaggerated scale).

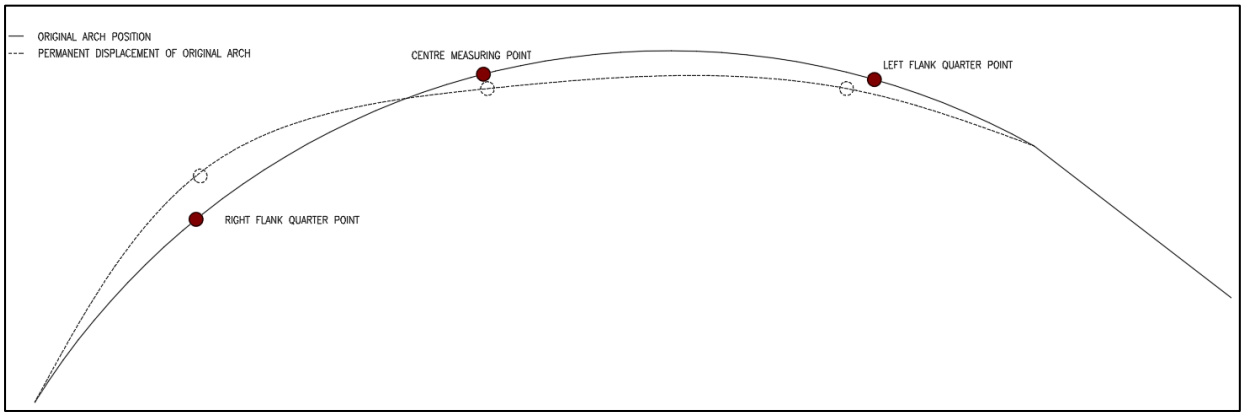

Figure 7-3: Schematic of permanent x-y displacement of Thabina Dam

The largest average annual strain rates are in the vertical direction. Generally, this is due to the fact that the concrete is mostly unrestrained in this direction, except at the interface with the abutments. As can be expected, the vertical strain rates increase towards the centre of the dam. Upstream drift is only evident at the right flank quarter point, but the centre of the dam and the left flank has moved in a downstream direction. The tangential movements show that the right and left flank have moved towards each other.

More recently, there seems to be a distinct increase in the average strain rates at Thabina Dam (refer to Table 7-4 which shows strain rates since 2010). It is possible that these increased strain rates are caused by AAR. However, experimental tests and further field observations will have to be performed to confirm this.

Table 7-4: Average strain and displacement rates at Thabina Dam since 2010

Thabina Dam Dam crest swelling rates since 2010		
Radial Displacement Rate (mm/annum)	**Right flank quarter point**	-1.1
	Middle point	-1
	Left flank quarter point	0.4
Tangential Strain Rate (με/annum)	**Right flank quarter point**	-3.6
	Left flank quarter point	8.8
Vertical Strain Rate (με/annum)	**Right flank quarter point**	2.6
	Middle point	3
	Left flank quarter point	3.4

It is noted that the presence of Blast Furnace Slag in the concrete significantly reduces the likelihood of the development of AAR. However, there is no guarantee that AAR will be completely prevented.

8. Conclusions and Recommendations

8.1. Summary

AAR is one of the leading causes of ageing in concrete arch dams in South Africa. It is becoming increasingly more important to understand and study the effects that AAR have on these dams and data gained from both visual inspections and instrumentation installed at the dams provide valuable insight into their behaviour. Understanding the behaviour will shed more light on the possible consequences of swelling due to AAR and how it impacts on the safety of concrete arch dams.

The purpose of this research is to compare the behaviour of three different arch dams in South Africa. In each case, the factors that affect AAR were different (i.e. different climate regions, different construction materials and different patterns of moisture exposure of the concrete). The dams that were considered during the study are Hartebeeskuil Dam, Poortjieskloof Dam and Thabina Dam. The South African National Department of Water and Sanitation uses *inter alia* geodetic surveys, trivec installations, crack width gauges, stress measuring cells and piezometers to monitor the behaviour of their arch dams. For the purpose of this study, a visual inspection of each dam was performed, and all available instrumentation data was collected and analysed.

The sections below present the conclusions of this research as well as recommendations regarding future work relating to the topic.

8.2. Conclusions

The visual inspections and instrumentation results of all three dams confirmed the typical behavioural phenomena that are associated with swelling concrete due to AAR. Such phenomena are the response of the structure to the internal stresses that are the result of swelling that occurs on a microscopic scale, but eventually manifests on a macroscopic scale in the form of permanent upstream and downstream displacements, permanent rising of crest levels, peripheral cracks on the downstream face close to the abutment and separation of horizontal construction lift joints. At two of the dams, namely Hartebeeskuil Dam and Poortjieskloof Dam, AAR-related deterioration has been reported on in statutory dam safety inspection reports compiled by the DWS over the years. At Thabina Dam there have been no reported confirmation of the presence of AAR. SKC and Keller Consulting Engineers (1997) did, however, make mention that there is a possibility that the structure may still develop AAR.

Of the three dams, the oldest, Poortjieskloof, exhibited the worst observed deterioration due to AAR. The downstream face of the arch dam wall is cracked severely, and the horizontal construction lift joints show clear separation on the downstream face of the dam. A maximum average vertical strain rate of 9 με/annum was recorded in the centre of the arch and a maximum average tangential strain rate of 3.1 με/annum towards the right abutment was recorded at the right flank. Generally, the swelling rates show a decrease since 2010. It is possible that the rate of AAR in the concrete is decreasing.

The second oldest dam, Hartebeeskuil Dam, exhibited less observed deterioration due to AAR. Peripheral cracks were visible on the downstream face of the arch dam wall close to the abutment contact. A maximum average vertical strain rate of 1.4 με/annum was recorded at the

centre of the arch and a maximum average tangential strain rate of 1.8 με/annum were recorded at both flanks (expanding towards the abutments). The geodetic survey showed small average annual upstream displacement rates (maximum 0.3 mm/annum at the right flank). Generally, the swelling rates remain fairly constant when looking at the more recent rates (since 2010).

Thabina Dam is the youngest of the three dams and visually it exhibits the least deterioration. Only one major crack on the right flank downstream face was observed close to the abutment contact. One of the horizontal lift joints was exhibiting active seepage. A maximum average vertical strain rate of 2.2 με/annum was recorded at the centre of the arch and a maximum average tangential strain rate of 1 με/annum was recorded at the left flank (expanding towards the right flank). The geodetic survey showed small average annual upstream and downstream displacement rates (maximum 0.2 mm/annum upstream at the right flank and maximum 0.4 mm/annum downstream at the left flank). The strain rates showed a definite increase since 2010. The entire arch has started to move permanently upstream and strain rates have increased significantly especially in the vertical and tangential directions.

8.3. Recommendations

It is recommended that diagnostic tests be performed to determine whether AAR has indeed developed at Thabina Dam.

It is recommended that a full-scale finite element analysis be carried out for Poortjieskloof Dam to determine what effect the deterioration of the concrete due to AAR has on the long-term ability of the structure to resist the loading due to significant overtopping events.

Further studies into creating a calibrated finite element model to predict the long-term safety of arch dams subjected to swelling due to AAR would be useful. Such a finite element model could be calibrated to simulate an accurate AAR swelling mechanism and could also be used to investigate possible remedial measures to alleviate the effects of the swelling if deemed necessary.

9. References

Addis, B. 1998. *Fundamentals of Concrete.* Owens, G. (ed). Cement and Concrete Institute. Midrand, South Africa.

Alexander, M. & Beushausen, H. 2009. Chapter 8: Deformation and volume change of hardened concrete in Owens G. (ed.) *Fulton's Concrete Technology.* Ninth Edition. Cement and Concrete Institute, Midrand, South Africa. 111-154.

Amberg, F. 2011. *Performance of Dams Affected by Expanding Concrete*. Proceedings of ICOLD Symposium 2011. Lucerne, Switzerland.

Beukes, H.J. 2008. Hartebeeskuil Dam: Third Dam Safety Inspection Report. Report Number: 20/2/K100-02/C/1/22/4. Directorate: Strategic Asset Management, Department of Water Affairs and Forestry. Pretoria, South Africa.

Beukes, H.J. 2005 Thabina Dam: Second Dam Safety Inspection Report. Directorate Civil Design, Department of Water Affairs and Forestry. Pretoria, South Africa.

Botha, A.J., Campos De Carvalho, A., Chipuazo, J., Carvalho, E., Boulat, L., Hensi, D. & Chatron, C. 2016. *Practical Lessons Learnt from the Rehabilitation of Spillway Gates at Cahora Bassa Dam*. Proceedings of ICOLD Symposium on "Appropriate technology to ensure proper development, operation and maintenance of dams in developing countries". 18 may 2016. Johannesburg, South Africa. 2a-209 to 2a-218.

Boulat, L., Hensi, D., Chatron, C., Chipuazo, J.Z.J., Botha, A. & Campos De Carvalho, A. 2015. *Cahora Bassa rehabilitation: Challenges and solutions to restore total availability of the spillway gates.* Hydro 2015 Advancing Policy and Practice. 26-28 October 2015. Bordeaux, France.

Carvalho, E.F., Matsinhe, B.T. & Oosthuizen, C. 2016. *Monitoring System of Cahora Bassa Dam….The Past, Present and Way Forward.* Proceedings of ICOLD Symposium on "Appropriate technology to ensure proper development, operation and maintenance of dams in developing countries". 18 may 2016. Johannesburg, South Africa. 6-87 to 6-94.

Chappex, T. & Scrivener, K. 2012. *Controlling Alkali Silica Reaction by Understanding the Contribution of Aluminium Provided by Supplementary Cementitious Materials.* Proceedings of the Second International Conference on Microstructural-related Durability of Cementitious Composites. 11-13 April 2012. Amsterdam, The Netherlands. 605-612.

Charlwood, R. 2009. *Predicting the Long Term Behavior and Service Life of Concrete Dams*. Proceedings of the 2nd International Conference on the Long Term Behaviour of Dams. 12-13 October 2009. Graz, Austria. 1-11.

Charlwood, R. 2011. *Key Issues for Managing AAR in Dams*. Unpublished notes. EPFL Seminar on Alkali Aggregate Reaction Testing, Prognosis, Modelling & Avoidance. 14 September 2011. Lausanne, Switzerland.

Charlwood, R.G. 2016. Introduction and Key Issues. Unpublished notes. Theme D1: The Long Term Effect of the Aging of Concrete. Proceedings of ICOLD Workshop. 19-20 May 2016. Johannesburg, South Africa.

Charlwood, R., Scrivener, K. & Sims, I. 2013. *Recent developments in the management of chemical expansion of concrete in dams and hydro projects - Part 1: Existing structures*. Proceedings of ICOLD Simposium 2013. Seattle, USA.

Charlwood, R.G & Sims, I. 2013. *Prevention of AAR in New Dams in Africa*. Proceedings of the Africa 2013 Conference. 16-18 April 2013. Addis Ababa, Ethiopia.

Dorfling, C. 2008. *DWAF Crack-Width Gauges: A Journey through History*. Proceedings of the Short Course: Dam Monitoring and Surveillance. 15-18 September 2008. Stellenbosch University, Stellenbosch, Western Cape. 42-46.

Elges, H., Geertsema, A., Lecocq, P. & Oosthuizen, C. 1995. *Detection, monitoring and modelling of alkali-aggregate reaction in Kouga Dam (South Africa)*. (Report CONF-9510182—TRN: 95:008180-0012). Denver, CO, USA: Committee on Large Dams.

Geotechnisches Ingenieurbüro. 2004. *Stress-relief Methods with Triaxial Cell*. Am Reutgraben, 9. D-76275 Ettlingen, Germany.

Ghanaat, Y. (1993). *Theoretical Manual for Analysis of Arch Dams*. Technical Report ITL-93-1. Washington DC: U.S. Army Corps of Engineers.

Giorla, A.B., Cyrille, F.D., Scrivener, K.L. 2014. *Role of Creep on the Microstructural Damage Induced by Alkali-Silica Reaction*. Proceedings of the RILEM International Symposium on Concrete Modelling. 12-14 Ocotber 201. Beijing, China. 197-203.

Goldie, R. 2002. Hartebeeskuil Dam: Second Dam Safety Inspection Report. Report Number: K100-02-DY03. Directorate Civil Design, Department of Water Affairs and Forestry. Pretoria, South Africa.

Hagen, D.J. 1996. Poortjieskloofdam: Damveiligheidsinspeksie. Verslag Nommer: H300/01/DY03. Direktoraat Siviele Ontwerp, Departement van Waterwese en Bosbou. Pretoria, South Africa.

Hattingh, L.C. 2011. Kouga Dam: Fourth Dam Safety Inspection Report. Report Number: L820/01/DY04. Department of Water and Sanitation. Pretoria, South Africa.

Hattingh, L.C. and Oosthuizen, C. 2012. *Long Term Behaviour of Dam Materials*. Proceedings of the SANCOLD Annual Conference 2012. 1-3 August 2012.Pietermaritzburg, KwaZulu-Natal. 73-76.

Hattingh, L.C., Tembe, I. Carvalho, E. & Oosthuizen, C. 2014. *3D Swelling due to Chemical Reaction – the Cahora Bassa Dam Experience*. Proceedings of the SANCOLD Annual Conference 2014. 5-7 November 2014. Johannesburg, South Africa. 498-507.

ICOLD, 1991. *Alkali-Aggregate Reaction in Concrete Dams*. ICOLD Bulletin 79. Paris, France.

ICOLD, 1994. *Ageing of Dams and Appurtenant Works*. ICOLD Bulletin 93. Paris, France.

ICOLD, 2009. *Surveillance: Basic Elements in a "Dam Safety" Process*. ICOLD Bulletin 138. Paris, France.

Larive, C. 1998, *Apports Combin'es de l'Experimentation et de la Modélisation à la Comprehension el'Alcali-Réaction et de ses Effets Mécaniques.* PhD thesis. Thése de Doctorat Laboratoire Central des Ponts et Chaussées, Paris.

Lea, F.M. 1971. *The Chemistry of Cement and Concrete, Third Edition.* Chemical Publishing Co., Inc. New York, USA.

Liu, C., Chen, G., Ji G., Kong, X. & Ma, L. 2012. *The Effect of AAR on Concrete Mechanical Properties*. Second International Conference on Micro-structural-related Durability of Cementitious Composites. 11-13 April 2013. Amsterdam, The Netherlands. 568-576.

Mahlabela, C.N. & Oosthuizen, C. 2012. Lombardi slenderness coefficient as one of the criteria for the preliminary evaluation of proposed rehabilitation works at Kouga Dam in Alexander, M.G., Beushausen, H.D., Dehn, F. & Moyo, P. (eds.) *Concrete Repair, Rehabilitation and Retrofitting III (ICCRRR)*. London: Taylor & Francis. 233-234.

Martin, R.P., Bazin, C. & Toutlemonde, F. 2012. *Alkali aggregate reaction and delayed ettringite formation: common features and differences*. 14th International Conference on Alkali Aggregate Reaction ICAAR14. 20-25 May 2012. Austin, Texas, USA.

Menendez, E. 2016. Critical Parameters that Lead to the Evolution of ASR. Unpublished notes. Theme D1: The Long Term Effect of the Aging of Concrete. Proceedings of ICOLD Workshop. 19-20 May 2016. Johannesburg, South Africa.

Muller, H. 2006. Poortjieskloof Dam: Third Dam Safety Inspection Report. Report No.: 20/2/H300/01/C/1/22. Directorate Civil Design, Department of Water Affairs and Forestry. Pretoria, South Africa.

National Water Act, No. 36 of 1998. Regulation. 2012. *Government Gazette*. 560(35062). 24 February. Government Notice No. R139. Pretoria: Government Printer.

Naude, P. 2002. *Kouga Dam: Dam Safety Installation Report on Trivec System*. (Report Number: L820/01/DX02). Pretoria, South Africa. Directorate: Civil Design, Sub-Directorate: Dam Safety, Department of Water Affairs and Forestry.

Oberholster, B. 2009. Chapter 10: Alkali-Silica Reaction in Owens G. (ed.) *Fulton's Concrete Technology.* Ninth Edition. Cement and Concrete Institute, Midrand, South Africa. 189-218.

Oosthuizen, C. 2015. Dam Surveillance Techniques: Basic Instrumentation and Data Interpretation. Unpublished notes. Proceedings of the short course: The Design and Construction of Hydraulic Structures. 28 September - 01 October 2015. Stellenbosch University, Stellenbosch, South Africa.

Oosthuizen C., Goldie, R.H. & Dorfling, C.J. 2003. *An Attempt to Explain the Complex Behavious of a 'Simple' Cylindrical Arch Dam.* (ISBN 90 5809 602 5). Field Measurements in Geomechanics. Proceeding of the 6th International Symposium. 23-26 September 2003. Oslo, Norway. 261-266.

Oosthuizen, C., Naude, P.A. & Dorfling, C.J. 2003. *A Simple 3-Dimensional Crack-Width-Tilt Gauge Out of Africa.* (ISBN 90 5809 602 5). Field Measurements in Geomechanics. Proceeding of the 6th International Symposium. 23-26 September 2003. Oslo, Norway. 599-604.

Pretorius, C.J. 2008. *Geodetic Surveying, Is It Worth the Effort*. Proceedings of the Short Course: Dam Monitoring and Surveillance. 15-18 September 2008. Stellenbosch University, Stellenbosch, Western Cape. 28-35.

Prins, Z.J. 2013. Hartebeeskuils Dam: Fourth Dam Safety Evaluation Report. Report Number: 20/2/K100-02/C/1/22/5. Directorate: Civil Design, Department of Water Affairs and Forestry. Pretoria, South Africa.

Prins, Z.J. 2014. *Dynamic Loads and Their Significance in Understanding the Behaviour of Concrete Arch Dams.* Proceedings of the SANCOLD Annual Conference 2014. 5-7 November 2014. Johannesburg, South Africa. 154-163.

Saouma, V. & Perotti, L. 2006. Constitutive Model for Alkali-Aggregate Reactions. *ACI Materials Journal*, 103(3): 194-202.

Shaw, Q.H.W. 2015. *The Structural Function of Different Arch Dam Types*. Proceedings of the SANCOLD Annual Conference 2015. 1-3 September 2015. Cape Town, South Africa. 320-332.

Sibanda, B. 2011. Poortjieskloof Dam: Fourth Dam Safety Inspection Report Carried Out In Terms of GN R1560 of 25 July 1986. Report No: H300/01/DY/02. Directorate: Strategic Asset Management, Department of Water Affairs and Forestry. Pretoria, South Africa.

SKC & Keller Consulting Engineers. 1997. Thabina Dam: First Dam Safety Inspection in Terms of the Dam Safety Regulations. Report Number: B801/82/DY01. Directorate: Civil Design, Department of Water Affairs and Forestry. Pretoria, South Africa.

Van Den Berg, C.L. 2008. *Visual Observations - Guidelines for Site Inspections*. Proceedings of the Short Course: Dam Monitoring and Surveillance. 15-18 September 2008. Stellenbosch University, Stellenbosch, Western Cape. 8-15.

Ulm, F., Coussy, O., Kefei, L. & Larive, C. 2000. Thermo-Chemo-Mechanics of ASR Expansion in Concrete Structures*. Journal of Engineering Mechanics*, 126(3): 233-242.

United States Army Corps of Engineers. 1994*. Arch Dam Design.* (Engineering Manual no. 1110-2-2201). Washington, DC.

United States Bureau of Reclamation. 2017. *Glen Canyon Unit*. Available: https://www.usbr.gov/uc/rm/crsp/gc/ [2017, November 27]

United States Bureau of Reclamation. 2017. *Flaming Gorge Unit*. Available: https://www.usbr.gov/uc/rm/crsp/fg/index.html [2017, November 27]

Van Den Berg, C.L. 1994. Hartebeeskuil Dam: Dam Safety Inspection Report. Report Number: K100-02-DY02. Directorate Civil Design, Department of Water Affairs and Forestry. Pretoria, South Africa.

Van Der Spuy, D. 1987. Damveiligheidsinspeksie Poortjieskloofdam. Verslagno.: H300-01-DY02. Departement van Waterwese, Direktoraat Siviele Ontwerp. Pretoria, South Africa.

Vezi, M. 2014. *Dynamic Modelling of Arch Dams in the Ambient State*. Master's Dissertation. Faculty of Engineering and Built Environment, University of Cape Town, Cape Town, South Africa.